



DELFT UNIVERSITY OF TECHNOLOGY

MSC THESIS PROJECT

Sensitivity Analysis for Expansion of Transmission Systems with High Amounts of Renewables

Author:
Evangelos Galinas

Supervisors:
Ass. Prof. Madeleine Gibescu
Dip.-Ing. Jens C. Boemer

March 15, 2013

“When setting out upon your way
to Ithaca, wish always that your
course be long, full of adventure,
full of lore.”

— *K.P. Kavafis*

Preface - Acknowledgements

Nowadays, climate change and global warming has been continuously raising public awareness about drastic actions that need to be taken in order to mitigate their detrimental effects. The cost-benefit analysis produced by Nordhaus, George Bush's economic consultant at that time, proved that climate mitigation actions were not economical; the 2006 Stern Review on climate change [1] however concluded different views. It was the first report that substantiated the problem, daring to proclaim that something was going wrong, thus putting the US governmental actions into the eye of the storm.

Seven years later, and although the United States still have not ratified the Kyoto Protocol, great progress has been achieved in reducing carbon emissions and increasing the renewable energy share at least in the European continent. Following the 20-20-20 European Commission directive [2], the EU Member States have agreed on reducing their carbon footprint and investing on clean energy alternatives. The Fukushima accident in March 2011 accelerated the sequence of events, since it forced the German government to a historical decision to gradually decommit its nuclear power plants and rapidly integrate renewable energy sources onto the German power system. Despite the harsh economic crisis, it drastically changed the map of renewable energy shares in the EU that currently leads the way towards a carbon free society by 2050.

This thesis has been a fascinating journey in the world of European power systems, markets and policy. Concepts such as network modelling, data mining and optimisation algorithms where of its main focus as well. Despite the countless sleepless nights I encountered, I discovered a lot about the importance of self-motivation and time-management. The closest the date of completion came, the more I learned to stay calm, focus and limit my curiosity to a healthy level. This thesis finally set the bar quite high as far as my productivity and physical strengths are concerned.

For all these, I would like to thank my thesis supervising professor, Madeleine Gibescu, for the opportunity she gave me to cooperate with the Power Systems group of TU Delft. Her support during decisions of critical importance and her willingness to help at every problem encountered is greatly appreciated. Furthermore, I want to express my honest gratitude to my supervisor, senior consultant and PhD candidate Jens C. Boemer, for his encouragement, guidance, help and mentoring from the beginning till the very end of this project. Without him, this project would definitely not have been the same. Moreover, I want to thank the whole Power Systems and Markets team in Berlin, for the flawless collaboration we had during the first part of this project. Also, the NTNU PhD candidate, Ida Fuchs for her support and guidance while implementing the Ant Colony Optimisation approach and the TU Delft PhD candidate Ana Ciupuliga for the New England benchmark system data that she provided me with. Last but not least my family, for their limitless support and encouragement.

Evangelos Galinas, March 2013

Abstract

The increasing share of Renewable Energy Sources (RES) in today's electricity mix has introduced new challenges for the ageing European power networks. Optimal large scale deployment of wind and solar units around Europe necessitates the upgrade of the transmission system. Identifying transmission bottlenecks for fully accommodating high amounts of renewables comprises the objective of the so called Transmission Expansion Problem (TEP). However, in times of high RES in-feed and consequently high network congestion, minor RES curtailment could potentially be more economical than reinforcing another network branch. The related annualised investment costs of these transmission lines can be larger than the value of the respective RES energy integrated into the power system. Primary objective of this thesis is to perform certain sensitivity analyses in an attempt to optimise between renewable power curtailment and network reinforcement investment costs.

A new heuristic approach that employs Optimal Power Flow (OPF) as its main tool, termed Least Upgrade Curtailment Sensitive Pseudo Optimisation (LUCSIPO) was developed for this purpose. The LUCSIPO approach, integrated with a statistical branch overload ranking, is a simple, straight-forward methodology that determines the least upgrades needed for obtaining a feasible solution. Its novel feature is the sensitivity on the curtailment limits applied. It is a key part that actually guides the algorithm towards a minimal cost solution, since it considers the trade-off between network upgrades and curtailment of RES power.

In order to validate the LUCSIPO results, a modern Meta-Heuristic TEP approach that utilises the Ant Colony Optimisation (ACO) concept was also developed. This nature inspired algorithm, mimics the collective behaviour ants exhibit while searching for food. When an ant locates a food source, it travels back to its nest and emits a certain serum called Pheromone. Trailing this serum effectively guides the other ants towards the food source. The most visited paths will exhibit the highest pheromone concentration and thus will form the shortest ("optimum") path to the nest. When applied to the TEP, a path corresponds to a set of upgraded network branches while the path length represents the total system costs.

The IEEE-39 bus New England Test System has been employed as the testing platform for the two developed approaches. Sensitivity analysis results prove the existence of an economic optimum between grid upgrades and RES curtailment. They further highlight the importance of network upgrades and high non-synchronous penetration limits for secure and cost-efficient large scale RES integration. For the selected high installed wind capacity system, the sum of curtailment and investment costs is minimised and thus regarded as the "optimum" in the at curtailment limit region between 30% and 60% of the installed wind capacity. The merit order effect, however, has a direct impact on the trade-off between RES curtailment and grid extension. The previously identified "optimum" is shifted to a curtailment limit of about 70-80% (discarding c.a. 0.75% of the available wind energy) if the operational costs are also taken into account.

The LUCSIPO's approach efficiency in providing solutions that minimise the total costs involved, has been compared against the ACO algorithm. Results show that the LUCSIPO approach introduces major calculation time speed-ups while providing solutions very close to the ACO methodology.

The final goal of this thesis was to create a continental Europe High Voltage network model for potentially applying the developed approaches. Employing similar modelling techniques and assumptions as in pan-European grid integration studies, led to the development of a consistent, spatial resolution flexible DC load flow modelling platform. It integrates publicly available consumption data with externally supplied RES time series and network information for effectively modelling the European HV network.

Abbreviations

ACO	Ant Colony Optimisation
ACS	Ant Colony System
AC	Alternating Current
AIS	Artificial Immune Systems
BC	Base Case
BIP	Binary Integer Programming
BSF	Best So Far
CEST	Central European Summer Time
CET	Central European Time
CSP	Concentrated Solar Power
DC	Direct Current
DEP	Distribution Expansion Problem
DE	Differential Evolution
DLS	Day Light Savings
DMA	Discrete Monkey Algorithm
DP	Dynamic Programming
DSM	Demand Side Management
ED	Economic Dispatch
EEZ	Exclusive Economic Zones
ENTSO-e	European Network of Transmission System Operators for Electricity
ES	Evolution Strategies
EU	European Union
EWIS	European Wind Integration Study
FIT	Feed In Tariff
FLH	Full Load hours
FS	Fuzzy Sets
GA	Genetic Algorithms
GEP	Generation Expansion Problem
GIS	Geographic Information System
GRAS	Greedy Randomised Adaptive Search
HL	High Limit
HVDC	High Voltage Direct Current
HV	High Voltage
HWHL	High Wind High Limit
HWLL	High Wind Low Limit
HWRO	High Wind Risk of Overload
HW	High Wind
HiRLAM	High Resolution Limited Area Model
ICPPCRO	Investment Cost Per Per-Cent of Risk of Overload

LF	Load Flow
LL	Low Limit
LMP	Locational Marginal Pricing
LP	Linear Programming
LUCSIPO	Least Upgrade Curtailment Sensitive Iterative Pseudo-Optimisation
LW	Low Wind
MC	Marginal Cost
MINL	Mixed Integer Non-Linear
MIP	Mixed Integer Programming
MOMA	Multi-Objective Memetic Algorithm
MRCGP	Minimum Required Conventional Generation Penetration
MS	Member State
NEP	Netzentwicklungsplan
NE	New England
NLP	Non-Linear Programming
NREAP	National Renewable Energy Action Plan
NTC	Net Transfer Capacity
NUTS	Nomenclature of Territorial Units for Statistics
ODBC	Open Database Connectivity
OLM	Overhead Line Management
OPF	Optimal Power Flow
PSEP	Power System Expansion Problem
PSO	Particle Swarm Optimisation
PS	Pump Storage
PTDF	Power Transfer Distribution Factor
PV	Photovoltaic
REI	Radial Equivalent Independent
RES	Renewable Energy Sources
RL	Residual Load
ROR	Run Of River
RO	Risk of Overload
SA	Simulated Annealing
SCOPF	Security Constraint Optimal Power Flow
SFL	Shuffled Frog Leap
SNSP	System Non-Synchronous Penetration
TAL	High Temperature ALuminium Conductor
TEP	Transmission Expansion Problem
TOA	Taguchi's Orthogonal Array
TS	Tabu Search
TYNDP	Ten Year Network Development Plan
UCTE	Union for the Coordination of Transmission of Electricity
UCT	Universal Coordinated Time
UC	Unit Commitment
WYI	Wind Year Index

Nomenclature

A	Annuity
\mathbf{B}'	Nodal reactance matrix
B_{ij}	Imaginary part of the nodal admittance ij^{th} element
C_{curt}	Curtailment cost
CE	Curtailed energy in %
C_i	Curtailed energy per hour in MWh
c_i	Cluster's centroid value
$C_{inv,pa}$	Investment costs
C_{op}	Operating costs
$C_{op,pol}$	Operational policy costs
c_p	CO ₂ price
C_{pen}	Penalty Cost Factor
C_t	Total cost
$C(x)$	Objective function
$\Delta\tau_{i,e}$	Branch pheromone Update for the i^{th} branch
m	Current ant expedition
M	Max number of ant expeditions
e_f	CO ₂ emission factor
FIT	2012 FIT rate
FIT_a	Adjusted FIT rate
FIT_{av}	FIT weighted average
\mathbf{F}_{max}	Vector of maximum power flow branch limits
f_p	Fuel price
f_p^i	Cost function for the i^{th} generator
G_{ij}	Real part of the nodal admittance ij^{th} element
$g(x)$	Inequality constraint
h	Simulated hours
h_f	Branch flow inequality constraints
$h(x)$	inequality constraint
i	Inflation rate
Inv_i	Investment cost index ICPPCRO for the i^{th} branch
l	Line length
lim	Max loading limit in % of the branch capacity
m	Current ant mission
M	Max number of ant missions
m_e	Mean overload for the i^{th} branch
N	Number of network buses
n	Investment's lifetime
N_b	Number of branches

n_g	Number of generators
P_{cur}	Curtailement Limit
\mathbf{P}_d	Demand vector
\mathbf{P}_g	Active power injections vector
p_g^i	Active power dispatch of the i^{th} generator
$p_g^{i,max}$	Maximum allowed loading for the i^{th} generator
$p_g^{i,min}$	Minimum allowed loading for the i^{th} generator
ϕ^{global}	Global pheromone reduction rate
ϕ^{local}	Local pheromone reduction rate
P_i	Net active power injected at bus i
PV	Present value factor
q_k	ACO quality
Q_i	Net reactive power injected at bus i
r	Interest rate
RO_i	Risk overload for the i^{th} branch
r_{pu}	Line resistance (p.u.)
R_t	Typical line resistance in Ω/km
S_b	Base power in MVA
S_k	TEP Solution
S_l	TEP partial Solution
S^{RO}	Set of branches identified as overloaded
$\tau_{i,m}$	Pheromone amount at s_i for the m^{th} mission
$\tau_{i,m+1}$	Pheromone amount at s_i for the $(m+1)^{th}$ mission
$\tau_{i,e}$	Pheromone amount at the global s_i for the e^{th} expedition
$\tau_{i,e+1}$	Pheromone amount at the global s_i for the $(e+1)^{th}$ expedition
Θ	Voltage angle vector
θ_{ij}	Voltage angle between the i^{th} and the j^{th} bus
u	Decision variable
V_b	Base voltage in kV
$ V_i $	Voltage magnitude the i^{th} bus
$ V_j $	Voltage magnitude the j^{th} bus
W_i	Available wind energy per hour in MWh
x	State variable
X_t	Typical line reactance in Ω/km
x_j	Observation
x_{pu}	Line reactance (p.u.)
Z_a	Actual line impedance in Ω
Z_b	Base impedance in Ω
Z_t	Magnitude of typical line impedance in Ω/km
z_{pu}	Magnitude of line impedance (p.u.)

List of Definitions

Curtailed wind energy

The fraction of the discarded wind energy over the available wind energy. Wind Energy can be curtailed due to transmission bottlenecks but also due to operating policy limitations.

Curtailment Limit

The minimum power limit that the RES units can be dispatched to. The RES units operate between the available hourly in-feed and this limit. It can be defined either as a dynamic or a static limit.

Dynamic Curtailment Limit

It is the curtailment limit defined as a fraction of the available RES infeed.

Economic dispatch

The process of deciding what the individual power outputs of the scheduled generating units at each time-point should be.

Merit Order Effect

The effect that the integration of RES-E introduces in an electricity market and alters the order in which power plants are dispatched. In general, it reduces the system operating costs.

MRCGP limit

The Minimum Required Conventional Generation Penetration due to power system stability reasons. It comprises the fraction of the hourly demand that should at least be covered from conventional generation (must-run) units.

SNSP Limit

The System Non-Synchronous Penetration limit. It forms the maximum allowed RES penetration limit defined as a fraction of the hourly consumption. It holds true that $SNSP = 1 - MRCGP$

Static Curtailment Limit

It is the curtailment limit defined as a fraction of RES units nominal power.

Unit commitment

The process of deciding when and which generating units in a power plant to start-up and shut-down.

Contents

Preface - Acknowledgements	ii
Abstract	iii
Abbreviations	iv
Nomenclature	vi
List of Definitions	viii
List of Figures	xii
List of Tables	xv
1 Introduction	1
1.1 Grid challenges arising from renewable energy sources development	1
1.2 Problem definition	2
1.2.1 Transmission Expansion Problem Including Curtailment	2
1.2.2 Flexible and Consistent Data Management	2
1.3 Objective	2
1.4 Research Approach	2
1.5 Scientific Contribution	3
1.6 Outline of the report	3
2 Literature Survey	5
2.1 Optimisation Problems	5
2.2 The Transmission Expansion Problem	6
2.2.1 Definition	6
2.2.2 Classification	7
2.2.3 Methodologies	9
2.3 Previous Work on European Network Expansion	14
2.4 Conclusions	19
3 Methodology	20
3.1 Tools Overview	22
3.1.1 PowerFactory	22
3.1.2 MatPower/Matlab	22
3.2 The Load Flow (LF)	22

3.3	The Optimal Power Flow (OPF)	24
3.3.1	The OPF as a Transmission Expansion Tool	25
3.4	Statistical Transmission Branches Overload Ranking	26
3.4.1	Risk of Overload (RO)	26
3.4.2	Investment Cost Per Per-Cent of Risk of Overload (ICPPCRO)	26
3.5	The Unit Commitment Approach	27
3.6	The TEP methodologies	29
3.6.1	The LUCSIPO methodology	30
3.6.2	The ACO methodology	35
3.7	Representative Hours	42
3.8	Conclusions	43
4	Results	45
4.1	Case Study: The New England System	46
4.2	Sensitivity Analysis	49
4.3	Results	50
4.3.1	K-means	50
4.3.2	LUCSIPO	53
4.3.3	ACO	63
4.3.4	ACO - LUCSIPO comparison	68
4.3.5	MatPower/Matlab - PowerFactory comparison.	69
4.4	Conclusions	72
5	Flexible Computer Aided Transmission Network Modelling for Europe	74
5.1	Tools Overview	75
5.1.1	Database Management System	75
5.1.2	Geographic Information System	75
5.1.3	Network Simulation Tool	76
5.2	Data Overview	76
5.3	The European DC-LF model	81
5.3.1	Interface between Postgres & PowerFactory	81
5.3.2	Network Model Regions	82
5.3.3	High Level Region Components	83
5.3.4	Network Components Modelling	84
5.3.5	Chronological Correlation	93
5.4	Network Reduction	93
5.4.1	Short Literature Review	94
5.4.2	Reducing the European DC-LF model	96
5.5	Conclusions	97

6	Main Findings and Recommendation for Further Research	98
6.1	Conclusions	98
6.1.1	Potential savings in total costs and transmission line upgrades by network- optimised RES curtailment	98
6.1.2	Impact of a Minimum Required Conventional Generation Penetration (MRCGP) limit	99
6.1.3	Impact of the curtailment compensation scheme	99
6.1.4	Methodology Discussion	100
6.1.5	The European DC-LF model	100
6.2	Recommendations for further research	100
	Bibliography	102
A	TEP Simulation Results	112
B	European Network Model Data	130

List of Figures

2.1	Non-Convex and Convex function. Source: [Own Representation]	12
2.2	Piecewise Linearisation of the Non-Linear of Losses and Generating Costs functions . Source: [3]	16
	(a) Line Losses as a square function of the Active Power Flow	16
	(b) Generating Costs as a Second Order Polynomial function of the Active Power	16
2.3	Input data and genetic algorithm implementation for the TEP problem. Source: Own Representation based on [4]	17
2.4	Collective animal behaviour have inspired the creation of Meta-Heuristic algorithms	18
	(a) Ants and their collective behaviour.	18
	(b) A flock of birds exhibiting swarm intelligence.	18
3.1	The non inter-temporal unit commitment approach.	28
3.2	Approach Comparison on utilising Statistical Ranking and the DC-OPF.	29
3.3	LUCSIPO Flow Chart.	30
3.4	Dynamic and Static Curtailment Limit for a 1600 MW WPP.	31
3.5	LUCSIPO Implementation. Inputs, outputs and lower level algorithmic implementation.	34
3.6	Mechanical analogy. Spheres in Bowls representing Pheromone Quants.	37
3.7	ACO implementation for the TEP problem. based on [5]	40
3.8	Clustering 1000 observations into 3 clusters. Source: [6]	43
3.9	From the 8760 Residual Load values, 100 clusters are created that contain a subset of hours representative of the annual network's state. The first hour of the year that belongs to each circle (k means cluster) is used for representing the grid at this point.	44
4.1	The New England Region. Source: [7]	46
4.2	Single Line Diagram of the reduced New England LF Model. In Red the ID of each branch. In Brown the technology of each generating unit. The appendix Table A.27 presents the network model's branch data. in PowerFactory	48
4.3	Residual Load Duration Curves for the two temporal resolution cases.	52
4.4	Weighting the two temporal resolution runs.	52
4.5	HW Scenario. Investment and Operation Costs.	56

4.6	Total Costs and Operating Costs as a function of the curtailed energy.	56
	(a) Curtailed energy.	56
	(b) Congestion induced curtailed energy.	56
4.7	Comparing the conventional power integration limits for the HW case.	59
4.8	HW Scenario. Comparing the Ranking Approach effect on the total system costs.	60
4.9	HW Scenario. Curtailment Limits Comparison	61
4.10	Overload ranking for the HWRO case.	85
4.11	HW Scenario. Branch convergence for the ACO approach.	66
4.12	Total Cost Comparison for the LUCSIPO and the ACO approach.	72
4.13	Calculation Time Comparison for the LUCSIPO and the ACO approach.	72
5.1	High Level Transmission System Network Modelling.	75
5.2	2010 Transmission Network Corridors in Europe. based on [23].	77
5.3	2010 German Power Networks - Conventional Power Plants. based on [23].	77
5.4	Area (Longitude: 12° W to 30° E - Latitude: 35° S to 70° N) covered by HiRLAM. Source: [102]	79
5.5	Renewable shares in The EU - 2020. Source: [115]	80
5.6	Offshore Wind Farms at the North Sea. Source: [106].	81
5.7	Voronoi diagram. Source: [116]	82
5.8	DC-LF Network Model: Germany (Voronoi), surrounding countries (NUTS2) and rest of Europe (NUTS1).	83
5.9	High level components.	84
5.10	Geo processing. Source: [118]	85
5.11	HV terminals modelling. Source: [118]	85
5.12	Transformers modelling.	86
5.13	Gas turbine power plant consisting of three units. Source: [118]	88
5.14	Assigning the plants at the voronoi regions decision making process. Sub refers to Substation.	89
5.15	Assigning the plants.	89
5.16	Internal and External Subsystems of a Power System.	94
5.17	Major Reduced Network Equivalencing Techniques. based on [130] and [129]	95
	(a) Ward	95
	(b) REI	95
	(c) Extended Ward	95
5.18	LMP Illustration. NUTS 2 Regions of similar color have similar nodal prices and thus can be further aggregated into wider regions.	95
5.19	Original network and Reduced network using the PowerFactory Ward Reduction built-in function. In green the equivalent impedances between the 5 boundary buses.	96
5.20	Voronoi Regions and Transmission Corridors for Germany. In Red the simulated above 80% loaded (N-1 overloaded) lines on 01:00:00 1/1/2010.	97

A.1	Total Cost Comparison for the three wind cases.	120
A.2	Total Cost Comparison for the three wind cases.	120
A.3	LUCSIPO. Comparing the conventional power integration limits for the HW case from an operating costs point of view.	121
A.4	LUCSIPO. Comparing the conventional power integration limits for the HW case from a curtailed energy point of view.	121
B.1	Offshore Regions. Source: Representation by LEnGISS.	130
B.2	Typical German winter and spring week. Total [105] and Vertical [18] Load comparison	134
B.3	EU Wind Capacities in 2010	135
B.4	EU Biomass and Biogas Capacities in 2010	135
B.5	EU Solar Capacities in 2010	136
B.6	EU Solar Capacities (GW). Source: [115]	136
B.7	EU Wind Capacities (GW). Source: [115]	137
B.8	EU Hydro Capacities (GW). Source: [115]	137
B.9	EU Biomass Capacities (GW). Source: [115]	138
B.10	DC-LF Network Model: EU NUTS0.	138
B.11	DC-LF Network Model: Germany (NUTS2) and rest of Europe (NUTS1).	141

List of Tables

2.1	Installed Capacities in Germany by 2030. Source: BMU [8])	9
2.2	Short comparison of the different studies	10
3.1	Technical figures for Conventional Power Plants. Source [9]	35
3.2	Probability/ Pheromone Concentration	37
4.1	New England Modified System, Power Plants. Source: [10]	47
4.2	Development of Fuel prices in $\text{€}_{2010} \backslash \text{MWh}_{\text{th}}$. For CO_2 the costs are in $\text{€}_{2010} \backslash \text{t CO}_2$. Source: [9]	47
4.3	Total annual demand for the three areas of the New England system.	47
4.4	Economical figures assumed for the New England Study case. Source: [64,94–97]	49
4.5	Installed Wind Capacity Scenarios	49
4.6	MRCGP Limits assumed	50
4.7	Base case and selected sensitivity scenarios.	51
4.8	Comparison of the round-the-year and representative subset case.	51
4.9	Base Case Scenario Results	53
4.10	Base Case Scenario Upgraded Branches	54
4.11	BC and LW - HW comparison	55
4.12	BC and LL - HL cases comparison	57
4.13	HW and LL - HL comparison	58
4.14	HW and HWRO comparison	59
4.15	Sequence of upgrades for the HW case when the ICPPCRO and RO rankings are applied.	60
4.16	HW and HWS comparison	61
4.17	HWS and IFLH comparison	62
4.18	ACO Inputs	63
4.19	Selected Input Parameter Sensitivity Scenarios.	63
4.20	ACO Tuning Tests, Part I	64
4.21	ACO Tuning Tests, Part II	65
4.22	ACO Tuning Tests, Part III	65
4.23	BC and HW - LW cases comparison for the ACO implementation	66
4.24	BC and LL - HL cases comparison for the ACO implementation	67

4.25	HW and HWLL - HWLL cases comparison for the ACO implementation	68
4.26	BC and MC, RO case comparison for the ACO implementation	69
4.27	ACO and LUCSIPO Results Comparison for the Base Case.	70
4.28	ACO and LUCSIPO Results Comparison for the High Wind Case.	70
4.29	PowerFactory and MatPower Comparison for the HWS case.	71
4.30	PowerFactory and Matpower Dispatch comparison	71
5.1	Spatial Resolution of the provided EuroWind data	78
5.2	Typical Transmission line Impedance values. Source: [125]	87
5.3	Line Ratings	88
5.4	Installed Offshore capacities in Germany. Source: [106,107]	92
A.1	LUCSIPO MC Scenario Results	113
A.2	LUCSIPO HW Scenario Results	113
A.3	LUCSIPO HW Scenario upgraded branches	114
A.4	LUCSIPO HWS Scenario Results	115
A.5	LUCSIPO HWS upgraded branches	115
A.6	LUCSIPO LW Scenario Results	116
A.7	LUCSIPO LW Scenario Upgraded Branches	116
A.8	LUCSIPO LL Scenario Results	117
A.9	LUCSIPO HL Scenario Results	117
A.10	LUCSIPO HWHL Scenario Results	118
A.11	LUCSIPO HWHL Scenario Upgraded Branches	118
A.12	LUCSIPO HWLL Scenario Results	119
A.13	LUCSIPO HWLL Scenario Upgraded branches	119
A.14	LUCSIPO HWRO Scenario Results	122
A.15	LUCSIPO HWRO Scenario Upgraded Branches	122
A.16	ICPPCRO/RO ranking comparison for a 90% curtailment limit. The first ranking corresponds to the original network while the second takes place after one branch has been already reinforced.	123
A.17	ICPPCRO/RO ranking comparison for a 90% curtailment limit. The first ranking corresponds to the original network while the second takes place after one branch has been already reinforced.	123
A.18	LUCSIPO HWRO Scenario Results	124
A.19	LUCSIPO HWRO Scenario Upgraded Branches	125
A.20	ACO and LUCSIPO Results Comparison for the Low Wind Case.	125
A.21	ACO and LUCSIPO Results Comparison for the High Wind High Limit Case.	126
A.22	ACO and LUCSIPO Results Comparison for the High Wind Low Limit Case.	126
A.23	ACO and LUCSIPO Results Comparison for the Low Limit Case.	127
A.24	ACO and LUCSIPO Results Comparison for the High Limit Case.	127
A.25	ACO and LUCSIPO Results Comparison for the Marginal Cost Case.	128
A.26	ACO and LUCSIPO Results Comparison for the RO Case.	128
A.27	NE Test System Branch Information	129

B.2	Installed RES capacities in EUROPE on 2010. Source: [113] [104]	130
B.3	2010 Installed RES Capacities (MW)in Germany per 2 Digit Postal Code . . .	131
B.1	Installed conventional capacities in DE and surrounding countries on 2012. Source: [23].	134
B.4	Basic PowerFactory objects	139
B.5	DE North Sea Offshore Capacities. Source: [106]	140
B.6	DE Baltic Sea Offshore Capacities. Source: [106]	140
B.7	Average Indicative costs for different grid technologies. Source: [97]	141

Chapter 1

Introduction

1.1 Grid challenges arising from renewable energy sources development

During recent years, the share of Renewable Energy Sources (RES) in the European electricity mix has been increasing rapidly. The main drivers so far have been the EU dependency on imported fossil fuels and high carbon emission environmental effects. Meeting the 20-20-20 European Commission target as defined in the Energy Package [2], will require further penetration of inherently fluctuating renewable power.

This strong growth of inherently fluctuating renewable sources results in new, more variable flow patterns that challenge to existing power systems. Network bottlenecks not only hinder the complete RES integration but also jeopardise the system stability. In order to guarantee reliability of supply, the European electricity distribution and transmission infrastructures have to be modernised and extended.

Moreover, it has been claimed that optimally deploying renewable sources in regions of high wind and solar potential throughout Europe could possibly boost the RES penetration level in a cost efficient way. Rather than reaching each Member State's individual targets, high renewable integration can be effectively supported by further reinforcing cross-border transmission corridors [11]. Thus, the European power network has to be further upgraded in order to transfer bulk amounts of renewable power from remotely located regions (e.g. offshore wind farms in the North Sea) to the large industrial and residential load centres.

Nonetheless, in times of high RES in-feed (e.g. on a windy Saturday night), curtailing the excess of generated energy in a certain network region could prove to be more economical than reinforcing another network branch. Nowadays, it is common practice for wind turbines to reduce their power output or even halt their operation -so termed curtailment-, when their power cannot be further integrated in the network. Although there are no consistent figures in a European level, it is indicative to mention that only for China in 2011, more than 10 billion kWh of wind energy were discarded because of insufficient grid capacity [12]. Thus, the PV and Wind industry's interests conflict with the interests of the utility companies. The latter have to provide the high voltage network that cost effectively carries the generated green power to the large load centres. As a result, determining the economic optimum between discarding green power and upgrading the existing network infrastructure is the next step for the transformation of the existing power system in the context of energy transition [13].

1.2 Problem definition

1.2.1 Transmission Expansion Problem Including Curtailment

Many of the existing renewable energy integration studies start with the assumption that grid extensions will be sufficient in order to enable full integration of renewable energy in-feed into the system and curtailment is allowed only as a last measure to maintain system stability. However, a consistent analysis aiming at finding an optimum between grid extension and RES curtailment has not been presented yet. Consequently, the optimal trade-off between network reinforcement and curtailment of renewable (mainly solar and wind) power in future power systems is the main focus of this research project.

1.2.2 Flexible and Consistent Data Management

The ongoing rapid increase of strongly fluctuating RES penetration into the EU energy mix has created further challenges from a network modelling perspective. Extensive techniques are needed in order to safeguard system security but also to determine the required extensions for the power grid of tomorrow. Modern high computational power has enabled the development of pan-European transmission network models in order to tackle the problem. Nevertheless, the models are usually static from a (lower or higher) spatial resolution point of view. A flexible platform that employs geo-processing in order to build and scale the network model components accordingly, has not been presented yet. The platform employs a consistent European-wide dataset that includes geo-referenced generation, demand and network information. This dataset creates the basis for a High Voltage (HV) network model that can perform interregional linearised Load Flow (LF) simulations as an attempt to efficiently provide information for future states of the European power grid.

1.3 Objective

The objective of this thesis is three-fold:

- Prove¹ that there is an economical optimum between RES power curtailment and network reinforcements.
- Develop a consistent methodology for performing sensitivity driven transmission expansion planning in linearised load flow network models. This methodology forms an attempt to identify pseudo-optimal solutions that minimise the total system costs.
- Develop a flexible platform for modelling the Continental Europe HV network where the developed Transmission Expansion Problem (TEP) methodology could be potentially applied.

1.4 Research Approach

The main objective of this thesis is to develop a consistent approach for achieving a near optimal trade-off between RES power curtailment and transmission network upgrades. Due to the non-convex nature of the optimisation problem, an absolute optimum cannot be found. Hence, a new heuristic TEP methodology was developed. This new approach is termed Least Upgrades Curtailment Sensitive Iterative Pseudo Optimisation (LUCSIPO). It is an iterative approach that employs hourly minimum cost DC Optimal Power Flows (OPFs) in order to identify a set of branches that will minimise the sum of curtailment costs, network upgrades

¹If an optimum can be achieved, then we have proved that it exists. It does not involve any mathematical proof.

costs and system operation costs. At every iteration a different RES power curtailment limit is applied in order to force the algorithm towards pseudo-optimal solutions. The LUCSIPO approach includes a statistical branch overload ranking methodology that takes place after every infeasible OPF run.

In order to test the performance of the suggested approach in identifying good quality solutions, a swarm intelligence optimisation technique, the Ant Colony Optimisation (ACO) algorithm as found in [5] is used and extended. The ACO approach imitates the collective behaviour ants exhibit while searching for food. Minimum cost OPFs with the same objective function as the LUCSIPO approach are applied, that pinpoint the optimal set of branches to be reinforced.

The IEEE - New England 39 bus Test System as presented by Ciupuliga et al in [10] was used for testing and comparing the two TEP methodologies. Demand and wind power time series were used in order to yield the hourly system's Residual Load (RL). The latter was used to determine a hundred hour network congestion representative subset via employing the k-means clustering technique. The software tools involved were Mathworks Matlab coupled with the MatPower toolbox extension and DigSILENT PowerFactory.

Finally, a flexible consistent linearised load flow² modelling platform was developed through similar modelling techniques and assumptions as in pan-European grid integration studies [11, 14]. This platform integrates publicly available consumption data with externally supplied RES time series and network information. It is an attempt to effectively model the European HV transmission network in different spatial resolutions for performing transmission expansion planning in European power systems. A PostgreSQL server has been employed for managing the consistent dataset behind the network model.

1.5 Scientific Contribution

This thesis makes four contributions to the scientific discussion on transmission expansion planning in systems with high amounts of RES power:

- The development of an iterative approach - so termed LUCSIPO - for identifying the pseudo-optimum between network expansion and RES curtailment;
- The modification of an existing ACO algorithm in order to account for the trade-off between wind curtailment and reinforcing the grid;
- The introduction of a new transmission branch overload ranking index that couples a round-the-year overload ranking with the investment costs involved in upgrading each branch;
- The identification of a subset of hours, representative of the round-the-year grid congestion. The sampling is based on the network's residual load and employs the k-means clustering methodology [6].

1.6 Outline of the report

This introduction formulated the problem definition, research objective and approach and also highlighted the scientific contributions of the thesis. Chapter 2 presents a literature review

²a linearised load flow is also termed in literature as DC load flow.

on European grid integration studies and introduces the Transmission Expansion Problem. Chapter 3 describes the developed methodology for solving the TEP with the objective of optimising the trade-off between grid upgrades and wind curtailment. Chapter 4 illustrates the IEEE - 39 bus New England system that was used as the network model for applying the two TEP methodologies. It further describes the sensitivity cases used and the related results obtained during the various runs. Chapter 5 lists the principles and basic assumptions employed for constructing the flexible network modelling tool that was developed during the cooperation with the industrial partner, Ecofys Berlin. Finally, Chapter 6 describes the main conclusions and gives recommendations for further actions and development.

Chapter 2

Literature Survey

Power system expansion has been one of the most daunting tasks for the utility companies over the past century. The Power System Expansion Problem (PSEP) involves the upgrade of the Transmission (TEP) and Distribution system (DEP) but also the extension of the system's Generating capacities (GEP). Nevertheless, due to the deregulation of modern power systems, generation and transmission/distribution cannot be co-optimised.

This thesis is dealing exclusively with the Transmission Expansion Problem and the methodologies applied for determining a (pseudo) optimum expansion of national and international power systems. This second chapter presents the conducted literature survey with regard to transmission expansion studies. First, it introduces generic optimisation problems concepts and presents widely applied programming techniques. Next, it focuses on the TEP and its classification. It also describes basic concepts behind the various methodologies that have been suggested for effectively addressing the TEP and it illustrates the most important techniques. Finally, it presents grid integration studies that deal with European-wide transmission expansion planning and attempt to identify (inter)national bottlenecks for effectively accommodating large scale renewable power.

2.1 Optimisation Problems

An optimisation problem formulation aims to identify the optimal solution among all feasible solutions. Every optimization problem includes [32, 33]:

- Optimisation (or decision) variables,
- Constraints which determine if specific decision variables lead to feasible solutions,
- An objective function, which is the function to be minimized (or maximized) depending on the decision variables

Formally written,

$$\min_x C(x) \tag{2.1}$$

subject to

$$g(x) \leq b \tag{2.2}$$

$$h(x) = a \tag{2.3}$$

where,

$$\begin{aligned}x &= \text{vector of decision variables,} \\C(x) &= \text{objective function,} \\h(x) &= \text{equality constraints,} \\g(x) &= \text{inequality constraints.}\end{aligned}$$

The branch of mathematics that specialises in formulating and solving optimisation problems is called *operations research*. The algorithms used while searching for an optimum are called *programming techniques*. Based on the problem formulation, several classes or families of programming techniques have been established.

One of the most widely applied programming techniques is the so called **Linear Programming (LP)**. LP is the procedure of solving a system of linear constraints, the so called *(in)equalities* over a set of unknown decision variables with a linear *objective function* to be minimised (maximised). **Non-Linear Programming (NLP)**, on the other hand, is the programming technique where some of the constraints and/or objective function are not necessarily linear.

The decision variables can, in general, take any real values (subject to constraints). In case there are specific variables which correspond to e.g. indivisible goods, the variables are assumed to be integer values only. In such a situation, the method applied for solving the (non) linear problem is termed **Integer Programming (IP)**. In case the variables are restricted to be binary (0/1), then a **Binary Integer Programming (BIP)** problem is formed. If only some variables are restricted to be integer and the rest are continuous, then the problem is known as **Mixed Integer Programming (MIP)**.

An optimisation problem can be further classified either as a **Convex Problem** or a **Non-Convex Problem**. An optimisation problem is a convex problem in case the objective function and all the constraints are convex functions. In simple terms, a function is convex if and only if any line segment between two points of the function graph lies on or above it. Figure 2.1 depicts a convex ($y = x^2$) and a non-convex function ($y = \sin(x)$). Convex problems can be solved efficiently up to very large size since every local optimum is simultaneously the global optimum. In the situation though, where a number of constraints or the objective function are non-convex, this becomes a non-convex problem. It can have several optima and consequently may need exponential time to determine the global optimum (if any) across all feasible solutions [34].

Dynamic programming (DP) is an optimisation approach that decomposes a multi-dimensional problem into a collection of overlapping sub-problems [35]. The multi-stage structure of the DP optimisation procedure is widely applied for solving complex problems of all previous types.

2.2 The Transmission Expansion Problem

2.2.1 Definition

According to the classification viewed in section 2.1, the transmission expansion problem is a mixed integer, non-linear, non-convex, multi-stage problem which is “extremely difficult if not impossible to solve” [30]. Its main objective is to define when, where and what network reinforcements are needed for the power system in order to satisfy the predicted demand, generation and system security criteria while minimising the operational and/or investment costs [36].

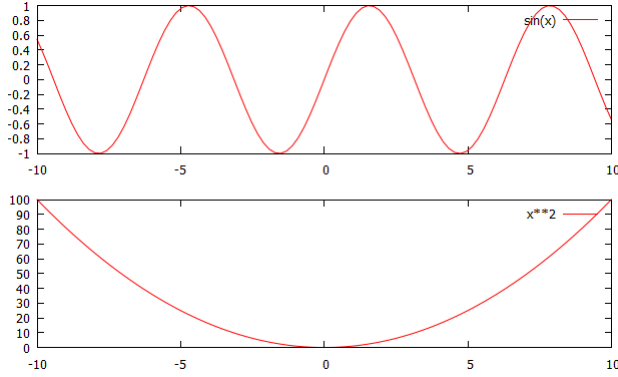


Figure 2.1: *Non-Convex and Convex function. Source: [Own Representation]*

2.2.2 Classification

The planning horizon of the problem or the optimization technique employed are commonly used for classifying the various TEP methodologies. When the planning horizon is in the main focus, the TEP can be:

■ Static

For the Static Case, the TEP optimises for a single planning horizon, i.e. a specific year in the future. It considers forecasts of system conditions that correspond to the year in focus and determines the optimal solution S_k , given by Equation (2.4). Each partial solution S_l can be 0 or integer multiples of 1. It corresponds to the number of circuits each branch is upgraded with.

$$S^k = [S_1^k \quad S_2^k \quad \dots S_l^k \quad \dots S_n^k] \quad (2.4)$$

where,

- S_l = Partial solution of the l^{th} branch,
- n = Number of network branches,
- k = Candidate plan,
- l = Current branch.

In such a situation the decision maker is not interested in when the extra circuits should be installed, but only in finding the optimal network configuration for the projected future year [36] [37].

■ Dynamic

Nevertheless, from its nature, the TEP is a dynamic problem. For the dynamic (multi-stage) problem it is important not only to define where, but also when the grid reinforcements should be implemented. Basically, it involves optimising through several intermediate stages between the base year and the final stage, in order to arrive at the solution matrix S_t^k given by Equation (2.5) [36].

$$S_t^k = \begin{bmatrix} S_{11}^k & S_{12}^k & \cdots & S_{1l}^k & \cdots & S_{1n}^k \\ S_{21}^k & S_{22}^k & \cdots & S_{2l}^k & \cdots & S_{2n}^k \\ \vdots & \vdots & \ddots & \vdots & \vdots & \vdots \\ S_{t1}^k & S_{t2}^k & \cdots & S_{tl}^k & \cdots & S_{tn}^k \\ \vdots & \vdots & \vdots & \vdots & \ddots & \vdots \\ S_{y1}^k & S_{y2}^k & \cdots & S_{yl}^k & \cdots & S_{yn}^k \end{bmatrix} \quad (2.5)$$

where,

- S_{tl} = Partial Solution of the l^{th} branch for the t^{th} stage
- y = Number of stages,
- t = Current stage.

The dynamic formulation of the problem and the time constraints that optimising through several years introduce, render the dynamic problem extremely complex. Due to this time dependent nature, the dynamic formulation of the problem results into prohibitive computational times. Thus, pseudo-dynamic approaches using sequences of static (single-stage) problems are generally employed. There are three fundamental approaches for the pseudo-dynamic TEP [37]:

1. The **forward** approach, which determines sequentially the optimal network starting from the first stage and gradually configures the optimal solution for the final stage [38].
2. The **backward** approach in which, the final stage is assumed to be the step that stresses the power grid the most. Therefore, it determines the final optimum network and proceeds with backward changes till the initial network state is reached [39]. It is believed, that the backward approach generates better solutions than the forward approach [37].
3. The **backward-forward** approach. This method determines the optimum multi-stage expansion plan by comparing backward and forward changes [37,38].

On the other hand, the several TEP methodologies can be classied according to the solving procedure of the optimisation problem. There are three main categories:

- **Mathematical models**

When a mathematical model is employed, an optimum is determined by a calculation procedure that solves a mathematical formulation of the TEP [37].

- **Heuristic approaches**

On the contrary, the heuristic techniques apply, instead of a classical mathematical procedure, a step by step, trial-and-error approach that selects and evaluates expanding scenarios by using empirical rules [37].

- **Meta-heuristic concepts**

Finally, the meta-heuristic approaches simulate the selection of better candidates across the solution search space mostly based on behaviours found in nature. They combine characteristics of both the mathematical and heuristic models [32,37].

2.2.3 Methodologies

Since the TEP exhibits high complexity, several methods and algorithms have been suggested in order to deal effectively with the challenges it involves. Nevertheless, *the TEP is a matter of decision making and not solely of optimisation* [37]. And since *optimisation requires knowledge but decision needs courage* [40], TEP is a complicated problem that requires intensive time and effort in order to achieve acceptable pseudo optimum results.

This section presents the basic methodologies employed for all three TEP families but also a short comparison between them. Then, it shortly describes the most promising algorithms encountered from those families.

Basic Techniques

Among the most popular techniques for solving the TEP is to introduce a largely simplified mathematical model and employ a classical optimisation problem approach. As described earlier, this involves a problem formulation with optimisation variables, an objective function and various constraints. Several methodologies are widespread in literature which apply classical operational research approaches like **Linear Programming** [41,42], **Non-Linear Programming** [43], **Dynamic Programming** [44] or **Mixed Integer (Non-)Linear Programming** [3, 45 - 47]. As an attempt to decrease the complexity of the TEP problem, several decomposition techniques like **Benders** [48, 49] or **Hierarchical** [50] have been suggested. Further combining a decomposition methodology with other approaches is the basis to form a **Branch and Bound** algorithm [51, 52].

On the contrary, several other models are found in the literature that implement a sophisticated trial-and-error concept. Through the guidance of logical rules or sensitivities, they generate and evaluate solutions till the point when no better solution can be achieved. One of the first attempts to implement a so called *Heuristic* approach was made by Fischl in 1972 who introduced the **Adjoin Network** concept. It used a DC load flow to guide the solutions towards a (pseudo) optimum [53]. Other methods include the use of **Sensitivity Analysis**, varying from electric sensitivities [54] to load curtailment sensitivities [55] or **Least Effort Criteria** [56]. Other Heuristic Optimisation models include the use of **Expert Systems** [57] and **Guide Numbers** [58] that build up the new expanded network one branch at a time. **Tree Formats** [59] have been also employed in order to decompose the original problem into sub-problems.

Nevertheless, several algorithms can be found in literature that combine the characteristics of both heuristic and mathematical approaches. They are in general termed as *meta-heuristics* and can be further classified into:

- **Evolutionary algorithms**

Greatly inspired by Charles Darwins theory of evolution, this category includes **Genetic Algorithms (GA)** [4, 60], **Artificial Immune Systems (AIS)** [61], **Differential Evolution (DE)** [62] and **Evolution Strategies (ES)** [63] algorithms. They differ from each other on the basis the evolution mechanisms are applied.

- **Swarm Intelligence algorithms**

The meta-heuristic approaches of this group include mainly the **Ant Colony Optimisation (ACO)** [64] and the **Particle Swarm Optimisation (PSO)** [65,66]. They also include the more recently developed **Shuffled Frog Leap** [67] algorithm and the **Discrete Monkey Algorithm (DMA)** [68]. Inspired by animal behaviour, they are based on the collective behaviour that certain groups exhibit when their individuals interact with each other.

- **Other**

Several other meta-heuristic approaches have been suggested for solving the TEP problem. They range from thermodynamic principles like the **Simulated Annealing (SA)** [69] to memory effects like the **Tabu Search (TS)** [36]. Quite widespread is also the **Greedy Randomised Adaptive Search (GRASP)** [70] as well as the so called **Multi-Objective Memetic Algorithm (MOMA)** [71] approaches. Finally, concepts like **Fuzzy Set (FS)** [72] and **Taguchi's Orthogonal Array (TOA)** [73] have been also employed.

Comparison

The non-convex and high complex nature of the TEP problem formulates a major draw-back for any kind of **mathematical** model. Mathematical approaches can guarantee a local optimum but not necessarily a global optimum. The latter can be reached only for simplified cases. Moreover, a quite complex initialization process is usually required while it can be extremely computationally expensive to acquire an feasible solution.

The **heuristic** approaches cannot guarantee reaching the global optimal solution either. They cannot even indicate how close the solution is to the optimum. Nevertheless, they are less complex and less computationally intensive when identifying a feasible solution. However, the optimality of the solution is questionable.

Finally, the more novel **meta-heuristics**, produce highly approximate solutions to the global optimum but disregard pareto¹ solutions [71]. Moreover, prior knowledge on each objective function is required as well as good quality initial sequences to guide the search towards better solutions. A combination with another approach for the evaluation of the solutions obtained is also necessary. On the other hand, the meta-heuristics are relatively simple algorithms that have shown potential of solving extremely complex problems in a reasonable amount of time. By exploring the problem structurally, they have exhibited results of avoiding premature convergence due to imprisonment in local optima [36].

The information technology boom of the last decade has fundamentally altered the TEP formulation. Accuracy, as well as complexity has increased in the models used. The extensive computational power of modern hardware has resulted into a trend towards novel, non-mathematical algorithms that can produce reliable, pseudo-optimal results.

Modern TEP Optimisation Techniques

A mathematical approach suggested by Barbulescu et al (2011) is to solve the **Mixed Integer Non-Linear** TEP Problem by applying specific gradient methods, so termed Fletcher Reeves, and Lagrange multipliers. The aim is to minimise an auxiliary function Φ that consists of:

- the problem's objective function, i.e. sums of investment and operational costs,
- factors that correspond to the Lagrange multipliers (equality constraints),
- penalty coefficients.

The rather complex MINL auxiliary function Φ , found in [47], considers a complete AC Load Flow model. AC-LF methods are out of the scope of this thesis, and therefore it will not be studied in any further detail.

¹The set of solutions that can improve specific individuals while decreasing the quality of the rest [74].

A widely applied approach to reduce the complexity of the TEP is to gradually transform the non-linear problem into a **Linear Programming** problem. Since the planning takes place at the transmission level, the DC-LF equivalent provides an acceptable approximation. It comprises a largely simplified description of the network model that eliminates certain non-linearities of the AC case. The DC-LF model neglects the system reactive power and considers the bus voltage angles sufficiently small to treat the sinusoidal functions as linear (i.e. $\sin(x) \simeq x$). The result is a lossless network model where all voltages are set at 1 p.u..

Zhang et al. have presented several other approximations in order to eliminate further non linearities and form a MILP Multi-Stage TEP Problem. Figure 2.2 illustrates the piecewise linearisation process followed for the power losses and generating costs. The MILP arrives at an optimum when the social welfare is maximised. This is determined by the minimisation of the discounted operating and investments costs [3].

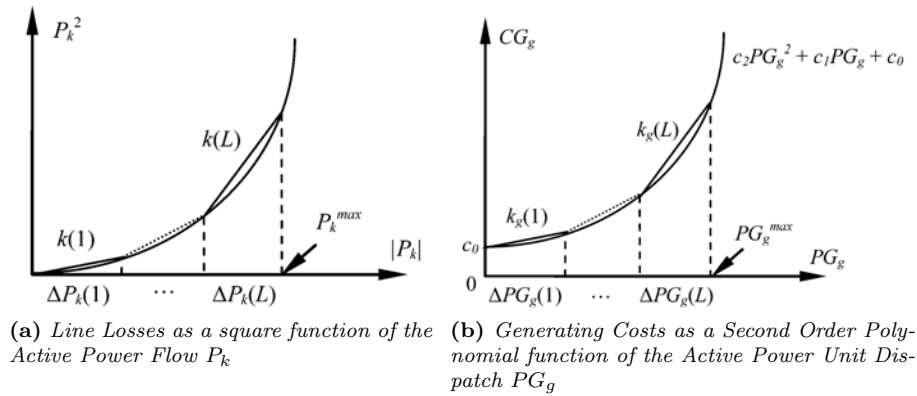


Figure 2.2: Piecewise Linearisation of the Non-Linear of Losses and Generating Costs functions . Source: [3]

The **Bender's Decomposition** applied by Pereira et al [75] was one of the first attempts to decompose the original complex MINL problem into two iteratively solved sub-problems, the *Master* sub-problem and the *Operation* sub-problem. The former is a binary integer problem that identifies the candidate expansion plans and searches for minimum investment costs. The Operation sub-problem is a mixed integer linear problem that investigates the feasibility and the constraint violation of the candidate solutions. In case a violation occurs in the operation sub-problem, a Bender's cut (i.e extra constraint in terms of investment variables) is introduced and added in the operational sub-problem. The process continues until convergence is achieved [48] [75].

Another fundamental technique to solve the MINL TEP is the **Branch and Bound** algorithm, an approach quite similar to the divide and conquer concept. It employs two basic strategies known as relaxation and separation. The former's concept is to *relax* the integrality of the problem constraints and solve the corresponding candidate problem. In case the solution is an integer value, the global optimum has been found. Otherwise, the problem is *separated* into two sub-problems by selecting an integer variable with currently non-integer values, thus creating a list of sub-problems to be solved. After initialising and selecting a candidate solution (sub-problem) there are two main stages that take place. The so called *Fathoming Test* which verifies the existence of more promising solutions and the *Branching Operator* which determines the size of the algorithm search tree [51].

Genetic Algorithms are classified as evolutionary algorithms. They are based on the nature inspired principle of *survival of the fittest*. The approach generates population sequences

through three basic mechanisms: *Selection*, *Crossover* and *Mutation*. After initializing the population (network) and calculating its fitness, the reproduction begins with the *Selection* of two parent solutions (set of branches). The *Crossover* operation follows, which interchanges the values of the parents' chromosomes (branches), and thus randomly assigns their characteristics at their children. Finally, the *Mutation* process takes place in order to alter the offspring characteristics in a more arbitrary way. The fitness of each individual is calculated and evaluated through the value an objective function obtains. This is usually the total system costs a network load flow yields [4, 32]. The flowchart in Figure 2.3 illustrates the procedure that Osthuies et al. implemented while applying a Genetic Algorithm into the TEP problem.

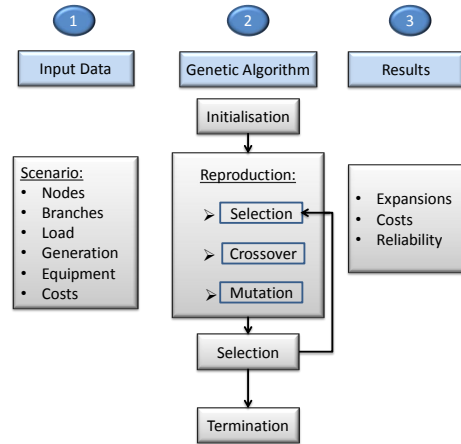


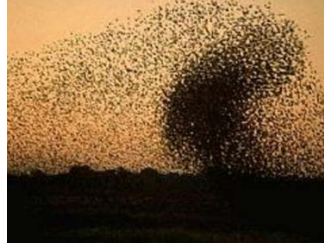
Figure 2.3: *Input data and genetic algorithm implementation for the TEP problem. Source: Own Representation based on [4]*

Artificial Immune Systems is another meta-heuristic approach classified in the family of evolutionary algorithms. The algorithm tries to imitate some principles of the human immune system based on genetic concepts like Reproduction and Hyper-mutation. The CLON-ALG algorithm presented by Honorio et al (2011), employs the *Reproduction* process to clone antibodies (network paths) and create identical copies with the aim of generating multiple solutions. What follows is the stage of *Hyper-mutation*, which changes their characteristics and creates higher affinity antibodies. During the *Selection process*, the best antibodies created by the parent antibodies and their mutated clones are selected. The *Receptor Editing* process picks the best solutions obtained from the previous step. The general objective of the AIS algorithm is first to identify the set of best sequences (and not only the best) and while avoiding local optima imprisonment, to identify the global optimal solution [36, 76].

One of the nature inspired algorithms that has exhibited efficient results when solving the TEP [36] is the methodology termed **Ant Colony Optimisation**. It is classified as a meta-heuristic technique and belongs to the family of the swarm intelligence algorithms. It considers equally fast ants randomly scattered in the vicinity of their nest with the aim of locating a food source. The first ant to find food, travels back to its nest and emits a serum called pheromone in order for the other ants to trail its path. Due to pheromone evaporation though, different ants will follow less or more substantially different paths. After a certain time-point, there will be several paths with different pheromone concentration. The most travelled path exhibits the highest pheromone concentration, and therefore, is supposed to comprise the optimum solution [5]. Among other ACO algorithms, the Ant Colony System (ACS) has exhibited high performance for solving computationally intensive problems [77]. To avoid premature convergence, it couples two separate search paths, the global and the



(a) *Ants and their collective behaviour. Source: [78]*



(b) *A flock of birds exhibiting swarm intelligence. Source: [79]*

Figure 2.4: *Collective animal behaviour have inspired the creation of Meta-Heuristic algorithms*

local path. As presented by Fuchs and Gjengedal [64], it utilises DC-OPFs to validate the feasibility and rank the quality of each solution the ants have produced. The paths the ants follow represent candidate TEP solutions while the path length corresponds to total system costs.

The **Particle Swarm Optimisation** is a swarm intelligence algorithm, inspired by the movement of flocks of birds/fish. Although every individual moves independently, they share some kind of collective behaviour. Each individual considers the best position it has achieved but also the best position that the entire group has achieved. Thus, it determines its route by adjusting its velocity and position in order to follow the best positions obtained so far. When applied in transmission expansion studies, the PSO algorithm evaluates the position (objective function) the individuals (set of branches) have reached through upgrading the solution branches and performing a DC-OPF [32, 66].

Tabu Search is a widely found Meta-Heuristic technique that uses a memory list of the already visited states of the problem. This way it excludes premature convergence from already explored local optima. Its basic stage is the so termed *Neighbourhood* stage which creates a set of sequences that occur from basic modifications termed of the original network *Movements*. As an input to the next iteration, the *Intensification* procedure selects the best neighbours that belong to the Neighbourhood. Further, a *Tabu list* is created. It forms a set of rules that prevents the algorithm from visiting already identified solutions. The *Aspiration Criterion* contains exceptions to the Tabu list rules. Finally, a *Diversification* process is used to guide the approach into visiting regions not yet explored and, therefore avoid local optima [36, 80].

Simulated Annealing is a stochastic² optimisation process that was initially developed in the 1980s. It is based on the thermodynamic principle of annealing³, and the assumption that under thermal equilibrium, the cooling process results in the formation of crystals. In case of a minimum energy a state, a perfect crystal can form [32]. The SA algorithm, when applied to the TEP, consists mainly of two processes: the Transition Mechanism and the Cooling Scheme. The Transition mechanism is responsible for the generation of candidate solution sequences by randomly adding, swapping and removing network branches. The Cooling Scheme is defined by parameters like initial and final temperature as well as temperature change rate and number of transitions. It is the process that tries to achieve thermal equilibrium, i.e. minimum state of energy, and determines the efficiency of the algorithm. Romero et al. [69] claim that although it is extremely computationally expensive, the SA algorithm converges asymptotically to the

²In probability theory stochastic process is a set of random variables that represents the evolution of a system over time [81].

³The process of cooling a molten material.

global optimum. This as well as the fact that the quality of the solution is independent of initial configuration [69], render the suggested approach a major candidate for efficiently solving the TEP.

The **Greedy Randomised Adaptive Search** is another powerful meta-heuristic iterative sampling technique. It has exhibited quite satisfying results when applied to large combinatory problems [70]. It is composed of two main processes, a *Construction Phase* and a *Local Search*. During the *Construction Phase*, an iterative algorithm builds a feasible solution by randomly adding one variable, from a candidate list, at a time. An adaptive greedy function evaluates the benefit of each addition. In the work presented by Binato et al (2001), load shedding was used as the performance index in order to assess the solutions obtained from the construction phase. Through the *Local Search* operation, the algorithm attempts to locate a better solution in the vicinity of the feasible solution obtained from the previous step. To do so, it replaces some candidates till no better solution is found [70].

Finally, another two animal behaviour inspired algorithms have been suggested for solving the TEP. They both involve three stages in order to select the candidate network branches. The first one is known as the **Discrete Monkey Algorithm** [68] which was inspired by the tree climbing process that monkeys exhibit and involves a *Climb* process, a *Watch-Jump* process and a *Somersault* stage. The second algorithm is termed **Shuffled Frog Leap** [67] and is a population algorithm, in which a virtual frog population is leaping in a swamp towards a food source. They are both using a DC-LF guided process to select their candidate solution.

2.3 Previous Work on European Network Expansion

As a premise for further study, a short literature review on previous work by different sources is presented. A brief presentation of key results from every work is followed by a high-level description of the methodology used.

Zhou and Bialek (May 2005) [15] developed one of the first consistent models of a pan-European power grid. It uses a DC-PTDF approach and covers the former UCTE area except the Balkans. Publicly available data and a demand distribution, proportional to the population of each district, resulted in a network model consisting of 1254 buses and 378 generators. It has been used as a reference for several other studies.

The **TradeWind Project** (2009) [16] was the first study to look into large scale cross-border wind power transmission and market design at a European level. It also explored to what extent large-scale wind power integration challenges could be addressed by reinforcing interconnections between Member States. In order to catch the high wind penetration targets set by the EU, the Tradewind study identifies new directions for both the design and operation of the power system and the electricity markets. The two fundamental issues tackled are the weak interconnection between control zones and the inflexible nature of the European power markets. Furthermore, administrative barriers, lack of public acceptance, insufficient economic incentives for TSOs, and the lack of a joint European approach by the key stakeholders are highlighted as the major issues for the cumbersome integration of renewable power in Europe. The Tradewind consortium investigates the impacts of increasing wind power on cross-border power flows and suggests that the expected future wind power capacity will result into severe congestion on the French borders, between GB and Ireland and on some of the Swedish, German and Greek borders. Moreover, it identifies the necessity of upgrading 42 onshore interconnectors (and their corresponding time schedule) that will introduce yearly operational cost saving benefits of up to 1.5 billion €. Furthermore, the Tradewind study emphasizes on an EU-wide wind power contribution on system adequacy while arguing in favor of a power market design with intra-day rescheduling of crossborder exchange that will

not only lead to higher market efficiency but also further reduce operational costs of another billion €.

The grid model used consists of three synchronous areas of Europe consisting of the UCTE system (continental Europe), the Nordel system and Great Britain - Ireland. It is a highly reduced network model consisting of 132 nodes, 384 generators, 67 loads, 213 transmission lines and 6 HVDC links. The simulation tool is based on simplified grid representation, aggregated demand/capacities and marginal costs of each generator type, based on publicly available data from the UCTE, EURELECTRIC [17] and IEA. It treats the different synchronous zones in a separate way due to non-availability of network data for all regions and results into creating dedicated equivalents for each region. The UCTE synchronous area is represented by aggregated zonal PTDF matrices, similar to the approach followed by Bialek [15]. DC representations of individual lines are used for the OPF models for Nordel and UK, and these are converted to PTDFs when running simulations of the full European model, since PTDFs allow for faster calculations compared to solving the optimal power flow for each hour of the year.

The **European Wind Integration Study** (EWIS - 2010) [14] comprises the first time that a round-the-year market analysis was coupled with network representations for a set of snapshots that correspond to challenging conditions from a technical perspective. It mainly deals with the efficient integration of wind power while ensuring the quality and reliability of power supply, and achieving cost efficient network upgrades. The time horizon is the period until 2015. EWIS has focused on the immediate network related challenges by analysing detailed representations of the existing electricity markets. It suggests that high wind scenarios in continental Europe result into loop flows that differentiate substantially between the market transactions and the actual network power flows in Germany, Poland Czech Republic and the Benelux countries. EWIS also examined the systems dynamic behaviour by studying the effects of transient and frequency response in the event of voltage dips or sudden generation loss. It concludes that improvements in stability performance are required for reducing the frequency stability barrier that limits large-scale wind integration. Furthermore, EWIS pinpoints the need for TSO coordination and improved wind forecasting techniques. Finally, EWIS demonstrates that network development costs are likely to be modest compared to the benefits brought by wind generation although the capital costs included are substantial in absolute terms. Thus, national regulatory frameworks and international cost sharing mechanisms should be given suitable priority by the establishment of a new European regulatory authority and the development of European grid code requirements.

EWIS uses two models for its simulations: The EWIS market model and the EWIS network model. The market model produces a representation of market operation throughout a year, ignoring all network limitations except cross-border limits which are implemented as Net Transfer Capacities (NTC). To derive the actual network flows for the year-round market exchanges, an approximation of the full load flow calculation based on PTDFs is used. The PTDF market model hourly runs allow for determining congestion on cross-border lines. Nevertheless, they do not provide neither detailed national transmission corridor overload information nor indications of real flows which could potentially exceed physical thermal capacities. The latter results in the so called loop flow difference. Due to these reasons, specific point in time scheduled cross-border exchanges, calculated by the market model are fed into the EWIS network model which allows detailed DC load flow simulations. The network model used is the well-known UCTE model, consisting of approximately 10,000 nodes, 13,500 lines, 1,800 transformers and 3000 generators. The national development plans (till 2015) have also been integrated.

The Energynautics - EWI report **Roadmap 2050 - a closer look** (Oct 2011) [11] compared a moderate extension of the European grid according to the ENTSO-E Ten Year Net-

work Development Plan (TYNDP) [108] with an optimal grid extension scenario in which no restriction in line upgrading was present. The optimal scenario assumes renewable plant development in areas with favourable conditions rather than country-specific and subsequently transmission of power throughout Europe. It results in 228,000 km of extra lines needed (together with 1217 GW of new grid capacity) by 2050 whereas in the moderate scenario less than half of them are required. Due to the more favourable sites though, less investment costs in RES are involved while more conventional (consisting mainly of natural gas) plants are needed for back up. The total costs involved are slightly lower, on the order of 3.6%, in the case of the optimal scenario.

An electricity market model and a 224 node grid model using the DC Optimal Power Flow (OPF) was built for this purpose. The models run in 5-year steps while one typical day per season, divided into 6 slices, is simulated for each year. 47 onshore and 42 offshore wind sites throughout Europe were considered, together with 38 photovoltaic technology regions and 6 concentrated solar power (CSP) regions (including North Africa). A general increase on the electricity demand (0.3-1.95% pa, country-specific) was assumed along with a small increment in the fuel prices. Finally, storage facilities including pumped hydro and compressed air (CAES) were taken into account. As far as transmission technologies are considered, HVDC networks were incorporated into offshore connections only.

The Energynautics - Greenpeace **European Grid Study 2030/2050** (Jan 2011) [16] developed a grid extension scenario with the aim of optimizing the European sustainable sources use and achieving a 90% RES penetration. The need for transferring solar power from southern countries and Wind power from Northern regions to the large load centres in central Europe is identified. By optimally extending the grid and applying a prioritization scheme, the study managed to produce results that would reduce the curtailed renewable power from 12% (in Greenpeaces Energy [R]evolution scenario 2009) down to 4%. Should the curtailed power be reduced to 1% though, further grid upgrades between offshore parks at the North Sea and the mainland would be required. It is finally concluded that, with an assumption of electricity price 10 ct/kWh, the costs of curtailment are significantly higher than upgrading the grid.

The 224-node Energynautics grid model is used here as well. Also, a simplified approach for accounting of (N-1)- contingencies, by limiting the line load at 80 % of its nominal power, is considered. Hourly feasibility check OPF simulations are executed, and an extreme event (winter 1997) is used for testing the Security of Supply (SoS). The load is assumed to be the same as today since high-efficient devices will compensate for the higher future load. The optimal upgrade level is defined as the point where upgrade costs equal losses due to curtailed power. The penetration of renewable power is assumed to be 68% in 2030 and a rather high 97% for 2050. Demand data are obtained from ETSOVISTA database [18]. Weather data are provided from satel-light [19] and NOAA [20]. Finally, sensitivity scenarios of three levels of demand reduction using DSM have also been investigated that. Despite allowing more efficient penetration of local renewable power, they do not significantly relieve grid congestion.

The **KEMA-RAP-ECF** Power perspectives 2030 (Nov 2011) [21] attempts to determine the route to a carbon free economy by 2050, focusing on the shorter term of 2030. It clearly points out the trend in power systems of shifting from operational expenditure to capital investments. To reduce high curtailment levels, CO₂ emissions and additional back up conventional power, the urgent need to upgrade the grid infrastructure, employ DSM measures and facilitate inter-country cooperation, is identified. By 2030 a grid investment cost of about 115 billion and a total upgrade of 75 TwKm, or an additional capacity of around 173 GW (relatively low compared to the 450 GW predicted from [11] for the same period), needs to be realised, as the only way to keep the system reliable and secure. DSM and efficiency measures are considered of fundamental importance for the realization of the EU CO₂ emission reduction targets. Finally, it highlights the problems and delays in the installation of network upgrades that may occur due to lack of public acceptance.

that may occur due to lack of public acceptance.

The methodology includes an electricity market and grid model coupled with a generation model, used to simulate the 2030 EU power system without any interaction between them. The grid model consists of 48 nodes, 76 inter-country lines, a few intra-country lines (for example 6 lines in Germany) and 12 connections with non-EU countries. Together with the base case (which is in terms with the Roadmap 2050) a wide selection of sensitivity scenarios is investigated, that range from higher or lower RES penetration to less onshore transmission. The demand assumptions are for the base case 1.8% growth p.a. while for the high efficiency scenario 0.3%. Load data are taken from the PRIMES report “EU energy trends to 2030” [22], Installed RES capacities from country-specific NREAPs while non-RES data are from PowerVision [23]. Hourly simulations are implemented for a time series of 8760 hours, accounting for both short-term and long-term reserve.

The **EWI working paper, Michaela Fürsch et al** (Feb 2012) [24] attempts to pinpoint, where (European Wide) and at what level it is more cost effective to upgrade the grid rather than discarding/storing the surplus of generated renewable energy. It also gives a detailed insight on how the market and the load flow grid model of [11] were constructed. A dynamic linear dispatch and investment model produces the trade flows that are constrained due to line restrictions occurring from the grid model. Their interaction produces as an outcome the transmission lines that are more economically attractive for upgrades.

Jarass and Obermair (Aug 2010) [13] have developed a consistent method of monetizing the benefit from renewable power generation in order to apply the general economics problem of finding the optimum in a cost benefit analysis. They conclude that the optimum is the point where the marginal cost of upgrading the grid, equals the marginal benefit of discarding more renewable power, or in other words where the further revenue for the RES suppliers exceeds the additional costs for grid upgrades. They also claim that installing transmission infrastructure of only 70% of the installed wind power suffices for transmitting almost 99% of the wind energy yield.

Schaber et al. (Dec 2011) [25] using the so called URBS-EU model (consisting of 83 zones) and applying a parametric cost optimization approach, found that more than 80% of RES penetration can be achieved in a European level. For this, RES capacity exceeding the peak load tenfold is required. A long-term 8-year (2000-2007) time series, both for the demand and the RES production is employed. The load is assumed to be equal to today’s profiles. They conclude that less back up facilities are needed and less curtailment is expected if a grid extension of almost 25% of the expenditure needed for RES investment is realised.

Schaber et al. (Feb 2012) [26], while giving a more detailed explanation of their model in [25], investigate the effects that a potential grid extension may induce to the 2020 electricity markets. Both cables (in order to account for public acceptance issues) and overhead lines are considered. It is concluded that a pan-European grid significantly reduces the overall costs and spurs the RES integration.

Ciupuliga et al. (2012) [27] implemented hourly unit commitment-economic dispatch simulations using a PowrSym3 model for several sensitivity scenarios of a 2030 Europe. The study concluded that the RES curtailment/integration is mainly affected by the flexibility of the power system.

More focused in the German sector is the **Dena Grid study II** (Nov. 2010) [28]. It focuses on the German power electricity grid, attempting to determine the correct strategy for achieving 39% RES penetration by 2020. Several transmission technologies, including Overhead Line Management (OLM), high Temperature conductors (TAL) and HVDC are investigated, as well as scenarios with partial and full storage of non-transmissible power. It

is concluded that the most cost effective solution is the upgrade of the conventional HVAC transmission lines. It is also highlighted that the storage facilities involve extreme expenditure without significantly alleviating the system congestion. The Dena II report concludes that 3600 km of new HVAC 380 kV transmission lines, accounting for grid investment costs of about 1 billion e p.a., are adequate to transfer the renewable power generated throughout Germany by 2020. This includes 37 GW of onshore wind parks and 14 GW of offshore, 6 GW of biomass units and 18 GW of PV installations. DSM, improved forecast method, balancing power from renewables and the close cooperation of the several German TSOs are suggestions that may prove beneficial in the future.

A temporal resolution of 15 minutes and a spatial resolution consisting of 1186 high and extra-high voltage onshore grid nodes together with 46 offshore wind farms was applied. Wind data produced from a weather model combined with measured data from IWES [29] were used to produce the time series. The same temporal resolution is used for the PV technologies, but the spatial resolution is 14 km x 14 km. The solar radiation data are obtained from SODA [30]. In order to account for the (N-1)- contingencies, the line capacity was limited to 70% of its actual rating. The nuclear phase out policy of the federal German government as defined in the atomic energy act (2002) has been taken into account (the 2002 consensus agreed on the phase out of nuclear power plants, resulting in a capacity of only 6.7 GW by 2020). as well as a total load reduction of 8% due to the assumption of high-efficiency devices by 2020. A linear Power Transfer Distribution Factor (DC-PTDF) approach is used to model the grid and identify the non-transmissible inter-regional power, while an iterative process of opposing balance calculations is implemented for determining the necessary grid upgrades.

The “**BMU Leitstudie**” 2010 (Dec 2010) [8] focuses on the future German energy supply system, trying to implement an in-depth analysis of its future structure. Pre - Fukushima scenarios on the prolongation of nuclear plants in Germany as well as the penetration of H₂ and electric vehicles in everyday life are investigated. Up to 2030, a load decrease of 13% compared to 2008 levels is assumed while later on, it is considered stable. A renewable share of 40% by 2020 and a 65% by 2030 is assumed while the German transportation sector is considered to be composed of electric vehicles by up to 66% by 2050. DSM, flexibility of conventional plants, higher energy efficiency (electricity, heat, transport) and grid extension are identified as the most significant measures for a carbon free future.

The study uses a simplified unit commitment and dispatch model that does not consider inter-temporal restrictions (e.g. ramping rates). The assumed installed capacities of renewable technologies by 2030, are presented in Table 2.1.

Technology	Capacity 2010(GW)	Capacity 2030(GW)
Wind Onshore	27.1	43.7
Wind Offshore	0.09	23.5
PV	17.3	61
Biomass	6.34	10
Hydro	4.4	4.92
Geothermal	0.01	1
CSP (Import)	0	3.6

Table 2.1: *Installed Capacities in Germany by 2030. Source: BMU [8]*

In August 2011 (post-Fukushima), the German government decided a fast exit from nuclear power and at the same time a rapid increase of the RES share in the German power system. §12a-d of the German Energiewirtschaftsgesetz (energy act) regulates the commission of the German **Netzentwicklungsplan** (network development plan)(Aug 2012) [31]. The

NEP represents future situations of the German power infrastructure in order to achieve a full exit from nuclear power until 2022 and an 80% renewable penetration until 2050. It contains recommendations for grid upgrades and the construction of new transmission corridors in the German transmission network. It is provided by a collaboration between the German grid agency (DNA) and the four TSOs that are in charge of the modernisation and extension of the German HV grids: 50Hertz, Amprion, TenneT and TransnetBW.

A short comparison on the various grid models that the different sources used is presented in Table 2.2.

Source	Grid Model Nodes	Method	Temporal Resolution
Energynautics-EWI [11]	224	DC OPF	4 d
DENA II [28]	1232	DC PTDF	8760 h
KEMA-ECF [21]	48		8760 h
Energynautics-Greenpeace [16]	224	DC OPF	8760 h
TradeWind [16]	132	PTDF	8760 h
EWIS [14]	33/10000	PTDF / DC-LF	8760 h / n/a
Schaber et al. [25, 26]	83	Transp Problem	6 w
Zhou and Bialek [15]	1254	DC - PTDF	n/a

Table 2.2: *Short comparison of the different studies*

2.4 Conclusions

This chapter introduced the concept of the mixed integer non-linear (MINL) transmission expansion problem. It also presented the classification of the various TEP methodologies and described the most established concepts for achieving pseudo-optimal TEP solutions. Finally, it presented the main European-wide grid integration studies and the key results each of them achieved.

Chapter 3

Methodology

This chapter attempts to provide detailed explanation on the methodology used during this thesis. Its main objective is to present a technique that can effectively provide a pseudo-optimum Solution for expanding the current grid while optimising between upgrades and RES curtailment. Two different methods were developed. A robust performing, state-of-the-art meta-heuristic approach, named Ant Colony Optimisation (ACO) and a new heuristic approach, called Least Upgrade Curtailment Sensitive Iterative Optimisation (LUCSIPO). The LUCSIPO was developed both in Matlab/MatPower and in DIGSILENT PowerFactory as an attempt to compare performances and solver results between a free academic software, MatPower and a commercial software like PowerFactory. The part of comparing the solution quality provided by the new heuristic approach LUCSIPO with the solution generated by a modern optimisation technique like the ACO was implemented only in MatPower.

This 3rd chapter illustrates the methodology applied for performing transmission system expansion planning. First, after briefly presenting the software tools employed, it shortly describes the backbone of the TEP methodologies, the DC-Optimal Power Flow. It also presents two concepts for executing statistical line overload ranking, strongly linked to the two developed TEP approaches. Furthermore, it provides a detailed description of the two methodologies and gives an overview of the developed scripts. Finally, it illustrates the concept applied for gaining a 100 h representative sample of a 8760 h set for the demand and RES time series.

Prior to proceeding, it is essential to define a few terms:

- *Unit Commitment*

It is the process of deciding when and which generating units in a power plant should start-up or shut-down.

- *Merit order effect*

The effect that the integration of RES introduces in an electricity market. It alters the order in which power plants are dispatched. In general it reduces the system operating costs.

- *Curtailed wind energy*

It is the fraction of the discarded wind energy over the available wind energy. Wind energy can be curtailed due to transmission bottlenecks but also due to operating policy limitations.

- *Curtailment limit*

It is the minimum Power limit that the RES units can be dispatched to. The RES units

operate between the available hourly in-feed and this limit. It can be defined either as a dynamic or a static limit. Specifically:

- *Static Curtailment Limit*

It is defined as a fraction of RES units nominal power.

- *Dynamic Curtailment Limit*

It is defined as a fraction of the available RES in-feed.

- *MRCGP limit*

It is the Minimum Required Conventional Generation Penetration limit as defined by the policy maker. It comprises the fraction of the hourly demand that should at least be covered from conventional generation, connected via synchronous generators to the network (must run units), due to power system stability reasons.

- *SNSP limit*

It is the System Non-Synchronous Penetration limit. It forms the maximum allowed RES penetration limit defined as a fraction of the hourly consumption. It holds true that $SNSP = 1 - MRCGP$.

3.1 Tools Overview

3.1.1 PowerFactory

DIgSILENT stands for “*D*igital *S*imuLation and *E*lectrical *N*eTwork calculation program” [82]. DIgSILENT PowerFactory is an advanced interactive software package for electrical power system analysis with the perspective of handling the main objectives of planning and operation optimisation [83]. PowerFactory is supposed to lead the way towards integration of data management, modelling capabilities and overall functionality. Its capabilities and flexibility are further extended due to the provided database interface (DGS), the C++ like programming language (DPL) and a smooth integration with GIS system standards [82, 84, 85].

3.1.2 MatPower/Matlab

Matlab is the well known MATrix LABoratory Software created by Mathworks [86]. A necessary open-source add-on for power system studies is MATPOWER, created by Zimmerman in Cornell University [87]. MATPOWER is a package of MATLAB M-files for solving (optimal) power flow problems. It is intended as a simulation platform for researchers that is relatively easy to use and modify. It is designed to give the best performance possible while keeping the code simple to understand and adjust.

3.2 The Load Flow (LF)

The Power Flow or Load Flow study is a problem widely found in power engineering. It involves solving for the set of voltages and flows in a network of predefined generation, demand and topology. The AC load flow is a non-linear problem that requires an iterative approach without the guarantee of converging to a solution. It consists of a set of equations which, by using numerical analysis methods (e.g. Newton-Raphson or Gauss-Seidel), arrive at a solution for the vector of complex bus voltages (i.e. magnitudes and voltages). This solution must satisfy the system’s equilibrium as expressed in Equations (3.1) for active and reactive power injections at all $i = 1 \dots N$ buses [87-89].

$$\begin{aligned} P_i &= \sum_{j=1}^N |V_i||V_j|(G_{ij} \cos(\theta_{ij}) + B_{ij} \sin(\theta_{ij})) \\ Q_i &= \sum_{j=1}^N |V_i||V_j|(G_{ij} \sin(\theta_{ij}) - B_{ij} \cos(\theta_{ij})) \end{aligned} \tag{3.1}$$

where,

P_i = Net (Generation - Demand) active power injected at bus i

Q_i = Net reactive power injected at bus i ,

N = Number of network buses,

$|V_i|$ = Voltage magnitude of the i^{th} bus,

- $|V_j|$ = Voltage magnitude of the j^{th} bus,
- G_{ij} = Real part of the nodal admittance matrix' ij^{th} element,
- B_{ij} = Imaginary part of the nodal admittance matrix' ij^{th} element,
- θ_{ij} = Voltage angle difference between the i^{th} and j^{th} bus

However, transmission expansion studies involve time-consuming simulations of large network models which integrate future system state scenarios under specific uncertainty. Accuracy is not of high importance and as a result the complete load flow equations introduce unnecessary computation time. Instead, a linearised form of the load flow problem is widely employed. The so termed “*DC*” *Load Flow*, is a technique used to estimate power flows via a simplified, linear formulation of the load flow equations. It employs the following assumptions:

- All bus voltage magnitudes are equal to 1 p.u.
- Branches are considered lossless with negligible resistances and charging capacitances
- Voltage angle differences (in radians) are small enough that

$$\begin{aligned}\sin(\theta_1 - \theta_2) &= \theta_1 - \theta_2 \\ \cos(\theta_1 - \theta_2) &= 1\end{aligned}\tag{3.2}$$

According to the simplified DC model, the power flows in a branch is given by

$$P_{ij} = x_{ij}^{-1} \theta_{ij}\tag{3.3}$$

where x_{ij} corresponds to reactance of the branch. Consequently, the real power injection at a bus i is given by

$$P_i = \sum_{j=1}^K x_{ij}^{-1} \theta_{ij} = \left(\sum_{j=1}^K x_{ij}^{-1} \right) \theta_i + \sum_{j=1}^K (-x_{ij}^{-1} \theta_j)\tag{3.4}$$

where K is the number of lines connected to the i^{th} bus. For N system buses and since the reference bus is not participating in the solution ($\theta_{ref} = 0$), Eq. (3.4) can be put into a $(N - 1) \times (N - 1)$ matrix form as defined in Eq. (3.5):

$$\mathbf{P} = \mathbf{B}' \boldsymbol{\Theta}\tag{3.5}$$

where,

\mathbf{P} = vector of the net injections P_i ,

$\boldsymbol{\Theta}$ = vector of the bus angles θ_i ,

\mathbf{B}' = nodal reactance matrix with the following elements:

$$\begin{aligned}B'_{ij} &= -x_{ij}^{-1} \\ B'_{ii} &= \sum_{j=1}^K x_{ij}^{-1}\end{aligned}$$

Eq. (3.5) reveals that the DC-LF study is a linear problem that yields a non-iterative solution for $\boldsymbol{\Theta}$ by inverting the nodal reactance matrix \mathbf{B}' [87, 89]. The DC-LF results are by default less precise than an AC-LF analysis, but when applied to transmission expansion studies it forms a fast calculation tool of acceptable accuracy. Thus, this thesis is dealing exclusively with DC load flow problem formulations.

3.3 The Optimal Power Flow (OPF)

The *Optimal Power Flow* is a method that employs linear or non-linear programming techniques for determining a power flow solution that minimises or maximises an objective function. An apparent criterion is the cost minimisation of operating the power system considering different outputs of the various generating technologies. A basic objective behind operational costs minimisation is to perform economic dispatch while accounting for the constraints imposed by the network infrastructure, for example line thermal limits. However, a social welfare maximisation or a losses minimisation focus can also be applied. Finally, another widely applied objective function is to minimise the deviation from a given operating point. In practice, to minimise the unit re-dispatch from the outcome of a market model, due to bottlenecks in the grid.

A standard optimisation problem formulation involves an objective function (Eq. (3.6)) to be minimised subject to equality (Eq. (3.7)) and inequality (Eq. (3.8) and (3.9)) constraints. x represents the state variable while u is the independent (decision) variable of the problem.

$$\min_u f(x, u) \quad (3.6)$$

$$g(x, u) = 0 \quad (3.7)$$

$$h(x, u) \leq 0 \quad (3.8)$$

$$\begin{aligned} x_{min} &\leq x \leq x_{max} \\ u_{min} &\leq u \leq u_{max} \end{aligned} \quad (3.9)$$

It was mentioned earlier that the AC load flow problem is not in the scope of thesis. Neither is the AC OPF, so a detailed explanation is omitted. Applying the DC modelling assumptions and thus eliminating voltage magnitudes and reactive powers, allows for the real power vector \mathbf{P}_g to be modelled as linear functions of the voltage angle vector Θ . Therefore, the vectors of Eq. (3.10) comprise the optimisation variables x and u .

$$\begin{aligned} x &= \Theta \\ u &= \mathbf{P}_g \end{aligned} \quad (3.10)$$

The set of Equations (3.6) - (3.10) then takes the below described form. Eq. (3.11) comprises the objective (cost) function to be minimised while Eq. (3.12) represents the DC power equilibrium as the equality constraint g_P and a function of Θ and \mathbf{P}_g . Eq. (3.13) presents the h_f inequality constraint that corresponds to the branch flow limits as linear functions of the voltage angles Θ . Finally, the optimisation variables (in)equality constraints are represented by Eq. (3.14) and (3.15). They relate to the units technical limitations and the (set to zero) reference bus angle [87].

$$\min_{\mathbf{P}_g} \sum_{i=1}^{N_g} f_p^i(p_g^i) \quad (3.11)$$

$$g_P(\Theta, \mathbf{P}_g) = \mathbf{B}'\Theta + \mathbf{P}_d - \mathbf{P}_g = 0 \quad (3.12)$$

$$h_f(\Theta) = \mathbf{B}'\Theta + \mathbf{F}_{max}, i = 1 \dots n_b \quad (3.13)$$

$$p_g^{i,min} \leq p_g^i \leq p_g^{i,max}, \quad i = 1 \dots n_g \quad (3.14)$$

$$\theta_{ref} = 0 \quad (3.15)$$

where,

- f_p^i = Convex cost function of the i^{th} generator,
- p_g^i = Active power dispatch of the i^{th} generator,
- n_b = Number of branches,
- n_g = Number of generators,
- \mathbf{P}_d = Demand vector,
- \mathbf{P}_g = Active power injections vector
- \mathbf{F}_{max} = Vector of maximum power flow branch limits,
- $p_g^{i,min}$ = Minimum allowed loading of the i^{th} generator,
- $p_g^{i,max}$ = Maximum allowed loading of the i^{th} generator,

3.3.1 The OPF as a Transmission Expansion Tool

In practice, the OPF methodology is widely applied for operating the grid by the TSOs but it has also been extensively used in literature as a transmission expansion planning tool. It comprises a valuable approach that has been employed both for large scale European wind integration studies [11, 16] but also for developing state-of-the-art meta-heuristic TEP algorithms [4, 36, 64, 65]. In the first case, it is mainly utilised as a feasibility check algorithm while in the latter case, as a means to assess the quality of TEP solutions obtained by swarm intelligence or evolutionary optimisation algorithms.

This thesis employs operating cost minimisation OPF hourly runs as the main tool for performing transmission expansion planning. The DC-OPF problem as described by Eq. 3.11 - 3.15 functions as the means to evaluate potential solutions and drive the TEP algorithms towards a pseudo-optimum. Both in PowerFactory and MatPower, the built-in robust DC-OPF function is used in order to solve the optimal power flow problem and assess the outcomes of the TEP candidate solutions. The solutions involve changes in the topology, and thus a new \mathbf{B}' and \mathbf{F}_{max} is generated prior to the OPF runs.

However, a limitation of the standard OPF is that the operating constraints are satisfied only under normal operating conditions, i.e. when all network elements are in service. This does not guarantee the system security. Thus, a Security Constrained OPF should be developed that will consider N-1 contingencies (i.e. perform OPF checks for all N network element when 1 other element has failed). Developing or performing a SCOPF though, is out of interest for this thesis. The network security issue has been dealt with limiting the maximum line loading to 80 % of its nominal capacity. An empirical value used by several european grid extension studies [11, 16, 28].

3.4 Statistical Transmission Branches Overload Ranking

Overload sensitivity and criticality [90] are two important aspects that need to be taken care of, should the system's bottlenecks be determined. Therefore, special attention should be paid while identifying the highly overloaded network elements. A critical short time overload exhibits high potential for causing a cascading failure to the whole network. Nevertheless, an insignificant overload for a longer period of time may or may not be critical for the network operation.

Overload alleviation measures such as FLM or TAL are not in the scope of the thesis. Neither creating new transmission corridors is. The objective is to identify bottlenecks of the existing grid and upgrade the overloaded branches with standard HVAC technology.

Therefore, a statistical line overload ranking is of high importance in order to detect critical overloads. A statistical ranking is a core part of the LUCSIPO algorithm. It is also of great significance to the ACO approach since it provides a starting point for the iterations and thus guides the algorithm towards better solutions. Two different ranking approaches, described below, have been developed. Irrespective of the selected concept, in order to measure the line overload hourly, cost minimisation, branch limits unconstrained OPFs take place.

3.4.1 Risk of Overload (RO)

Ciupulinga et al [10] have suggested a severity ranking of the grid bottlenecks based on the total overloaded hours per year and the loading average for these hours. Omitting the N-1 contingency part, the formula suggested is the following:

$$RO_i = (m_i - lim)h \quad (3.16)$$

$$i = 1 \dots N_b$$

where RO_i = Risk of overload for the i^{th} branch

m_i = Mean overload for the i^{th} branch,

lim = The max loading limit in % of the i^{th} branch,

h = Simualted hours,

N_b = Number of branches

3.4.2 Investment Cost Per Per Cent of Risk of Overload (ICPPCRO)

The risk of overload severity index is an important index in order to effectively identify grid bottlenecks. Nevertheless, it does not include information about the cost effectiveness of each suggested upgrade. As a consequence, a new assessment index is introduced; the Investment Cost Per Per Cent of Risk of Overload (ICPPCRO). Eq. (3.17) presents the index formula.

$$Inv_i = \frac{C}{RO_i} \quad (3.17)$$

$$i = 1 \dots N_b$$

where RO_i = Risk of overload for the i^{th} branch

C = Investment Cost for upgrading the i^{th} branch,

Inv_i = Investment cost Index ICPPCRO for the i^{th} branch

Thus, dividing the branch investment cost with the RO index from [10], yields a new index that ranks the branches according to the most cost effective alleviation of 1% risk of overload. This way, an assessment of the economical effectiveness of each suggested upgrade is provided.

3.5 The unit commitment approach

Prior to proceeding with the developed TEP approaches, it is important to highlight the Unit Commitment (UC) concept. Determining the status of the system units, is a time intensive optimisation problem, due to the extremely large number of possible combinations [91]. As a result, performing UC runs is computationally expensive even for small sizes systems¹. Furthermore, an inter-temporal UC approach is out of the scope of this thesis. In order to perform realistic OPF simulations though, the following two alternative methods are suggested:

- **Minimum limit unconstrained DC-OPF**

In this case, the units are allowed to be dispatched below their technical limitations. The OPF will determine which units are not economical to use and therefore, they will be simply dispatched (close) to zero.

- **Non inter-temporal UC expanded DC-OPF**

The non inter-temporal UC approach does not consider ramp rates and start-up, shut-down costs. It performs a minimum limit unconstrained DC-OPF, as described above, and the units dispatched below their minimum loading limits are taken off-line. Then, a fully constrained OPF is applied for the units remaining online.

The second option provides more realistic results since the generating units operate within their actual range. Thus, it is employed for both the LUCSIPO and ACO approaches. It is also applied for the branch limit unconstrained DC-OPFs, as described in the statistical overload ranking section.

This non inter-temporal UC approach has been further extended in order to account for a Minimum Required Conventional Generation Penetration (MRCGP) limit. The MRCGP constraint, and its complementary, the System Non-Synchronous Penetration (SNSP) limit, are key parameters in determining the hourly economic dispatch and unit commitment profile of the system. The flowchart presented in Figure 3.1 portrays the steps that the proposed simplified UC approach follows.

In a situation where the conventional power output is higher than the MRCGP limit, then the status of the units with zero output is set as out of order. On the contrary, the units with non-zero production but still less than their technical limitations are considered to be on-line. This action is necessary because in case all the other generators are dispatched close to their maximum, decommitting the units would result in a infeasible OPF.

However, in case the RES generation is higher than the SNSP limit (i.e the conventional output is lower than the MRCGP threshold), non-congestion induced curtailment needs to

¹Moreover, PowerFactory does not yet support a UC function.

take place. This extra demand for dumping renewable power is linked to system stability and security reasons and it is irrelevant to transmission network bottlenecks. Nonetheless, it directly affects which units stay on-line and which not. This non-congestion induced curtailment is termed from now on *Operational Policy Curtailment*.

Thus, in case the system requires further non-congestion related RES curtailment, the sum of the maximum power output of all RES units is scaled to match the SNSP limit and all the zero output generators are set off-line. Then, the units, sorted by operating costs, are getting committed again until the sum of the first OPF run outputs and the min limits of the “just” committed units becomes higher than the MRCGP.

Nevertheless, if the system’s conditions do not allow for further RES generation reduction, for instance due to the curtailment limits set by the LUCSIPO methodology, storage measures are the only alternative solution. Since, the present thesis does not deal with energy storage applications, a different approach is needed. The maximum RES output is scaled again to the SNSP value while the min RES limits are set this time to zero. Furthermore, in order to avoid infeasibility, the conventional units are committed until the sum of their maximum ratings exceeds the MRCGP limit. After observing the graph in Figure 3.1, one can argue against

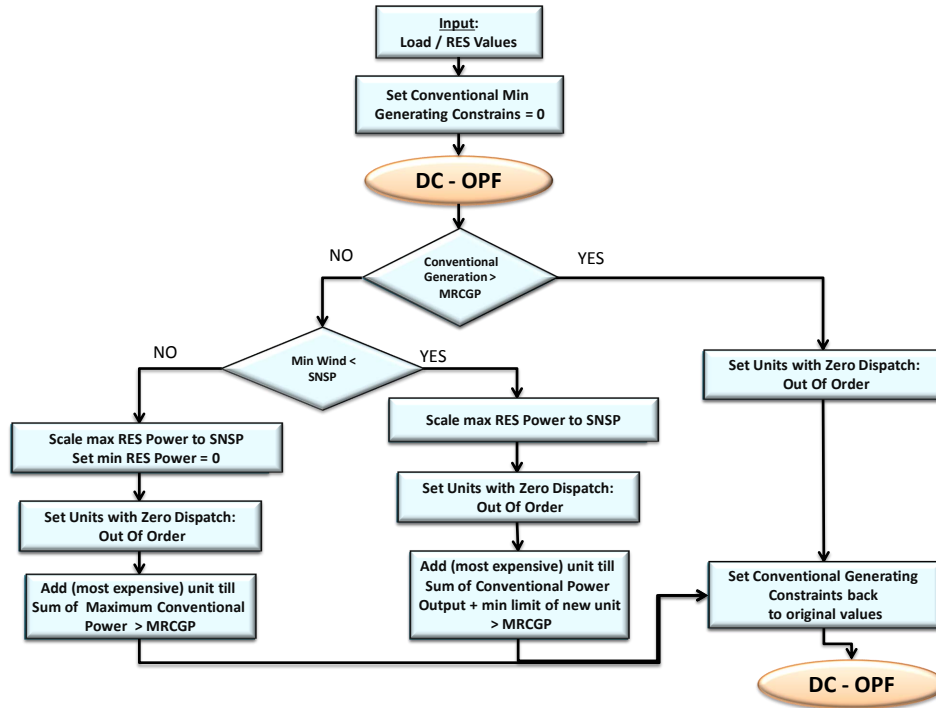


Figure 3.1: *The non inter-temporal unit commitment approach.*

using the most expensive unit in order to cover the extra SNSP limit demand for conventional power. Although it defies the unit merit order, it is used due to the flexibility of small gas turbines in contrast to larger lignite/coal units that would have been committed otherwise. Committing a small gas turbine produces a feasible solution, very close to the first DC-OPF outputs. Activating a larger unit though, substantially affects the flows in the whole system even when dispatched at its minimum production limit.

3.6 The TEP methodologies

It has been already highlighted that the main objective of this thesis is to perform transmission expansion planning while optimising the trade-off between grid extension and wind curtailment. A new heuristic approach, called Least Upgrade Curtailment Sensitive Optimisation (LUCSIPO) has been designed and developed in order to tackle the problem. For validating its results a state-of-the-art methodology, the Ant Colony Optimisation approach was also implemented. Both approaches utilise the above described DC-OPF concepts for arriving at a feasible solution.

Figure 3.2 depicts a high level comparison between the two approaches on a basis of utilising the methodology concepts. It also highlights the important role the DC-OPF plays. One can notice that the two approaches employ the hourly min cost DC-OPFs from a different perspective. The ACO focuses on the solution quality, meaning that applies OPFs and ranks the cost-quality of the solution obtained. On the contrary, the LUCSIPO employs the OPF as a means of verifying the feasibility of the solutions. If a feasible solution for a specific network configuration cannot be achieved, the topology changes and the algorithm starts over. Furthermore, the ACO applies the statistical ranking (either the RO or the ICPRO) only once, in the algorithm initialisation, while in LUCSIPO there is a constant interaction between the core algorithm and the ranking function.

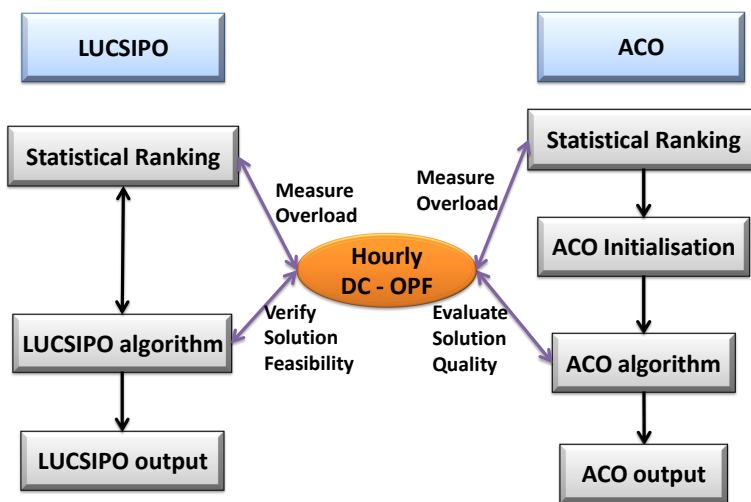


Figure 3.2: Approach comparison between the LUCSIPO and ACO methods on utilising the Statistical Ranking and the DC-OPF. The user can select between the two unit commitment approaches illustrated in section 3.5. Equation (3.11) is the objective function of the employed DC-OPF

As discussed in chapter 2, dynamic transmission expansion planning involves optimising through several intermediate stages between the base year and the final stage. Performing dynamic TEP is out of the scope of this thesis, so it exclusively deals with the static TEP and optimises for a single future year.

First, a detailed insight of the suggested LUCSIPO concept is presented together with a short illustration of the developed Matlab scripts. Then, a detailed description of the ACO approach and its development follows.

3.6.1 The LUCSIPO methodology

In order to identify the bottlenecks of the grid and upgrade the most appropriate existing transmission corridors, a new heuristic approach that applies an hourly minimum operational cost DC-OPF was designed. The flow chart of Figure 3.3 portrays the procedure followed in order to produce a feasible solution that will employ the least possible line upgrades towards an optimum solution. Different curtailment limits P_{cur} are applied with the aim of optimising the trade-off between grid extension and RES dumping.

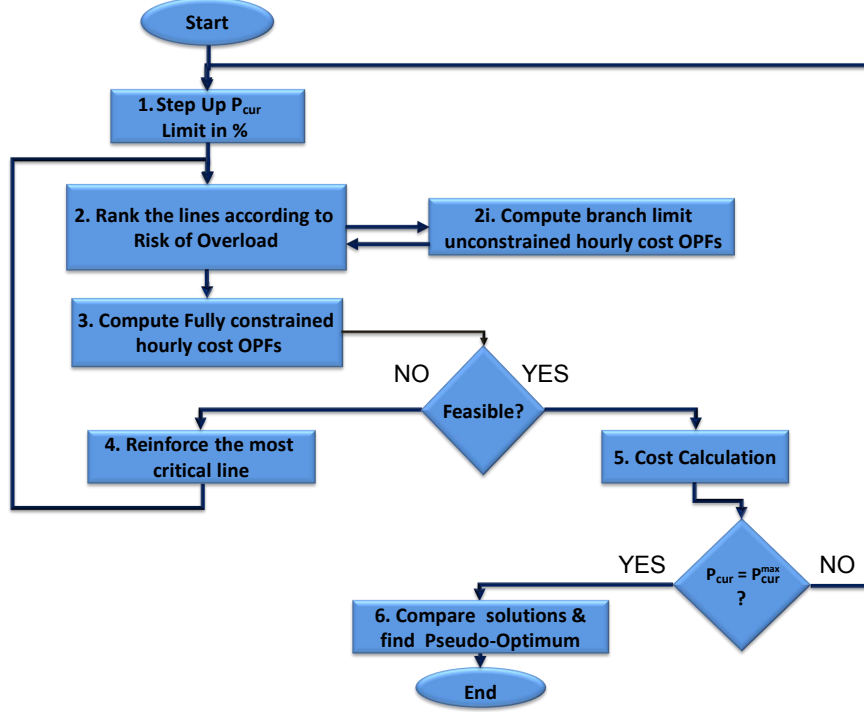


Figure 3.3: LUCSIPO Flow Chart.

Varying the RES curtailment limit and thus the minimum allowed RES production, is the novel part of the LUCSIPO approach². It is a key part that will actually guide the algorithm towards a minimal overall cost solution, since it considers the trade-off between grid reinforcements and curtailment of RES power. The same problem is solved for different curtailment limits P_{cur} which can be either static or dynamic. The dynamic curtailment limit is defined as a fraction of the available in-feed power while the static curtailment limit is a fraction of the installed wind power. Figure 3.4 further illustrates the distinction between those two limits. For a 1600 MW Wind Power Plant (WPP), the static 60% limit (in green) is flat at 960 MW. It allows wind power to be curtailed down to this limit, only for the hours of the year that the in-feed (in red) is higher than this value. On the contrary, the dynamic limit (in blue) follows the wind In-feed and allows curtailment for every hour of the year.

In case no curtailment is allowed (i.e. $P_{cur} = 100\%$), the algorithm produces a solution that upgrades all required transmission lines for fully accommodating the available wind in-feed. On the contrary, when there is no curtailment limitation (i.e. $P_{cur} = 0\%$) and in case

²The several limits P_{cur} that the LUCSIPO approach is run against is the reason for the *Curtailment Sensitive* term in the methodology name.

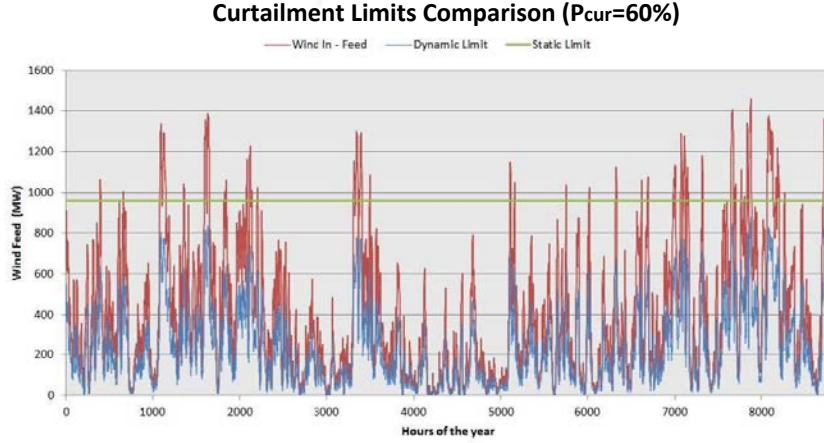


Figure 3.4: *Dynamic and Static Curtailment Limit for a 1600 MW WPP.*

of congestion, the excess of wind power will be simply dispatched down in order to mitigate network constraints. Both situations represent the worst case scenarios and result in high costs due to the high investment and/or curtailment costs involved in each of them respectively. The goal is to obtain a feasible solution that will optimise the sum of investment, operational and curtailment (congestion or non-congestion induced) costs. In other words, to investigate the existence of a feasible result that will provide the least network upgrades for the least RES curtailment. The most cost-effective solution is selected as the pseudo-optimum solution. The total system costs C_t in Eq. (3.18), comprise the LUCSIPO's objective function to be minimised as a function of P_{cur} . It is not minimised through exact mathematical methods, but through the heuristic search the LUCSIPO performs.

$$\min f(P_{cur}) = C_t = C_{op} + C_{curt} + C_{op,pol} + C_{inv,pa} \quad (3.18)$$

Algorithm Description

Step 1 comprises the key function that shifts the algorithm towards a minimal cost solution. It involves the manipulation of the minimum allowed generation limit for the RES units of the network model. It consists of the outer loop that forces the same problem to be solved for the different P_{cur} . This for loop ranges from a user defined starting curtailment percentage up to 100% in user defined steps.

Step 2 identifies the critical network elements. It consists of a round-the-year statistical overload ranking of the network branches, where either the RO or the ICPPCRO approach can be employed. *Step 2i* updates the load and RES time-series and measures the overload of all branch elements. Hourly cost OPFs that represent a user-defined number of the system's state snapshots, are applied without considering the branch capacity constraint. Thus, *Step 2i*, performs network unconstrained OPFs that do not consider congestion and produces results similar to a market simulation of the system. Next, according to the specified approach (RO/ICPPCRO), the actual ranking takes place in *Step 2*. It eventually pinpoints the most critical branch which is then fed as an input to *Step 4* as the branch to be upgraded next.

Step 3 verifies the feasibility of the provided solution, by also performing hourly OPFs but with activated branch constraints. The hourly network constrained DC-OPFs, account for

the cost of congestion and result in a different dispatch than *Step 2i*. *Step 3* calculates the operational costs and the curtailed energy that correspond to the network conditions for this specific hour. In case the marginal cost curtailment cost approach has been selected, *Step 3* also calculates the curtailment costs that correspond to this snapshot.

For both *Step 2* and *Step 3*, the non inter-temporal constrained UC approach presented earlier is optionally available. The user decides if no unit commitment (i.e. the conventional units minimum power limits are set to zero) or the non inter-temporal approach is used. For the latter case, the user defined conventional power MRCGP limit is also taken into account for the final OPF dispatch.

The constrained OPFs, nevertheless, can produce infeasible solutions. In such a case, an iterative approach is introduced in order to tackle the problem. The algorithm does not allow for infeasibility for any of the snapshots, so in case of a non-feasible solution, the round-the-year OPF run gets interrupted.

Step 4 follows, which upgrades the most overloaded branch so far, as identified in *Step 2*. A branch gets upgraded by adding one identical circuit to the transmission corridor. The process then starts over from *Step 2* and the algorithm proceeds with a new statistical ranking (*Step 2*). The algorithm iterates until it arrives at a network configuration that will produce a feasible OPF solution for each and every snapshot.

One could potentially argue against the necessity of performing a statistical ranking after every upgrade since the initial ranking could suffice. In such a case, after each infeasible OPF, *Step 4* would upgrade the branch that corresponds to its initial ranking position. However, after each upgrade, the algorithm performs a new ranking in order to identify the most critical branch only. The reason for this is the effect that a certain branch upgrade will have on the rest of the network. The initial ranking would become invalid.

At the point where the algorithm has obtained a set of upgrades that enables the system to provide an OPF solution for all hours under study, the approach moves forward with *Step 5*. *Step 5* calculates the costs related to operating the system, curtailing RES energy and upgrading the selected branches, for the solution each curtailment limit P_{cur} produced. The costs specifically involve:

- **Operating costs (C_{op})**

Assuming linear dependence, the hourly operational costs are defined as the production of all units multiplied by their incremental operating costs. Thus, the annual cost for operating the system is the sum of the round-the-year (or any other time unit) hourly operational costs. Based on the assumed cost figures, Eq. (3.19) describes the generation cost function f_p^i of Eq. (3.11) per technology class:

$$f_p^i = \frac{f_p}{\eta} + \frac{c_p e_f}{\eta}$$

$$\begin{aligned} \text{where: } f_p &= \text{fuel price,} \\ \eta &= \text{efficiency,} \\ c_p &= \text{CO}_2 \text{ price,} \\ e_f &= \text{CO}_2 \text{ emission factor} \end{aligned} \tag{3.19}$$

- **Curtailment costs (C_{curt})**

The costs related to RES Power curtailment. As also discussed in detail in chapter 5, there are two methods for calculating the curtailment costs: either the Feed-In-Tariff

(FIT) approach or the Marginal Cost (MC) approach. In the former case the curtailment costs are the curtailed energy multiplied by the FIT. For the MC approach, the calculation involves the summation of the hourly curtailed energy times the respective hourly marginal system costs.

- **Operational policy costs** ($C_{op,pol}$)

The costs related to non-congestion induced curtailment. They are monetised the same way as the curtailment costs but they form a separate category due to the System Non-Synchronous Penetration (SNSP) limit.

- **Investment costs** ($C_{inv,pa}$)

The investment costs involved when upgrading existing transmission corridors. The annuity formula of Eq. (3.20) is employed in order to project the investment costs as a series of payments to be periodically paid over the lifetime of the project.

$$PV = \frac{1 - \frac{1}{(1+r)^N}}{r}$$

$$C_{inv,pa} = A = \frac{C}{PV} \tag{3.20}$$

where,

- A = Annuity,
- C = Investment costs,
- PV = Present Value factor,
- r = Interest rate,
- n = Investment's lifetime

The first three factors in Eq. (3.18) are calculated via summing the hourly costs produced during a successful Step 3. For the investment costs, summing the lengths of the identified branches, yields a total length which multiplied by the line cost per km, generates the total capital cost. Applying the annuity formula to the total capital costs, yields the annual investment costs. Finally, Step 5 performs a summation of the four cost factors, providing the value that the final solution and the algorithm output depend on.

Next, the P_{cur} value gets updated and the iterations restart from *Step 1*. When all curtailment limits defined in *Step 1* have produced a solution, the algorithm proceeds with *Step 6*. The limits as well as the step resolution are user defined. As a default, the algorithm uses a 10% step that ranges from 0 to 100 % of the RES in-feed (dynamic limit). Finally, in *Step 6* a cost comparison of the generated solutions yields the most cost-effective solution as the pseudo-optimal point between extending the grid and RES Energy Curtailment.

Implementation

The LUCSIPO approach was developed both in MatPower and PowerFactory. In each case, the unique characteristics of the scripting languages were taken into account. The C-like Matlab language allowed for great flexibility and performance while the, object oriented C++ like, DigSILENT Programming Language(DPL) is a scripting language with certain limitations. Separate handling is in request for several actions during the algorithmic implementation, such as the OPF runs, the updating of the time series, the auxiliary vectors or the network model itself. Both in PowerFactory and MatPower the built-in OPF functions are utilised.

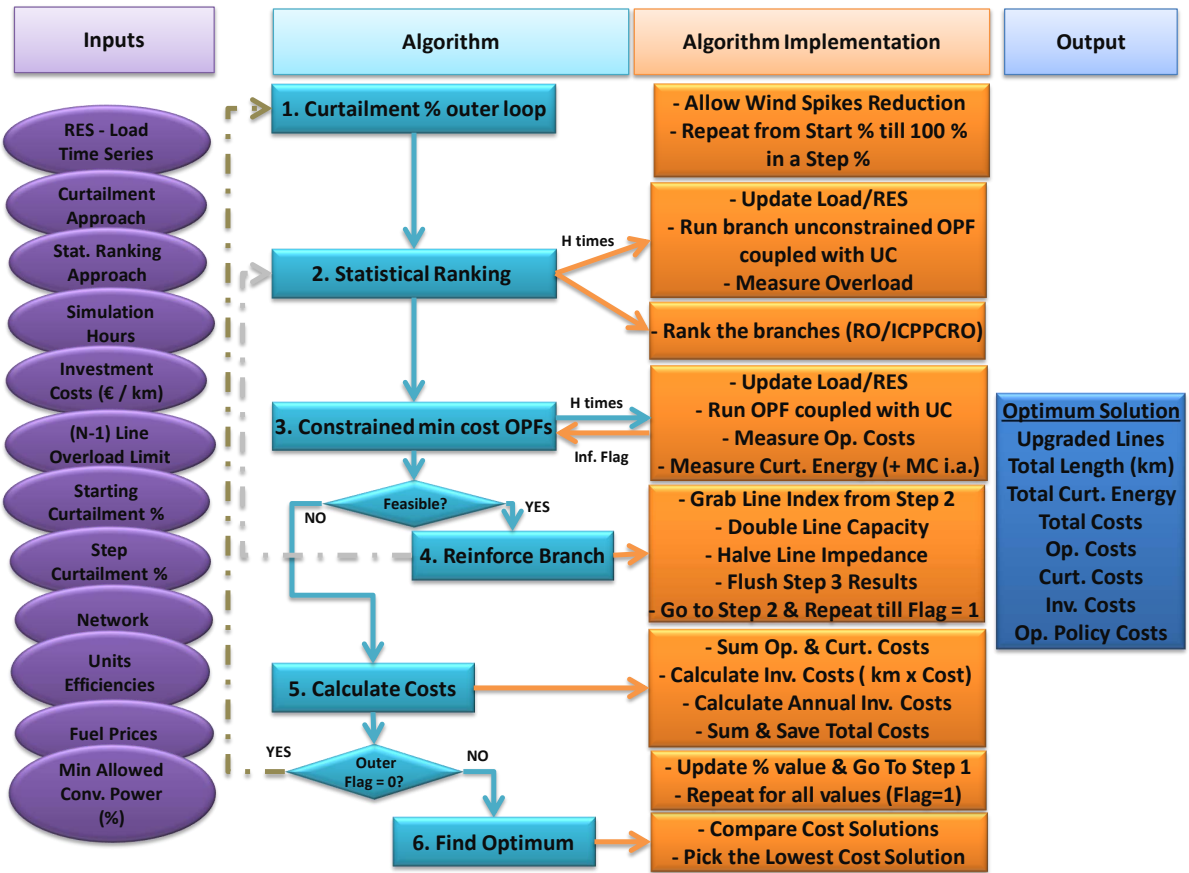


Figure 3.5: LUCSIPO Implementation. Inputs, outputs and lower level algorithmic implementation.

Figure 3.5 portrays the LUCSIPO approach inputs, outputs and lower level algorithmic implementation, common for both MatPower and PowerFactory scripts. On the left side (in purple), the inputs of the approach are presented. These include the several parameters, such as time-series, cost parameters and general limits. The central part depicts the several functions (in orange) that have been developed in order to successfully transform the algorithm as presented earlier (in light blue), into a functional TEP modelling approach. Finally, the right side (in dark blue) consists of the output of the approach. For the pseudo-optimum solution identified, this includes the:

- ID³ of the upgraded branches,
- Number of circuits added at each branch,
- Total length in km of the upgraded branches,
- Total costs involved,
- Total curtailed energy as a percentage of the total RES available in-feed, given by the

³Every branch comes with a unique identifier. The algorithm output contains the identifiers of the selected branches

following formula:

$$CE(\%) = \frac{\sum_{i=1}^h C_i}{\sum_{i=1}^h W_i} \quad (3.21)$$

where,

- CE = Curtailed energy in %,
- h = Number of hours,
- C_i = Curtailed energy per hour in MWh,
- W_i = Available wind energy per hour in MWh.

It is highlighted at this point that a different approach had to be used in order to account for the power limits of the various generating units. The maximum power limits for conventional plants are set as their nominal installed capacity while the minimum limits are determined by the technology class as presented in Table 3.1. For the RES units though, the case is different. The maximum power limits are set as the time series in-feed at any instant. *Step 1* defines the minimum RES unit generating limit, i.e. the fraction of the curtailment allowed.

	Emission Factors	Efficiency	Min Load
Lignite	0.406	0.43	0.3
Coal	0.305	0.46	0.3
Uranium	0	0.33	0.45
Oil	0.266	0.4062	0.2
Gas	0.201	0.4	0.2
RES	0	1	0
CCGT	0.201	0.6	0.4

Table 3.1: *Technical figures for Conventional Power Plants. Source [9]*

3.6.2 The ACO methodology

A nature inspired meta-heuristic, the *Ant Colony Optimisation* (ACO) was selected as the suitable TEP methodology to assess the results of the developed LUCSIPO approach. The reasons for this choice are multiple.

- The ACO has shown “*the best performance for solving different computationally intensive problems*” [77]. Moreover, “*Among several algorithms in literature, it has achieved better results to solve the TEP*” [36] and as a result it is believed to be an algorithm of high potential for efficiently solving the TEP.
- The ACO has exhibited signs of avoiding premature convergence. Furthermore it is highly flexible [5] and does not require initial good-quality sequences for moving towards better set of solutions.
- The potential of using parallel computing for the ACO implementation [5] and thus fundamentally decreasing computational time.

The above mentioned arguments render the ACO one of the most suitable algorithms for dealing with the daunting transmission expansion problem and justify its selection for evaluating the LUCSIPO technique.

Algorithm Description

As described in chapter 2, the ant colony optimisation is a swarm intelligence approach that mimics the collective behaviour of an ant population while searching for food. The pheromone that an ant deposits on its trace back to its nest, forms the backbone of the ACO algorithms, since the most visited path (i.e. the path that has accumulated highest pheromone concentration) comprises the pseudo-optimal solution.

An ACO methodology exhibits a solution quality dependent memory of candidates for solving the optimization problem under study. The memory is created via a probability array, that marks paths with pheromone, corresponding to a combination of pheromone deposit and evaporation rules. The amount of pheromone defines the probability value and is directly related to the quality of the solutions in the solution set.

The fundamental (and most challenging) feature of an ant colony optimisation approach is to effectively update every path's pheromone concentration after each iteration. Several ACO algorithms have been proposed in the literature; their main variation lies in the approach used for the pheromone update. The most important variants include the:

- **Ant System (AS)**. It comprises the first ACO algorithm proposed in 1992. The pheromone update, after each iteration, takes place by all the ants that have found a solution.
- **MAX - MIN Ant System (MMAS)**. It is an improved AS ACO algorithm, at which only the best ant (i.e. the best solution) updates the pheromone paths.
- **Ant Colony System (ACS)**. The novel feature is the introduction of a second, local pheromone update rule, that by decreasing the pheromone amount of a selected solution, forces the other ants to choose different trails [77].

The Ant Colony System *has exhibited the best performance for solving different computationally intensive combinatorial problems* [5, 77], and thus was chosen against the other two variations for this thesis.

The ACS, as presented by Fuchs in [5] consists of two pheromone update rules. The **Local** rule, which diversifies the candidate solutions and the **Global** rule that actually updates the most effective solutions.

The **Local** pheromone update rule reduces the pheromone concentration at the local trajectories, but not at the global paths, and as a result diversifies the solution search space. After an ant has completed a mission m , i.e. has travelled through the local solution space and formed a solution S_k , the pheromone reduction rule of (3.22) is applied only to the partial solution s_i that was chosen by that ant.

$$\tau_{i,m+1} = \begin{cases} \phi^{local} \tau_{i,m} & \text{if } s_i \in S_k \\ \tau_{i,m} & \text{otherwise} \end{cases} \quad (3.22)$$

where $\tau_{i,m}$ = Pheromone amount at s_i for the m^{th} mission

$\tau_{i,m+1}$ = Pheromone amount at s_i for the $(m+1)^{\text{th}}$ mission

ϕ^{local} = Local pheromone reduction rate

The example in Figure 3.6 comprises an attempt to visualise the relation between the pheromone concentration and the probability value of each partial solution s_i . The orange

spheres correspond to pheromone quants⁴ τ_{quant} , each bowl represents one partial solution s_i and each set of bowls with different number of spheres than the previous row, represents a solution set S_k .

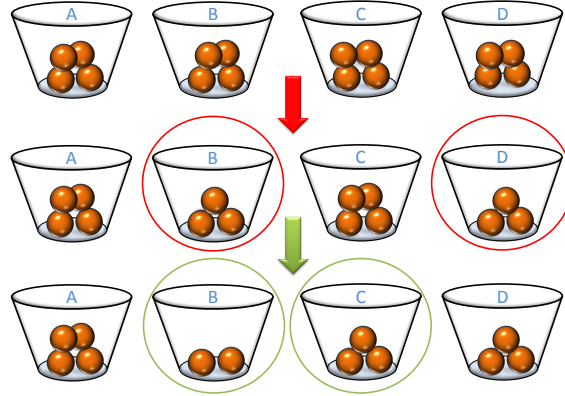


Figure 3.6: Mechanical analogy. Spheres in Bowls representing Pheromone Quants.

Figure 3.6 illustrates the local pheromone update rule, according to which, if a branch is selected by the algorithm, then its pheromone is reduced with the goal of exploring new, unvisited paths. Assuming that the system comprises of 4 paths, the local reduction rate corresponds to one orange sphere and every solution S_k consists of two bowls s_i , yields Table 3.2.

Since no initialisation has taken place, all bowls contain 4 spheres, i.e the same probability to be selected for the first mission. During the first ACO run, Bowls B and D form the solution S_k and consequently 1 sphere is removed from their contents. The sum of the balls is now 14 and the probabilities are updated accordingly. During the next run, Bowls B and C are selected and a sphere is taken out of the bowls. This yields the last row of Table 3.2 which determines Bowl A as the most probable bowl to be selected during the next run.

Probability/ Pheromone Concentration						
Mission	Param.	Bowl				SUM
		A	B	C	D	
m=0	Spheres	4	4	4	4	16
	Probability	0.250000	0.250000	0.250000	0.250000	1
m=1	Spheres	4	3	4	3	14
	Probability	0.285714	0.214286	0.285714	0.214286	1
m=2	Spheres	4	2	3	3	12
	Probability	0.333333	0.166667	0.250000	0.250000	1

Table 3.2: Probability/ Pheromone Concentration

The **Global** pheromone update rule is applied for updating the best solution(s) obtained during the local search. The “best” solution is usually either the local iteration-best⁵ or the best-so-far⁶ solution. Nevertheless, a ranking system can also be used for weighting each

⁴Smallest available pheromone unit

⁵Best solution obtained during the M missions of one local search

⁶Best Solution obtained through all the iterations

local solution according to the objective function improvement⁷. In case s_i is part of the best solution S^{best} , it receives pheromone according to the rule presented in Eq. (3.23). An expedition corresponds to a solution obtained for the global solution space.

$$\tau_{i,e+1} = \begin{cases} \phi^{global}\tau_{i,e} + \Delta\tau_{i,e} & \text{if } s_i \in S^{best} \\ \phi^{global}\tau_{i,e} & \text{otherwise} \end{cases} \quad (3.23)$$

where,

$$\begin{aligned} \tau_{i,e} &= \text{Pheromone amount at the global } s_i \text{ for the } e^{\text{th}} \text{ expedition} \\ \tau_{i,e+1} &= \text{Pheromone amount at the global } s_i \text{ for the } (e + 1)^{\text{th}} \text{ expedition} \\ \phi^{global} &= \text{Global pheromone reduction rate} \\ \Delta\tau_{i,e} &= \text{Pheromone received in iteration} \end{aligned}$$

$\Delta\tau_{i,e}$ is the value that updates the pheromone concentration according to the quality of the generated solution. Shorter global paths will receive higher amounts of pheromone. At the end of each iteration the pheromone of every partial solution s_i is multiplied with the global reduction rate in an attempt to represent the pheromone evaporation in time. Mathematically, this means that the solutions not visited any more, acquire a reduced probability to be selected again.

A similar bowl analogy as for the local rule can be performed for the global update. The only difference is that in case a bowl is selected, the solution quality will determine the number of orange spheres added. Moreover, the sphere concentration in all bowls will also be subject to evaporation.

Application to TEP

In order to apply the Ant Colony System into the Transmission Expansion Problem, the following analogies are established.

- The **Paths** s_i the ants walk on, represent the branches which receive reinforcements.
- The candidate **Solution** S_k , represent a set of branches to be upgraded.
- The **Path Length** from the ant's nest to the food source or the objective function to be minimised, is represented by a weighted sum of Total Costs C_k^t . These include investment, operational, operational policy and curtailment costs as an outcome of hourly applied minimum cost DC-OPFs.
- The path length also determines the **Solution Quality** q_k . This corresponds to cost reductions from a reference case as a result of network upgrades. It, thus, represents the difference of the path length.
- All pheromone values are multipliers of the smallest available pheromone unit, termed **Pheromone Quant** τ_{quant} . The value used by Fuchs accounts to 10% of the system's branches.

Eq. (3.24) presents the TEP solution matrix S that consists of the solution candidates S_k and subsequently of all branches s_i that receive reinforcements.

$$S = [S_1 \quad \dots \quad S_k \quad \dots \quad S_K] \quad (3.24)$$

⁷Difference from a reference path length

Even for moderate sized power networks, assessing all possible combinations of selected branches for upgrading is calculation time wise, unrealistic. Thus, the ACS by employing its solution memory feature and two pheromone update rules, diversifies the search space and moves to a pseudo-optimum TEP solution without evaluating all possible branch combinations

The flow chart depicted in Figure 3.7 portrays the basic functions of the ACS algorithm when applied into the TEP as described in [5]. Under the assumption that pheromone evaporates at all times, there are three main parts:

1. The local part, in green, locally updates the pheromone concentration of paths s_i that form a solution S_k obtained during a mission m . In order to avoid imprisonment in the solution's space local optima, the amount of pheromone corresponding to the branches that belong to the S_k is updated according to Eq. (3.22). M comprises the maximum number of solutions (S_k) that an ant can select during an expedition e .
2. The DC - OPF part, in orange, is the algorithmic part employed to evaluate the feasibility but also the quality of the solutions provided by the ants of the local part. An hourly cost minimisation DC - OPF is performed for all the locally selected solutions S_k . Depending on the approach chosen for identifying the best local solution S^{best} , it provides the branches s_i that belong to the S^{best} . Since, the iteration-best update rule avoids early convergence and delivers better results [92], it is the approach assumed in this thesis.
3. The global part, in cyan, globally updates the pheromone concentration of all (s_i) paths according to equation Eq. (3.23). E is the maximum allowed expeditions (global iterations) an ant can perform.

Optimising between RES curtailment and grid reinforcement

The classic ACO applied in Transmission Expansion Planning studies usually aims at fully integrating large scale wind power. Nevertheless, this thesis' goal is to optimise the trade-off between RES curtailment and grid extension. Some parts need to be adjusted compared to a classic ACO approach such as the methodology presented by Fuchs in [5].

Maximising wind integration, decreases the system operational costs due to the low RES operational costs (merit order effect). This is apparent on the objective function which comprises the summation of system costs and the annualised investment costs. For this work, the total system costs include another factor that corresponds to RES power curtailment costs. The objective function is then presented in Eq. (3.25).

$$\min_k f(k) = C_k^t = C_k^{op} + C_k^{curt} + C_k^{op.pol} + C_k^{inv.pa} + C_k^{pen} \quad (3.25)$$

Comparing Eq. (3.18) and Eq. (3.25), one can notice that a fifth factor, C_k^{pen} is introduced. The ACO approach does not break, in case of an OPF infeasibility. In contrast to the LUCSIPO approach, the ACO allows infeasibility for any number of hours by accounting for the penalty costs C_k^{pen} . If $C_{pen,f}$ is a penalty factor, the penalty costs are directly proportional to the number of hours H_{inf} the algorithm does not provide a solution. Specifically:

$$C_k^{pen} = C_{pen,f} H_{inf} \quad (3.26)$$

The calculated costs C_k^t define the solution quality q_k that provides the pheromone amount $\Delta\tau_{i,e}$ to be received in Eq. 3.23. The solution quality is provided by Eq. 3.27. The total cost

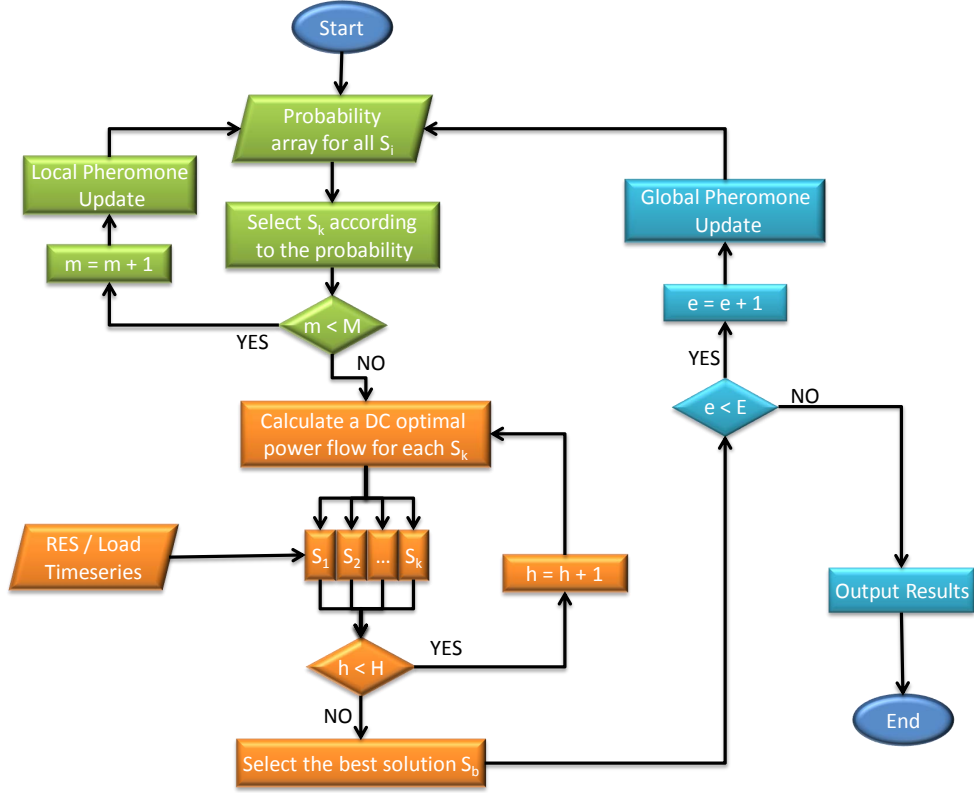


Figure 3.7: ACO implementation for the TEP problem. based on [5]

difference between the costs of a reference case C_{ref}^t and the costs of an obtained solution C_k^t comprises the solution quality q_k . In case the total system costs are higher than the reference costs, the quality is set arbitrarily to 1.

$$q_k = \begin{cases} (C_{ref}^t - C_k^t) & \text{if } C_{ref}^t \geq C_k^t \\ 1 & \text{otherwise} \end{cases} \quad (3.27)$$

The amount of pheromone update $\Delta\tau_{i,e}$ is then defined as:

$$\Delta\tau_{i,e} = \tau_{quant} q_k \quad \forall i \in S^{best} \quad (3.28)$$

Performing transmission expansion planning involves the integration of future wind capacity scenarios. A sane base case for performing cost comparison is the same system when omitting the future wind units. [5] uses the operational costs of the base case as the reference cost scenario and compares this figure with the operational costs of the obtained solution S_k . However, the different objective of this work, necessitates the investigation for defining alternative reference costs. Two base cases are defined:

1. **All Upgrades (AU)**. The base case integrates the future wind capacities but with all overloaded lines already upgraded. The reference costs are satisfactorily high due to full reinforcement of the grid.
2. **Full Curtailment (FU)**. The base case integrates the future wind capacities but no upgrades have taken place so any excess of RES power that cannot be integrated in

the network needs to be curtailed. The reference costs are high due to the extreme expenditure involved when discarding large scale RES power.

Performing transmission expansion planning involves the integration of future wind capacity scenarios. A sane base case for performing cost comparison is the same system when omitting the future wind units. [5] uses the operational costs of the base case, as the reference cost scenario and compares this figure with the operational costs of the obtained solution S_k . However, the different objective of this work, necessitates the investigation for defining alternative reference costs. Two base cases are defined:

$$\tau_i = \begin{cases} \tau^{quant}(1 + RO_i) & \text{if } i \in S^{RO} \\ \tau_{quant} & \text{otherwise} \end{cases} \quad (3.29)$$

where,

S^{RO} = Set of branches identified as overloaded during the statistical ranking

RO_i = Risk of Overload (in %) as identified from the RO approach

The above suggested formula cannot be employed for the ICPPCRO index since the cost indication is not of any value for this initialisation. Thus, another simplified approach is used that takes into account the ranking position RP_i each branch obtained during the ICPPCRO ranking. If α branches were found to be overloaded then:

$$\tau_i = \begin{cases} \tau^{quant}(1 + (\alpha - RP_i)^2) & \text{if } i \in S^{RO} \\ \tau_{quant} & \text{otherwise} \end{cases} \quad (3.30)$$

Implementation

Figure 3.5 presented a high level inputs/outputs representation of the LUCSIPO approach. With few adjustments needed, all the core power flow functions are similar to the functions applied in the ACS methodology. The main differences include the branches probability arrays introduced prior to the OPF runs in order to effectively simulate the pheromone update (both local and global) after each expedition and also the ACS related model inputs. The Matlab random generator via the built-in function *rand* is employed in order to generate random numbers and select the branches that form the candidate TEP solution. The pheromone amount in each branch (or bowl from Figure 3.6) represents its probability to get selected by the algorithm. The pheromone update rules adjust the margins of the cumulative distribution function that determine which branch corresponds to the randomly generated number.

Moreover, there is no curtailment limit P_{cur} applied, as introduced in the LUCSIPO approach. In case of congestion, the DC OPF can dispatch the wind production even to zero. The ACO algorithm is free to select the optimal number of upgrades versus the curtailed energy up to a maximum number of branch upgrades R . Each branch can be upgraded multiple times, if the algorithm decides to investigate such a solution.

Also, a Best So Far (BSF) solution (S^{BSF}) is introduced. After a predefined number of expeditions, an extra solution is put for investigation before entering the DC-OPF part. This solution consists of the R branches that have accumulated the highest pheromone concentration so far and can potentially augment the algorithm convergence.

The penalty factor $C_{pen,f}$ used for calculating the penalty cost C_k^{pen} of Eq. (3.26) can be anything large enough to drive the algorithm afar from infeasible solutions. For this thesis, the penalty factor $C_{pen,f}$ is defined as the operating costs of the reference case.

Finally a convergence check is also implemented in order to prevent the algorithm from unnecessary iterations when convergence is apparent. A quality margin ϵ between a solution

S_k and the best global solution so far $S_{g,best}$ is defined as the quantity, lower than which, the algorithm has reached convergence (Eq. 3.31). A value of $\epsilon = 2\%$ has been used in this work.

$$|S_{g,best} - S_k| < \epsilon \quad (3.31)$$

3.7 Representative Hours

Applying hourly cost OPFs either for the LUCSIPO or the ACO approach is a time intensive process that requires massive computational power as the size of the study case increases. Nevertheless, the results of the two algorithms can be assessed effectively by performing hourly OPFs to a representative subset of the 8760 round-the-year snapshots.

A widely applied clustering technique has been employed for obtaining a subset of the total snapshots. The observations used to perform the clustering are the hourly system's residual load figures and the number of clusters to be formed has been arbitrarily set to 100.

The Residual Load (RL), i.e the Demand subtracted by the RES feed, is a clear indicative of the congestion the network is subject to, at a particular point in time. The lower the residual load is, the higher the congestion becomes. For this work, Eq. (3.32) has been utilised in order to provide the residual load for the N areas of the network at any point in time.

$$RL_t = \sum_{j=1}^N Load_t - \sum_{j=1}^N RES_t \quad (3.32)$$

The approach termed *k-means* is a robust, widely used in data mining clustering algorithm with applications ranging from computer vision to astronomy or agriculture [93]. It partitions a set of n observations into k sets by forming clusters of observations according to the within-cluster sums of squared Euclidean distances. Figure 3.8 illustrates the data partitioning of 1000 observations into three clusters on the euclidean space. The algorithm aims at minimising the objective function F , given by Eq. (3.33).

$$F = \sum_{i=1}^k \sum_{j=1}^n ||x_j - c_i||^2 \quad (3.33)$$

where,

$$\begin{aligned} x_j &= \text{Obcervation} \\ c_i &= \text{Cluster's centroid value} \end{aligned}$$

The robust Matlab built-in k-means function is employed for performing the requested clustering. The function uses as input arguments the hourly residual load time series and produces as an output the cluster each of the 8760 values belong at, together with the centroid value of the cluster. However, as Eq. (3.33) describes the hourly residual load time series is the outcome of the summation of wind and load values corresponding to all areas of the network model. Thus, a single residual load centroid value cannot be used to extrapolate the value for each wind and load element. Utilising the centroid information then becomes an obstacle. The approach employed to overcome it, is to use the actual time series values that correspond to the first hour of the year identified as a member of each of the one hundred clusters. Figure 3.9 illustrates schematically the technique used for identifying a sample of one hundred hours that can effectively represent the round the year congestion in the network. The accuracy achieved suffices for this thesis' objectives.

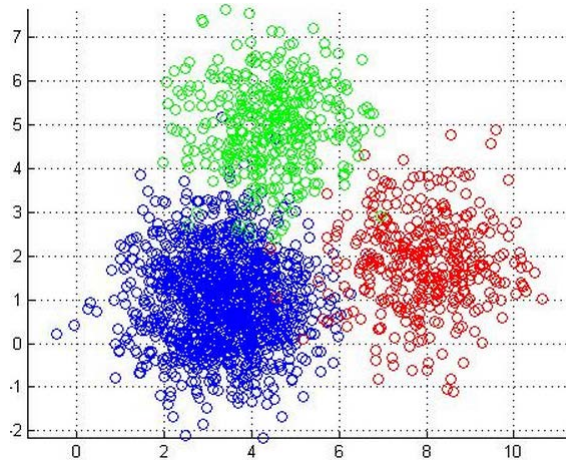


Figure 3.8: *Clustering 1000 observations into 3 clusters. Source: [6]*

3.8 Conclusions

This chapter presented the methodology applied in this thesis for dealing with the transmission expansion problem in systems with high amounts of RES. After providing background information on fundamental tools like the load flow and the optimal power flow study, it described the approaches developed for performing network optimised RES curtailment. The new heuristic LUCSIPO was illustrated as well as the modified ACO algorithm that was constructed for assessing the LUCSIPO's results. Finally, the k-means clustering technique employed for yielding a representative 100 h sample of the round-the-year snapshots, was also illustrated. In short, chapter 3 provided an insight in the details and the methodology challenges that were involved while developing an approach for performing transmission expansion studies.

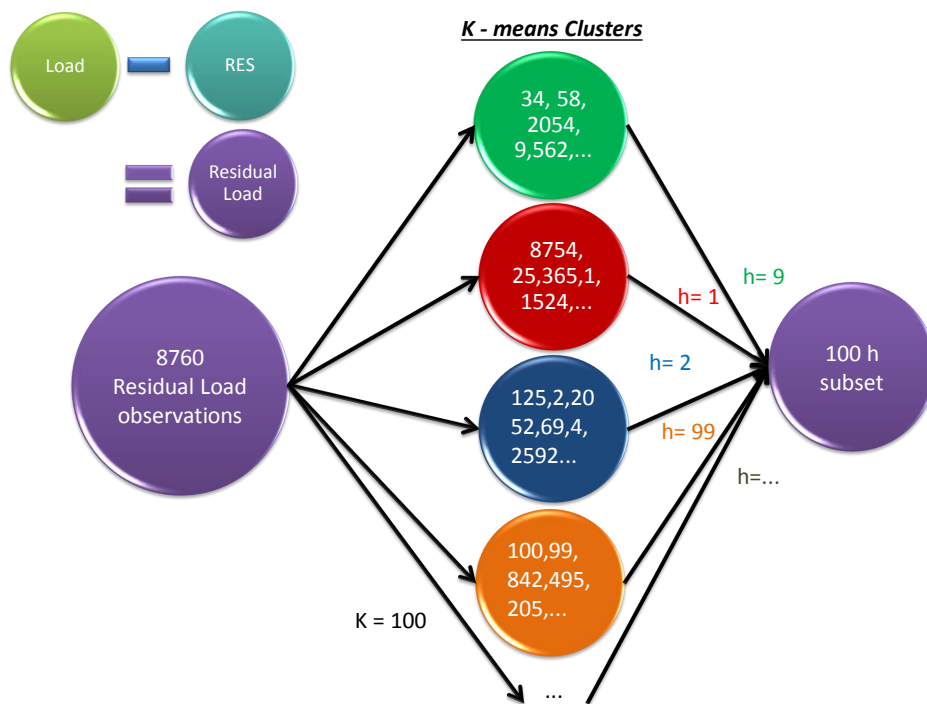


Figure 3.9: From the 8760 Residual Load values, 100 clusters are created that contain a subset of hours representative of the annual network's state. The first hour of the year that belongs to each circle (*k* means cluster) is used for representing the grid at this point.

Chapter 4

Results

The Least Upgrade Curtailment Sensitive Iterative Pseudo-Optimisation (LUCSIPO) approach has been developed as an attempt to prove the existence of a pseudo-optimum between RES curtailment and network reinforcements. To assess its outcomes, a modified Ant Colony Optimisation (ACO) approach was also developed.

The main goal of this chapter is to verify whether the developed TEP methodologies can identify transmission bottlenecks and upgrade the appropriate network branches. A small, flexible test system is needed for this purpose. A modified New England network model, presented in the first section of this chapter, is used for evaluating the two TEP methodologies.

Further, chapter 4 describes the sensitivity analyses undertaken and the scenarios developed for assessing the two approaches. Finally, it presents results obtained from the sensitivity cases assumed and compares the quality of the solutions that the LUCSIPO and ACO approach produced.

4.1 Case Study: The New England System

The IEEE - 39 bus New England (NE) benchmark system was chosen as a suitable testing platform. The NE system consists of a largely reduced network model of the actual New England region of North Eastern U.S.A., shown in Figure: 4.1



Figure 4.1: *The New England Region. Source: [7]*

The system model is organized into three areas and is a standardised system for testing purposes that has been widely used for both static and dynamic studies in power systems.

The 39-bus system consists of:

- 10 generators,
- 19 loads,
- 36 transmission lines,
- and 12 transformers.

The extended by wind power NE system presented by Ciupuliga et al. in [10] is used. Two extra buses (40 and 41) were introduced in order to account for two wind units in Area 1 and Area 2. Consequently two extra transformers were built between buses 25-41 and 21-40 for interconnecting the extra two units in the system. Moreover, modifications in the unit generating capacity and technology class were incorporated, for the purpose of integrating current technologies and fuel prices. Table 4.1 illustrates the specifications of the generating units assumed by [10] while the figures of Tables 3.1 (of chapter 3) and 4.2 describe the technical limitations and fuel prices used.

The time correlated wind in-feed and consumption time series used by Ciupuliga et al at [10] are employed for this case study. Due to lack of consistent publically available data, EU consumption profiles were used and the original load elements of the NE system were scaled according to the maximum value of the load profiles. Moreover, loads in buses 1 and 9 were removed from the test system. Table 4.3 contains the total annual consumption corresponding to each system region. Finally, the provided normalised regional wind in-feed time series are assigned to each of the wind units of the system.

Area	Tech. Class - Bus No	Installed Capacity (MW)
1	Lignite - Bus 37	965
	Gas - Bus 30	640
	Wind - Bus 41	300
2	Coal - Bus 39	1100
	Gas - Bus 32	185*2
	Wind - Bus 31	1200
3	Coal - Bus 38	1050
	Gas - Bus 33	200*2
	CCGT - Bus 35	790
	CCGT - Bus 34	625
	CCGT - Bus 36	699
	Wind - Bus 40	1200

Table 4.1: *New England Modified System, Power Plants. Source: [10]*

	2008	2015	2020	2025	2030
Lignite	1.4	1.4	1.4	1.4	1.4
Coal	17.3	15.3	13.4	13.6	13.8
Uranium	3.6	3.5	3.3	3.3	3.3
Oil	44.6	71.8	99	104.5	110
Gas	25.2	26.6	28.1	29.7	31.3
RES	0.1	0.1	0.1	0.1	0.1
CO2	10.2	16.4	22.6	27.2	31.8

Table 4.2: *Development of fuel prices in €₂₀₁₀ \MWh_{th}. For CO₂ the costs are in €₂₀₁₀ \t CO₂. The prices are further adjusted in order to correspond to 2012 values. Source: [9]*

Area	Total Demand (GWh)
1	7,249
2	13,306
3	15,280

Table 4.3: *Total annual demand for the three areas of the New England system.*

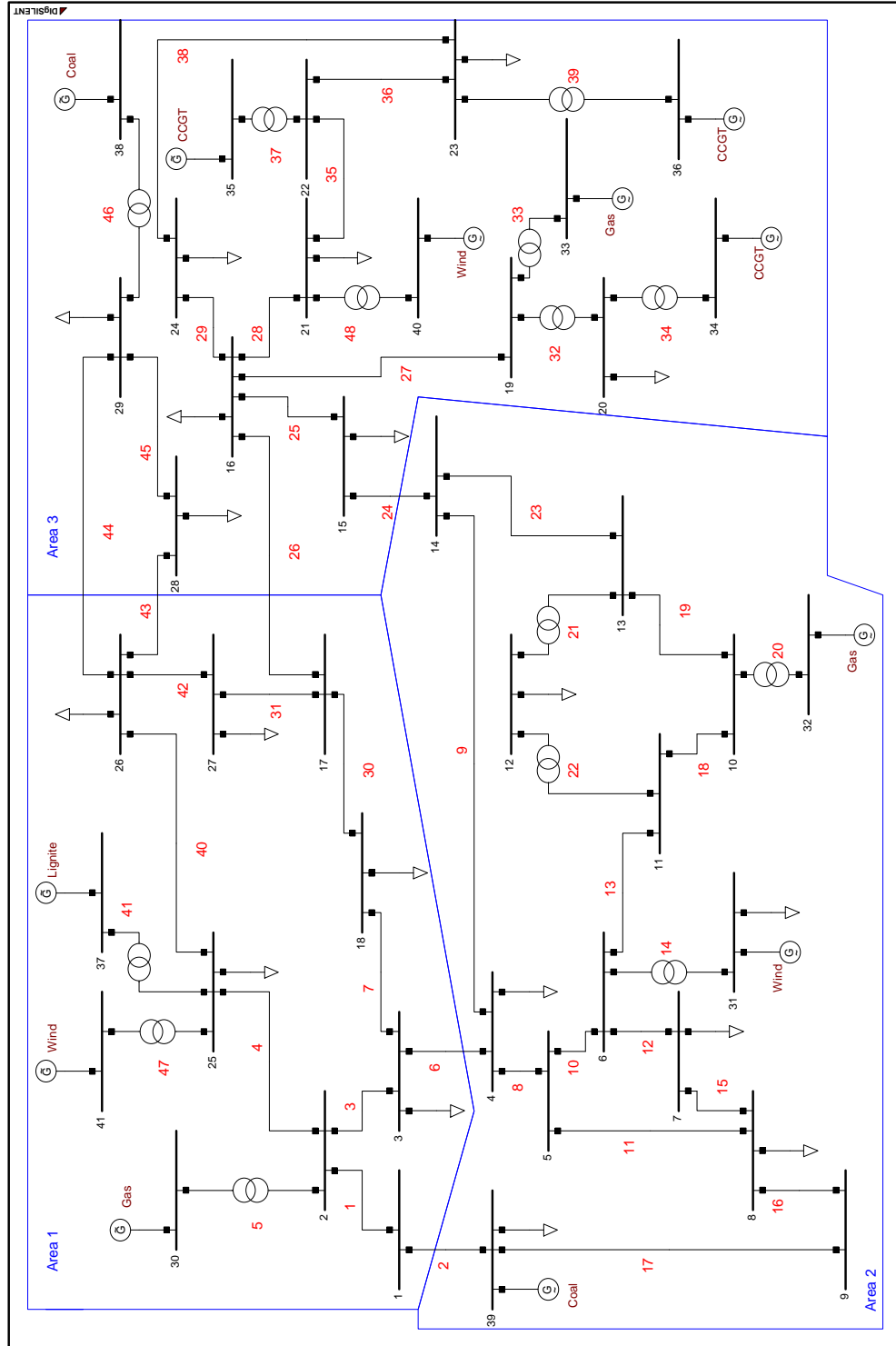


Figure 4.2: Single Line Diagram of the reduced New England LF Model. In Red the ID of each branch. In Brown the technology of each generating unit. The appendix Table A.27 presents the network model's branch data.

All branches were originally assumed by [10] to have a rated capacity of 900 MVA. Nevertheless, this rating was too high for illustrating the methodology proposed since it did not introduce sufficient congestion in the system. Thus, a lower branch capacity limit of 600 MVA is applied. Further, an 80% maximum loading constraint has been used in order to account for N-1 contingencies. Information on the length of the lines was obtained by using the p.u. line impedance as found in [87] and typical transmission line impedance values from [125]. Assuming a 345 kV base voltage and a 100 MVA base power, Eq. 3.5 yields the transmission line length.

$$Z_b = \frac{V_b^2}{S_b} \quad (3.1)$$

$$z_{pu} = |r_{pu} + jx_{pu}| \quad (3.2)$$

$$Z_t = |R_t + jX_t| \quad (3.3)$$

$$Z_a = Z_{pu}Z_b \quad (3.4)$$

$$l = \frac{Z_a}{Z_t} \quad (3.5)$$

where,

Z_b = Base impedance in Ω ,

V_b = Base voltage in kV,

S_b = Base power in MVA,

z_{pu} = Magnitude of line impedance (p.u.),

r_{pu} = Line resistance (p.u.),

x_{pu} = Line reactance (p.u.),

Z_t = Magnitude of typical line impedance in Ω \km,

R_t = Typical line resistance in Ω \km,

X_t = Typical line reactance in Ω \km,

Z_a = Actual line impedance in Ω ,

l = Line length

Transformers are not considered a bottleneck and thus their maximum capacity constraint has been deactivated. Nevertheless, in order not to disturb the power flows, their impedance values have not been modified.

The study case assumes that the load and wind time series relate to the installed capacities of the year 2030 and also includes the economical figures assumptions presented in Table 4.4. The feed-in-tariff is considered to have a flat rate of 9.3 ct/kWh as defined in [94]. In order to extrapolate the actual 2030 value an annual inflation rate of 2% has been assumed corresponding to the average inflation in the EU for January 2013 [95]. The interest rate is set a 9.05 % as defined by the German Federal Ministry of the Environment [96]. For line upgrade costs, the values presented for Germany by L'Abbate et al [97] are used.

Nevertheless, the FIT figure needs to be adjusted in order to meet today's value of money. FIT rates are set by European governments (in 20 year closed contracts) and are not adjusted to the inflation. Moreover, those rates are dependent on the construction date of each wind farm. The value in Table 4.4 is a weighted average that takes into account the installation

Parameter	Value	Unit
Line investment Cost	800000	€ ₂₀₁₂ /km
Lifetime	20	years
Interest rate	9.05	%
Feed in Tariff (2012)	93	€ ₂₀₁₂ /MWh
Inflation	2	%

Table 4.4: *Economical figures assumed for the New England Study case. Source: [64, 94–97]*

date of each farm. Since historically the rates have been decreasing, it is assumed that each year, 1/20 of the installed wind capacity is replaced by new wind capacity with a FIT compensation at 99% of the initial figure. Therefore, the rate in Table 4.4 does not represent the value of the FIT in 2030 and is adjusted by Eq. 3.6 and 3.7

$$FIT_{av} = FIT \left(\frac{19}{20} + 0.99 \frac{1}{20} \right)^{18} \quad (3.6)$$

$$FIT_a = \frac{FIT_{av}}{(1+i)^{18}} \quad (3.7)$$

where,

$$\begin{aligned} FIT_{av} &= \text{FIT weighted average,} \\ FIT &= \text{2012 FIT rate,} \\ FIT_a &= \text{Adjusted FIT rate,} \\ i &= \text{Inflation rate.} \end{aligned}$$

4.2 Sensitivity Analysis

Four main sensitivity analyses are considered in order to assess the influence of each sensitivity case to the final selected expansion. The sensitivities include:

Wind Capacity

Table 4.5 presents the three installed wind capacity scenarios, inspired by the wind scenarios [10] assumed. The variation of wind capacity requires different transmission expansion.

Area - Bus	Installed Wind Capacity (MW)		
	Low Wind	Moderate Wind	High Wind
Area 1 - Bus 41	300	300	300
Area 2 - Bus 31	800	1200	1600
Area 3 - Bus 40	800	1200	1600

Table 4.5: *Installed Wind Capacity Scenarios*

Curtailment Cost

As discussed in detail in Chapter 5, two policies for compensating the curtailed Energy

are differentiated. Feed-In-Tariffs (FIT) and Marginal Costs (MC). The FIT assumes a fixed compensation per curtailed MWh while the marginal system costs are calculated hourly since they are dependent on the system dispatch. These sensitivity cases can highlight which policy scenario is most attractive in respect with reducing the renewably generated energy curtailment.

Minimum conventional power in the system

It is a sensitivity analysis that evaluates how the grid upgrades / wind curtailment results depend on the Minimum Required Conventional Generation Penetration (MRCGP) limit. As defined earlier, it is the complementary of the System Non Synchronous Penetration (SNSP) limit. Three cases account for the limits set in Table 4.6:

MRCGP (%)	SNSP (%)
20	80
40	60
50	50

Table 4.6: *MRCGP Limits assumed*

The first two figures correspond to suggestions made by Ecofys to the Irish TSO EirGrid in 2009 [98], while the third value is the limit that EirGrid defined at that time.

Statistical Overload Ranking

This sensitivity is not related to governmental actions and policies. It is developed in order to evaluate the behaviour of the two TEP algorithms when the two different ranking options described in Chapter 3 are used.

4.3 Results

The algorithms were developed in the 64bit Matlab R2012b, using the open source MatPower 4.1 package and the IBM CPLEX optimisation studio 12.4 solver. THE LUCSIPO approach was also developed in the 32bit version of DigSILENT PowerFactory 14.1.3. The dedicated hardware employed a Quad-Core 3.4 GHz Intel Xeon E3-1240V2 processor (8 MB cache), and a physical memory of 16 GB.

Table 4.7 presents the sensitivity scenarios chosen to assess the results of the two TEP methodologies. The base case involves a moderate wind scenario (MoW), a FIT curtailment cost approach, a 40% MRCGP limit and the ICPPRO ranking approach. In order to study the effect each sensitivity case has on the system, the base case is compared against the solutions the other cases generate by altering a single parameter per run. For the high wind situation, a sensitivity case that applies static curtailment limits has been also included.

4.3.1 K-means

In order to present a sufficient variety of sensitivity cases for the developed approaches, it was unrealistic, computation time-wise, to perform extensive round-the-year simulations. A smaller subset of snapshots suffices for answering this thesis' research questions. A comparison between an 8760 hours run and a hundred representative hour subset run, obtained utilising the k-means function, is presented. Table 4.8 contains the base case scenario results, generated

Scenarios	Inst. Wind	Curt. Costs	MRCGP Limit	Ranking
Base Case	MW	FIT	0.4	ICPPRO
Low limit(LL)	MW	FIT	0.2	ICPPRO
High Limit(HL)	MW	FIT	0.5	ICPPRO
High Wind(HW)	HW	FIT	0.4	ICPPRO
Low Wind(LW)	LW	FIT	0.4	ICPPRO
MC Approach (MC)	MW	MC	0.4	ICPPRO
RO Ranking (RO)	MW	FIT	0.4	RO
High Wind/High Limit (HWHL)	HW	FIT	0.5	ICPPRO
High Wind/ Low Limit (HWLL)	HW	FIT	0.2	ICPPRO
High Wind/RO (HWRO)	HW	FIT	0.4	RO

Table 4.7: Base case and selected sensitivity scenarios.

for the two temporal resolution cases, when the LUCSIPO approach is employed. The investment costs p.a. for the k-means run have been downscaled simply by multiplying the resulting capital costs with a factor of $\frac{100}{8760}$. Although this is a large simplification, it is a straight-forward way to equally weigh the investment costs to the operating and curtailment costs that correspond to a 100 h operation.

Scenario	BC 100 h	BC 8760 h	100 h projection
Curtailment Limit (%)	100	90	
Upgraded Branches	5	7	
Curtailed Energy (%)	0.00	0.02	0.00
Curtailment Costs (M€)	0.000	0.105	0.001
Op. Policy Costs (M€)	0.000	0.000	0.000
Operational Costs (M€)	16.555	1,416.058	16.165
Investment costs p.a. (M€)	0.232	30.408	0.347
Upgraded Length(km)	231.4	345.7	
Upgraded Branches	3 4 26 28 42	3 4 26 28 31 35 42	
Calculation Time (sec)	851.8	160,677.63	
Total Costs (M€)	16.788	1,446.570	16.513

Table 4.8: Comparison of the round-the-year and representative subset case.

In order to enable the comparison of the two scenarios, the relevant figures (costs and energy) have to be projected into the same basis. The straightforward concept to divide the round-the-year case results by a factor of $\frac{8760}{100} = 87.6$ is presented in the third column of Table 4.8. It is *a priori* known that results obtained by employing a sampling technique, such as k-means, will introduce errors and significant solution deviation. Nonetheless, in case the gains of applying such a technique can outweigh some loss of accuracy, then it is important to at least be taken into consideration.

One can observe that the deviation of the cost and energy figures is not prohibitive. Indeed,

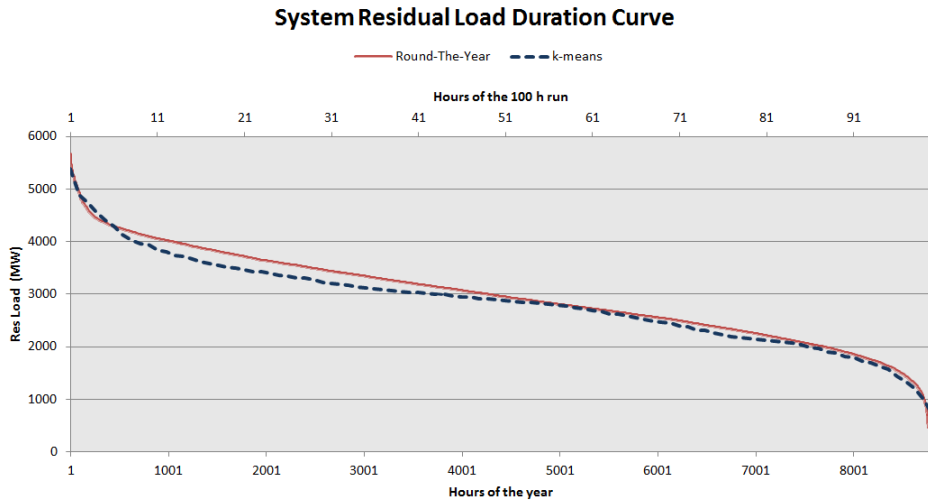


Figure 4.3: Residual Load Duration Curves for the two temporal resolution cases.

the 100 hour run has missed a few branch upgrades and the algorithm reached an optimal solution for different curtailment limits. However, the computation effort gain is massive and results in a rapid decrease in the simulation time. In fact, the 100 h run is 188 times faster. Simultaneously, and as shown in Figure 4.3, it has managed to represent efficiently the annual residual load duration curve, even for the high wind case.

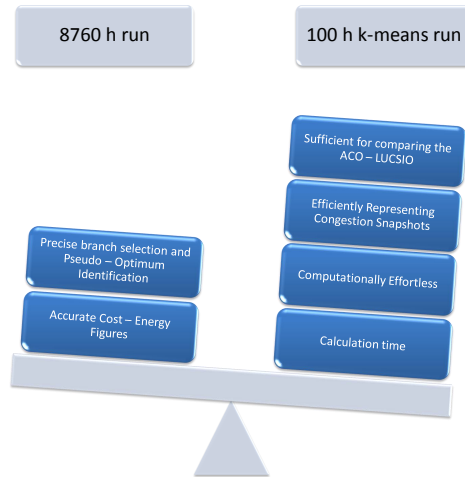


Figure 4.4: Weighting the two temporal resolution runs.

The goal of this thesis is to prove that there is an optimal trade-off between RES curtailment and grid upgrades and also to attempt to identify it via the LUCSIPO and the ACO approach. The 100 h k-means clustering efficiently provides a representative sample of the network congestion throughout the year, and therefore is sufficient for comparing and evaluating the two TEP methodologies and their sensitivity variations. Figure 4.4 illustrates a quick comparison of the advantages each temporal resolution approach provides. All the results

presented in this chapter are based on the three different 100 hour subsets that were obtained for the three wind capacity scenarios. The cost and energy figures also correspond to these 100 h subsets.

4.3.2 LUCSIPO

Iteratively increasing the wind curtailment limit is an integral part of the LUCSIPO methodology. For the dynamic limit case, the algorithm starts with allowing wind curtailment down to 20% of the available wind power in-feed. Attempting to detect an optimum, it proceeds with an increasing 10% step until no congestion-induced curtailment is allowed. The algorithm promotes solutions which do not result in Operational Policy costs, while, in case different curtailment limits produce the same solution, it selects the higher curtailment limit case.

Tables 4.9 and 4.10 present the LUCSIPO approach BC results for the various curtailment limits. Table 4.9 provides information on the number of branches selected for reinforcement, the curtailed energy and the total costs involved in each solution. Additionally, Table 4.10 explicitly pinpoints the upgraded branches that form the solution each iteration generated.

Curtailment Limit (%)	20	30	40	50	60	70	80	90	100
Upgraded Branches	2	2	2	2	2	2	5	5	5
Curtailed Energy (%)	3.27	3.27	3.27	3.27	3.27	3.27	0.00	0.00	0.00
Curtailment Costs (M€)	0.223	0.223	0.223	0.223	0.223	0.223	0.000	0.000	0.000
Op. Policy Costs (M€)	0	0	0	0	0	0	0	0	0
Operational Costs (M€)	16.878	16.878	16.879	16.879	16.879	16.879	16.555	16.555	16.555
Investment costs p.a. (M€)	0.096	0.096	0.096	0.096	0.096	0.096	0.232	0.232	0.232
Upgraded Length(km)	95.7	95.7	95.7	95.7	95.7	95.7	231.4	231.4	231.4
Total Costs (M€)	17.197	17.197	17.198	17.198	17.198	17.198	16.788	16.788	16.788

Table 4.9: *Base Case Scenario Results*

The figures presented in Table 4.9 reveal an apparent trend. Increasing the minimum generation limit of the wind units (i.e. decreasing the curtailment limit) results in an increase on the number of upgraded branches and a reduction of the curtailed wind energy. This outcome is expected since increasing the curtailment limit allows less wind power dumping and thus introduces congestion in the network. As a result, more branches need to be reinforced for transmitting the generated wind power. With more transmission capacity and hence more integrated wind, conventional plants outputs are reduced, resulting in lower operating costs.

The optimal solution the LUCSIPO achieved comprises the point where the total costs of operating the network, reinforcing the grid and curtailing wind power is minimised. For the base case scenario, the LUCSIPO approach claims that this happens at any curtailment limit between 80 and 100%, after upgrading 5 network branches. For the BC scenario, upgrading only the network without discarding any wind energy comprises the optimal solution.

Curtailement Limit (%)	Upgraded Branches
20	3 4
30	3 4
40	3 4
50	3 4
60	3 4
70	3 4
80	3 4 26 28 42
90	3 4 26 28 42
100	3 4 26 28 42

Table 4.10: *Base Case Scenario Upgraded Branches*

Sensitivity Scenarios

BC-MC

The LUCSIPO approach appears to be rather inelastic to changes with regard to the curtailment cost calculation approach. Table A.1 presents the solutions generated during the MC case. The non optimal solutions consider a small amount of discarded wind energy (in the range of 3%) which results in a more expensive system if the marginal cost approach is to be applied. Nevertheless, the optimal solution does not yield any wind curtailment, and it is identical to the base case.

BC-LW/HW

Table 4.11 illustrates a comparison on the network status for the HW and LW cases. The optimal solution for the HW case has resulted in an increase in the number of reinforced branches (from 5 to 9), consequently doubling the investment costs. Moreover, due to the increased wind generation, the curtailed energy (and related costs) have risen. This increase is outweighed though by the operational costs that have decreased significantly. As a consequence, the total cost savings for these 100 representative hours amount to 2.1 million €. Extrapolating this value to a full year, results in a major total system cost reduction and renders investment and curtailment costs insignificant.

Due to the merit-order effect, the low wind capacity case yields higher total costs. However, when compared to the base case, the number of upgraded branches has risen. This could be justified by the fact that the lower wind scenario results in higher conventional power plant dispatch and consequently different flows in the network.

The HW case is examined closely. As shown in the appendix Table A.2, the LUCSIPO approach finds a single optimum for a curtailment limit of 90%, where the optimal solution is achieved by upgrading 9 branches (of 427 km in total), the total costs amount to 14.564 million € and a 0.75% of the total wind energy has been curtailed.

Figure 4.5 illustrates the shift in curtailment and investment costs as a function of the curtailment limit. Including the operating policy costs, its sum is minimised between the 60 and 70% limit. Taking also into account the system operating costs though, as depicted in Figure A.1, shifts the optimum towards the 80% curtailment region.

Scenario	BC	HW	LW
Curtailment Limit (%)	100	90	100
Upgraded Branches	5	9	7
Curtailed Energy (%)	0.00	0.75	0.00
Curtailment Costs (M€)	0.000	0.026	0.000
Op. Policy Costs (M€)	0.000	0.041	0.000
Operational Costs (M€)	16.555	14.069	18.234
Investment costs p.a. (M€)	0.232	0.428	0.347
Upgraded Length(km)	231.4	426.6	345.7
Upgraded Branches	3 4 26 28 42	3 4 10 26 27 28 31 35 42	3 4 26 28 31 35 42
Total Costs (M€)	16.788	14.564	18.581

Table 4.11: *BC and LW - HW comparison*

The optimum found for the 90% limit with a slight difference of 6000 €, is an outcome of the MRCGP limit. Summing the operational policy and curtailment costs add up to the same figure since they are both multiplied by the FIT but, nevertheless, the approach prefers solutions which exclusively include congestion related curtailment. For the HW case, the 90% curtailment limit results in lower operating costs than the 80% limit, due to a small difference in the wind energy output that the MRCGP limit introduces.

Figures 4.6a and 4.6b present the HW total system and operational costs as a function of the curtailed energy. The data points of Figure 4.6a correspond to the total curtailed energy (both congestion and operational policy induced) while Figure 4.6b refers exclusively to network congestion related curtailment. As shown, due to the merit order effect, the operating costs get minimised when the least possible wind energy is discarded. Nonetheless, for both graphs, the total system costs are minimal when the solution yields a small fraction of curtailed energy.

BC-LL/HL

Results show that the BC scenario is inelastic when reducing the MRCGP limit variant (LL). This is due to the moderate assumption on the installed wind capacity incorporated in the BC. The system is sensitive though to increasing this limit since the installed wind capacity in the moderate wind scenario is high enough to cause minor congestion in the network. Table 4.12 summarises the results presented in detail in Tables A.8 and A.9.

The third column of Table 4.12 (HL) depicts the impact of the system's operational policy, even in cases of not highly congested systems. Increasing the MRCGP limit by 10% resulted in wind power dumping and further increase of the operating costs. This is due to the need of employing fossil fuel units (merit order effect). The total extra cost amounts to 50,000 €, which projected to an 8760 hour year can introduce extra costs of another 4 million €. Specifically, the appendix Table A.9 presents the HL scenario results where, due to the system operating policy, wind power needs to be curtailed in order for the system to meet the MRCGP limit. In the situation, though, where congestion based curtailment is not allowed (100% limit) and since no storage measures are considered, the wind units are forced to produce at the maximum allowed limit (SNSP). The extra costs involved with this non-congestion related curtailment are termed *Operational Policy Costs*. The algorithm gives priority to solutions not including operational policy costs when identifying the pseudo-optimum. The HL Scenario's optimum is found when curtailing 0.34% of the available wind energy.

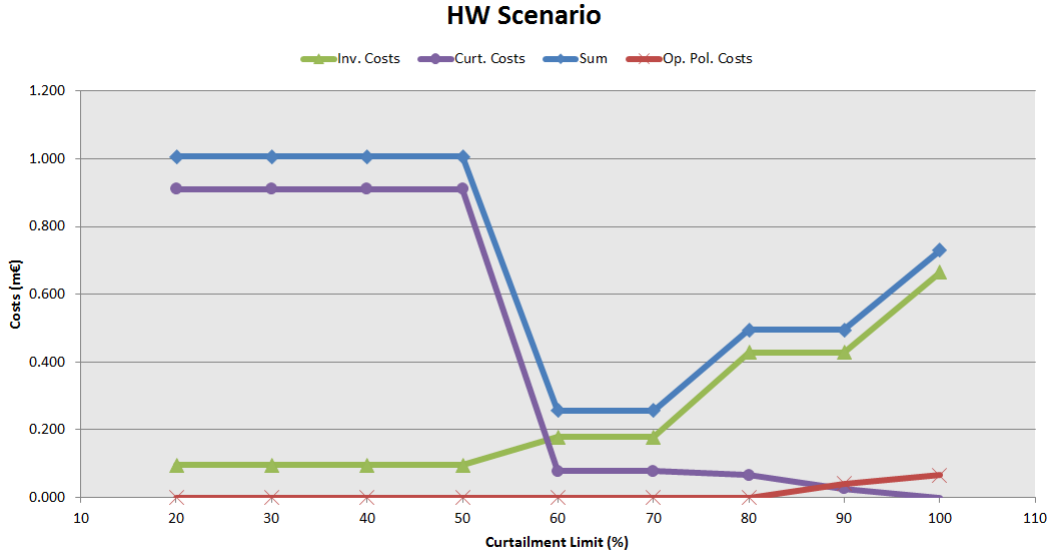
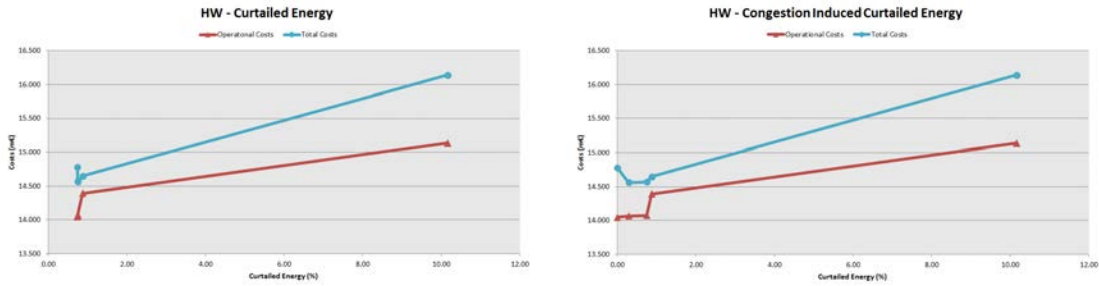


Figure 4.5: HW Scenario. Investment and Curtailment Costs.



(a) Curtailed energy.

(b) Congestion induced curtailed energy.

Figure 4.6: Total Costs and Operating Costs as a function of the curtailed energy.

HW - HWLL/HWHL

Table 4.13 presents a comparison between the HW scenario and the HWHL/ HWLL cases with the purpose of further testing the elasticity of the system to changes of minimum conventional operational policy. Full results for the HWHL and HWLL scenarios can be found in the appendix Tables A.10, A.11 and A.12, A.13 respectively.

The conventional power operational policy comparison reveals a clear trend. Altering the minimum required conventional generation penetration (MRCGP) limit in the system has a direct impact on the total costs involved. As Figure 4.7 illustrates, the reduction of the MRCGP limit to 20% of the total demand (HWLL case) results in lower total system costs. On the contrary, the increase of the limit to 50% (HWHL case) generates a solution half a million € less cost effective. This accounts for the price of security for the 100 k-means hours. Finally, the list of upgrades appears to be also sensitive to the MRCGP values due to the merit order effect which yields different flow patterns in the system. The appendix Figures A.3 and A.4 further illustrate the effect the SNSP limit has on the system.

Scenario	BC	LL	HL
Curtailement Limit (%)	100	100	90
Upgraded Branches	5	5	5
Curtailed Energy (%)	0.00	0.00	0.34
Curtailement Costs (M€)	0.000	0.000	0.023
Op. Policy Costs (M€)	0	0	0
Operational Costs (M€)	16.555	16.555	16.576
Investment costs p.a. (M€)	0.232	0.232	0.232
Upgraded Length(km)	231.4	231.4	231.4
Upgraded Branches	3 4 26 28 42	3 4 26 28 42	3 4 26 28 42
Total Costs (M€)	16.788	16.788	16.831

Table 4.12: BC and Low Limit - High Limit cases comparison

HW - HWRO

A comparison of the BC (utilising the ICCPRO ranking) with the RO ranking case show no differences since the network is not extensively congested. Therefore, the HW scenario, is used to test the ICPPRO and RO statistical ranking approaches. The appendix Tables A.14 and A.15 present the corresponding results for the HWRO Sensitivity Scenario while Table 4.14 shows the comparison of the optimal solutions that the HW and the HWRO scenario found.

The difference between the HW and HWRO cases is the ranking method used for the determination of the next upgrade the LUCSIPO approach performs. As shown in Figure 4.8, the two rankings upgrade the same branches and have identical results below the threshold of 70% curtailment limit. However, the investment cost ranking ICPPCRO identifies and upgrades a different sequence of branches which eventually results in lower total system costs and enable the HW scenario to yield a better solution. In fact, at the 80% limit the HWRO case upgrades 12 branches while the HW only 9 (see appendix). The reason for this behaviour is that the different branches the ICPPCRO upgraded first induced different power flows in the system and provided a feasible solution with less upgrades needed for the 80 and 90% steps. At the final 100% step, both HW and HWRO converge to the same solution.

Table 4.15 illustrates the sequence of upgrades for the two cases. The index value obtained is given next to each branch ID. As shown, the sequence is identical until the 9th upgrade. At this point the ICPPCRO ranking selects the 10th branch while the RO ranking upgrades the 4th branch for the second time. This choice, allows the ICPPCRO ranking to select a solution that involves less grid extensions. The appendix Tables A.16 and A.17 present the ranking positions each transmission line obtained during the 1st, 2nd and 8th, 9th ranking performed respectively. For the 1st ranking of the HWRO case, Figure A.10 presents the Risk of Overload for each branch in color code. In Red are the most overloaded branches. The branches that remain black, have not been overloaded at all throughout the hundred hour run.

Extra scenarios for the LUCSIPO approach

In order to further test the LUCSIPO approach, two extra scenarios were investigated. The first scenario integrates a static curtailment limit on the high wind case (High Wind Static, (HWS)), while the second assumes an increased wind in-feed in order to account for higher wind full load hours.

Table 4.16 presents the comparison between the HW and the HWS scenario. As shown,

Scenario	HW	HWLL	HWHL
Curtailment Limit (%)	90	90	60
Upgraded Branches	9	8	9
Curtailed Energy (%)	0.75	0.19	3.16
Curtailment Costs (M€)	0.026	0.017	0.274
Op. Policy Costs (M€)	0.041	0.000	0.000
Operational Costs (M€)	14.069	14.046	14.280
Investment costs p.a. (M€)	0.428	0.377	0.459
Upgraded Length(km)	426.6	375.5	457.5
Upgraded Branches	3 4 10 26 27 28 31 35 42	3 4 10 26 27 28 31 42	3 4x2 26 27 28 31 35 42
Total Costs (M€)	14.564	14.440	15.014

Table 4.13: HW and LL - HL comparison

the two scenarios produce the same pseudo-optimum solution but for different curtailment limits. The HW case finds the best solution for the 90% (of the available in-feed) limit while the HWS selects the 70% (of the installed capacity) limit. They both result in the same curtailed wind energy. The appendix Tables A.4 and A.5 present the HWS case results while Figure 4.9 illustrates a total cost comparison between the solutions obtained for each curtailment limit. The figure shows that, prior to locating the pseudo-optimum solution, they have followed different paths. It is important to clarify that the static and curtailment limit correspond to the two sides of the same coin. They always result in the same pseudo-optimum solution. Similar to the dynamic limit Figure 4.5, Figure A.2 of the appendix presents the curtailment and investment costs as a function of the static curtailment limit.

The full load hours of the wind in-feed in the three NE system regions correspond to 3,590, 2,094 and 3,334 hours respectively. In order to test the LUCSIPO output for more favourable wind conditions, the time series of the second system region were scaled up for 4,500 full load hours by a factor of 2.14. Nevertheless, in case the scaled hourly value was higher than the installed capacity, the corresponding wind feed was set to the rated figure. As a result, the resulting Increased Full Load Hours (IFLH) scenario accounts for 4089 full load hours. The static curtailment limit approach has been used for the IFLH scenario.

The appendix Tables A.18 and A.18 present the IFLH results while Table 4.17 illustrates a comparison between the HWS and the IFLH scenario. As shown, the “optimum” solution is reached at the 90% static limit. The operating costs and total costs are lower in the IFLH case and this is mainly due to the merit order effect. Nevertheless, the curtailment costs (accounting for 3.26% curtailed energy) are significantly high and they are dominated by expenditure related to the SNSP limit rather than network congestion. Finally, it is highlighted that the total upgraded length is quite similar to the HWS case but the branch candidate list is different. This is an outcome of the quite higher wind in-feed that alters the flows in the network.

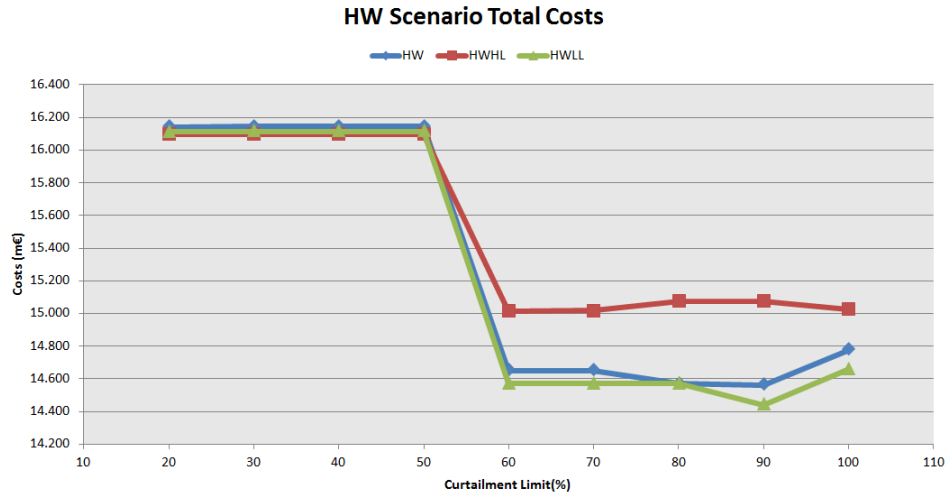


Figure 4.7: Comparing the conventional power integration limits for the HW case.

Scenario	HW	HWRO
Curtailment Limit (%)	90	70
Upgraded Branches	9	4
Curtailed Energy (%)	0.75	0.88
Curtailment Costs (M€)	0.026	0.078
Op. Policy Costs (M€)	0.041	0.000
Operational Costs (M€)	14.069	14.394
Investment costs p.a. (M€)	0.428	0.178
Upgraded Length(km)	426.6	177.5
Upgraded Branches	3 4 10 26 27 28 31 35 42	3 4 26 28
Total Costs (M€)	14.564	14.651

Table 4.14: HW and HWRO comparison



Figure 4.8: HW Scenario. Comparing the Ranking Approach effect on the total system costs.

HW case rankings. P _{curt} =90%				
Upgrades	HW		HWRO	
	Branch ID	ICPPCRO(M €)	Branch ID	RO(%)
1	4	0.47	4	68.66
2	3	0.85	3	52.27
3	26	0.92	26	28.29
4	28	1.67	28	23.59
5	42	2.56	42	16.83
6	27	10.15	27	5.62
7	31	12.81	31	3.95
8	35	34.11	35	1.20
9	10	35.97	4	0.49
10	n\a	n\a	26	0.42
11	n\a	n\a	7	0.25
12	n\a	n\a	10	0.23

Table 4.15: Sequence of upgrades for the HW scenario when the ICPPCRO and RO rankings are applied.

Scenario	HW	HWS
Curtailed Limit (%)	90	70
Upgraded Branches	9	9
Curtailed Energy (%)	0.75	0.75
Curtailed Costs (M€)	0.026	0.026
Op. Policy Costs (M€)	0.041	0.041
Operational Costs (M€)	14.069	14.069
Investment costs p.a. (M€)	0.428	0.428
Upgraded Length(km)	426.6	426.6
Upgraded Branches	3 4 10 26 27 28 31 35 42	3 4 10 26 27 28 31 35 42
Total Costs (M€)	14.564	14.564

Table 4.16: HW and HWS comparison

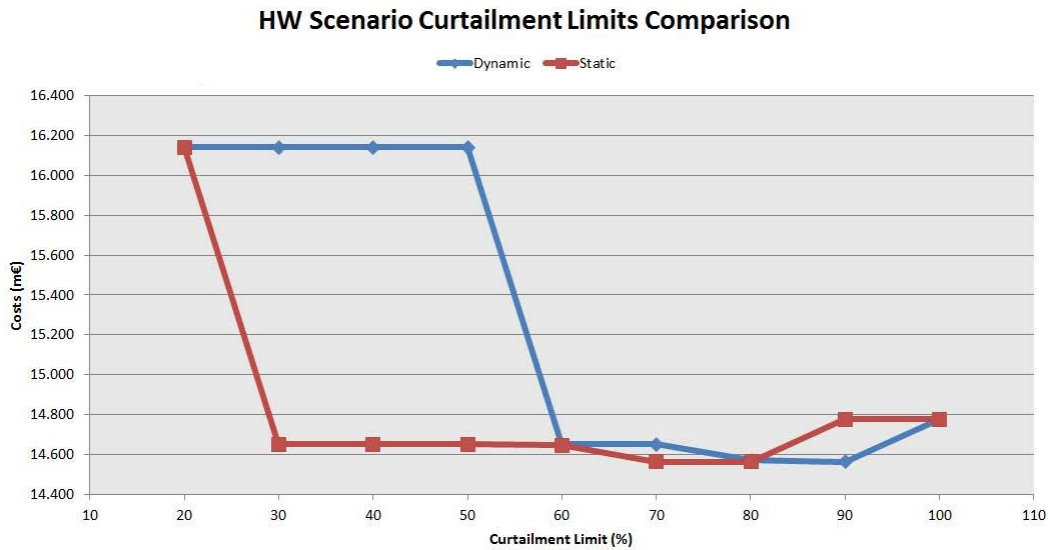


Figure 4.9: HW Scenario. Curtailment Limits Comparison.

Scenario	HWS	IFLH
Curtailement Limit (%)	70	90
Upgraded Branches	9	10
Curtailed Energy (%)	0.75	3.26
Curtailement Costs (M€)	0.026	0.003
Op. Policy Costs (M€)	0.041	0.351
Operational Costs (M€)	14.069	13.434
Investment costs (M€)	0.428	0.439
Upgraded Length(km)	426.6	437.6
Upgraded Branches	3 4 10 26 27 28 31 35 42	3 4 7 8 10 26 27 28 30 42
Total Costs (M€)	14.564	14.227

Table 4.17: HWS and IFLH comparison

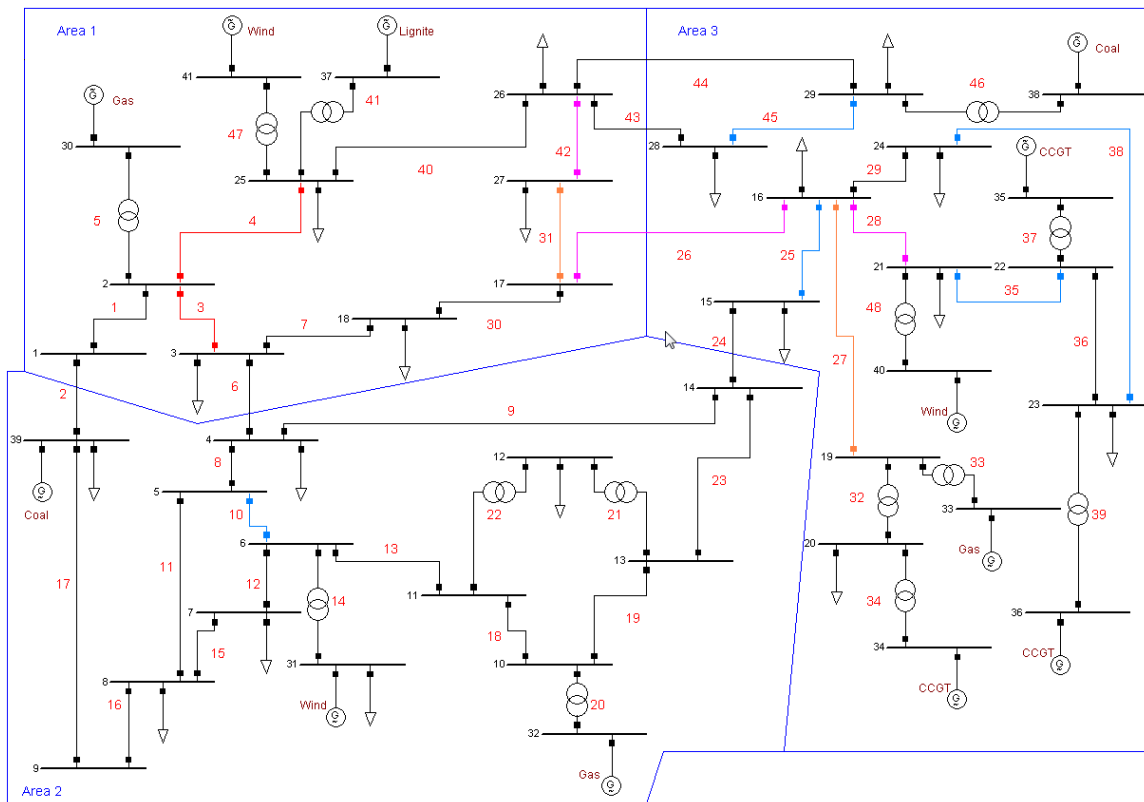


Figure 4.10: Ranking comparison for the HWRO case. In color code (from Red to Blue) the overloaded lines according to the values in Table A.16.

4.3.3 ACO

The Ant Colony Optimisation approach output is highly dependent on how its input parameters are tuned. Table 4.18 presents the basic input parameters and the values chosen.

Parameter	Value
Missions	5
Expeditions	100
Local Reduction Rate	0.7
Global Reduction Rate	0.95
Pheromone Quant	3.4
Max. number of upgrades	10
Reference Costs for Defining Quality	Full Curtailment (FC)

Table 4.18: ACO Inputs

Input Parameter Sensitivity

Before presenting the sensitivity scenarios results, this section illustrates the importance of tuning the ACO algorithm in obtaining reasonable results. Tables 4.20, 4.21 and 4.22, display a subset of different input parameter sensitivity runs, as defined in Table 4.19 and their effect on the optimum identified. The HW case defined for the LUCSIPO approach forms the base case for this comparison. The following factors that may affect the quality of the solution are analysed:

1. Number of missions per expedition the ants perform
2. Global pheromone reduction rate of the paths the ants follow
3. Behaviour of the algorithm against the maximum number of upgrades allowed
4. Whether forming a solution from the the most visited branches during the process (Best So Far (BSF) branches) augments the identification of a better solution
5. A combination of 2 and 4.

Input Parameter Combination	Missions	Max Upgrades	Global Rate	BSF
Base Case HW (BCHW)	5	10	0.95	YES
Missions (M)	2	10	0.95	YES
High Missions (HM)	10	10	0.95	YES
Global Rate (GR)	5	10	0.8	YES
Upgraded Branches (UB)	5	20	0.95	YES
No BSF (NB)	5	10	0.95	NO
No BSF, Global Rate (NBGR)	5	10	0.8	NO

Table 4.19: Selected Input Parameter Sensitivity Scenarios.

First, the ACO algorithm sensitivity is tested against the number of local missions the ants perform. Table 4.20 presents a comparison of the Base Case scenario (BCHW) with the M

Parameter Scenario	BCHW	HM	M
Expedition Conv. Break	59	51	51
Expedition	39	32	10
Curtailed Energy (%)	0.81	0.76	0.75
Upgraded Branches	6	7	9
Curtailment Costs (M€)	0.072	0.103	0.067
Op. Policy Costs (M€)	0.000	0.000	0.000
Operational Costs (M€)	14.134	14.202	14.085
Investment costs (M€)	0.304	0.348	0.474
Length(km)	302.7	346.8	472.4
Upgraded Branches	3 4 10 26 27 28 42	3 4 7 26 27 28x2	3 4 26 27 28 31 35 42 45
Total Costs (M€)	14.510	14.653	14.627

Table 4.20: *ACO Tuning Tests, Part I*

and HM scenario. As shown, a reduction of the number of intra-expedition missions from 5 to 2 results in the shrinking of the search space and thus produces a higher cost solution. On the other hand, further increasing the local missions to 10, over-diversifies the search space and does not allow for generating a lower cost solution. The BSF rule is of major importance in such a case since it determines the achieved solution. Table 4.21 compares the BCHW and the UB case where the maximum allowed number of upgrades has increased to 20. As shown, the ACO algorithm obtained a less cost effective solution, where the decrease of the operational costs was overcompensated by the additional capital costs which led to higher total system costs.

Moreover, Table 4.22 compares the BCHW, with a global reduction rate of 0.95, against the GR case with a rate of 0.8. Additionally, the NBGR and NB cases are presented, where a solution obtained from the Best branches So Far (BSF) is not evaluated against the ones identified by an ant mission. The results show total system costs of a few hundred e higher, and therefore less cost effective than the BCHW.

The graph in Figure 4.11 is used as an attempt to familiarise the reader with the branch convergence concept. It illustrates the branch pheromone accumulation for the HW scenario, as the number of expeditions the ants perform, increases in time. The vertical axis depicts the pheromone amount on each branch, corresponding to the probability for each specific branch to be part of the optimal solution. The depth axis portrays the number of expeditions, while the horizontal axis presents the New England system’s branches, also found in the appendix Table A.27. The graph shows that the branches 3, 4 and 28 are most visited by the ants and therefore become part of the optimal solution achieved. The last branch, termed “D” comprises a “dummy” branch that is implemented in order to allow the ACO algorithm to find solutions which contain less upgrades than the maximum limit defined in Table 4.18.

Parameter Scenario	BCHW	UB
Expedition Conv. Break	59	52
Expedition	39	19
Curtailed Energy (%)	0.81	0.80
Upgraded Branches	6	12
Curtailment Costs (M€)	0.072	0.072
Op. Policy Costs (M€)	0.000	0.000
Operational Costs (M€)	14.134	14.093
Investment costs (M€)	0.304	0.514
Length(km)	302.7	511.8
Upgraded Branches	3 4 10 26 27 28 42	3 4x2 10x2 26x2 27 28 31 42x2
Total Costs (M€)	14.510	14.678

Table 4.21: ACO Tuning Tests, Part II

Parameter Scenario	BCHW	GR	NBGR	NB
Expedition Conv. Break	59	54	52	56
Expedition	39	25	21	30
Curtailed Energy (%)	0.81	0.74	0.81	0.79
Upgraded Branches	6	8	7	9
Curtailment Costs (M€)	0.072	0.066	0.073	0.070
Op. Policy Costs (M€)	0.000	0.000	0.000	0.000
Operational Costs (M€)	14.134	14.133	14.129	14.129
Investment costs (M€)	0.304	0.384	0.359	0.408
Length(km)	308.7	382.0	358.0	406.6
Upgraded Branches	3 4 10 26 27 28 42	3 4 26 27 28x2 30 42	3x2 4 26 27 28 42	3 4 10 26 27 28 31 35 42
Total Costs (M€)	14.510	14.582	14.561	14.607

Table 4.22: ACO Tuning Tests, Part III

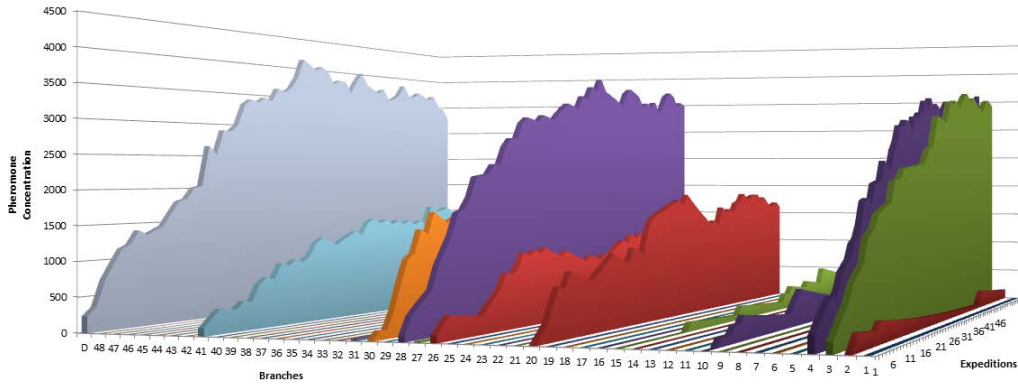


Figure 4.11: HW Scenario. Branch convergence for the ACO approach.

Sensitivity Cases

Tables 4.24, 4.23, 4.25 and 4.26 present the sensitivity cases equal to those performed for the LUCSIPO runs in order to evaluate whether the two methodologies exhibit the same behaviour.

Scenario	BC	HW	LW
Expedition Conv. Break	52	59	51
Expedition	48	39	10
Upgraded Branches	8	6	9
Curtailed Energy (%)	0.00	0.81	0.00
Curtailed Costs (M€)	0.000	0.072	0.000
Op. Policy Costs (M€)	0.000	0.000	0.000
Operational Costs (M€)	16.615	14.134	18.181
Investment costs (M€)	0.270	0.304	0.406
Upgraded Length(km)	268.5	302.7	404.0
Upgraded Branches	3 4x2 15x3 26 28	3 4 26 27 28 42	3 4 19 25 26 27 28 35 42
Total Costs (M€)	16.884	14.510	18.587

Table 4.23: BC and HW - LW cases comparison for the ACO implementation

First, the elasticity of the ACO algorithm to the three wind capacity scenario cases is tested in Table 4.23. The costs in the LW case are significantly higher (1.7 M€) and the main reason for the large difference is the operational cost. Nevertheless, as the LUCSIPO approach showed as well, the LW scenario requires additional expansion. The HW case, as anticipated, yields the lowest operating costs while discarding a small percentage (0.81 %) of the available wind in-feed.

Table 4.24 shows the MRCGP limit sensitivity scenarios when run against the Base Case. As expected, the total costs follow the changes in the operational policy. Increasing the MRCGP limit (HL), results in a slight increase in the total costs mainly due to wind energy

Scenario	BC	HL	LL
Expedition Conv. Break	52	51	51
Expedition	48	40	10
Upgraded Branches	8	9	9
Curtailed Energy (%)	0.00	0.34	0.00
Curtailement Costs (M€)	0.000	0.023	0.000
Op. Policy Costs (M€)	0.000	0.000	0.000
Operational Costs (M€)	16.615	16.534	16.355
Investment costs (M€)	0.270	0.356	0.474
Upgraded Length(km)	268.5	354.2	472.4
Upgraded Branches	3 4x2 15x3 26 28	3 4 26 27 28 31 35 42 45	3 4 18 25 26 28 29 35 42
Total Costs (M€)	16.884	16.912	16.830

Table 4.24: BC and LL - HL cases comparison for the ACO implementation

curtailment and consequently higher fossil fuel generation costs. On the contrary, reducing the MRCGP to 20% of the total system demand yields additional grid expansion needs but, nevertheless, leads to lower total system costs in the range of 50,000 €, compared to the BC.

The congestion that the MRCGP limit introduces in the network is further investigated in Table 4.25. Requiring the high operational limit for conventional generation in the HWHL case, increases the total system costs by half a million €, due to additional operational and curtailment costs. The 20% policy (LL), on the other hand, minimises both the curtailed wind energy and the total system costs although slightly higher investment costs are necessary

As shown in Table 4.26, the ACO methodology is sensitive towards the MC case because the curtailment costs are an integral part of the objective function that guides the algorithm towards better solutions. The marginal cost approach yields a slightly more cost-effective final solution (in the range of 50,000 €) when compared to the feed-in-tariff scheme, which is followed in the base case. The results obtained with the ACO algorithm when the RO ranking is used for its initialisation instead of the linear approach that was coupled with the ICPPRO index (BC), are also presented in Table 4.26. The RO ranking introduces a small difference in the total system costs in the range of 40,000 €.

An evident trend observable in the solutions obtained by the ACO is the lack of any operating policy costs. Since the ACO DC-OPFs are not constrained by any minimum wind curtailment limit P_{cur} as in the LUCSIPO case, the units are free to curtail as much energy as needed in order to produce a feasible solution.

It should be mentioned that the ACO gives no guarantee of absolute convergence. Although, there are indications of pheromone concentration convergence on certain branches, no global optimum has been obtained from a total system cost point of view. A reason for this behaviour could be the fact that the ACO runs on sub-optimal input parameters. Trial and error could lead to a different selection of parameters such as the pheromone update rates and the number of missions.

Scenario	HW	HWLL	HWHL
Expedition Conv. Break	59	55	91
Expedition	39	10	25
Upgraded Branches	6	9	8
Curtailed Energy (%)	0.81	0.10	3.14
Curtailed Costs (M€)	0.072	0.009	0.272
Op. Policy Costs (M€)	0.000	0.000	0.000
Operational Costs (M€)	14.134	14.019	14.303
Investment costs (M€)	0.304	0.428	0.423
Upgraded Length(km)	302.7	426.6	421.2
Upgraded Branches	3 4 26 27 28 42	3 4 10 26 27 28 31 35 42	3x2 4 26 27 28 35 42
Total Costs (M€)	14.510	14.456	14.999

Table 4.25: HW and HWLL - HWLL cases comparison for the ACO implementation

4.3.4 ACO - LUCSIPO comparison

This section presents a comparison between the optimum solution obtained by the two algorithms for the sensitivity scenarios defined in earlier sections. Tables 4.27 and 4.28 contain the best solutions achieved from the LUCSIPO and the ACO approach for the Base Case and High Wind scenarios respectively while the appendix Tables A.20 - A.26 present the results obtained for the rest of the sensitivity cases.

For the Base Case scenario, as shown in Table 4.27, the LUCSIPO approach has achieved a slightly lower total cost solution in the range of 100,000 €. None of the approaches resulted in any wind energy curtailment. Due to the quite different list of upgraded branches the operational costs are slightly higher for the solution obtained from ACO. However, the calculation time of the two methodologies differs significantly. The LUCSIPO approach solved the Base Case 5.5 times faster than the ACO implementation.

The High Wind case comparison is presented in Table 4.28. The ACO identified a better (from a total cost perspective) solution by a factor of 50,000 €. Although it resulted in higher curtailed wind energy (by 0.06%) and operational costs, the investment cost savings due to the fewer upgraded branches enabled the ACO to yield a more cost-effective solution. Finally, and as described earlier, the ACO implementation did not show any operational policy costs. The LUCSIPO approach, on the other hand, delivered a slightly worse solution but the speed gain achieved a factor of 3.6.

Figure 4.12 illustrates the solution quality comparison of the best solutions achieved by the two methodologies for the various sensitivity cases. The measure for comparing the solutions, is the total system costs. As shown, the resulting costs follow the same distribution over the sensitivity scenarios for both the ACO and the LUCSIPO methodologies, while the cost difference between the best achieved solution is relatively small. A closer look at the results reveals that the ACO performs slightly better in the highly congested cases (HW and HWHL) while, in the non-congested scenarios, the LUCSIPO yields more cost-effective solutions.

Calculation time wise though, the LUCSIPO is notably faster than the ACO. Figure 4.13 portrays the calculation time each approach needed for solving the same sensitivity scenario.

Scenario	BC	MC	RO
Expedition Conv. Break	52	51	51
Expedition	48	10	10
Upgraded Branches	8	9	9
Curtailed Energy (%)	0.00	0.00	0.00
Curtailement Costs (M€)	0.000	0.000	0.000
Op. Policy Costs (M€)	0.000	0.000	0.000
Operational Costs (M€)	16.615	16.356	16.410
Investment costs (M€)	0.270	0.453	0.433
Upgraded Length(km)	268.5	451.5	431.0
Upgraded Branches	3 4x2 15x3 26 28	3 4 25 26 27 28 31 35 42	3 4 26 27 28 30 31 36 42
Total Costs (M€)	16.884	16.809	16.843

Table 4.26: *BC and MC, RO case comparison for the ACO implementation*

For all cases the LUCSIPO has solved the TEP significantly faster. The LUCSIPO needs an average of 18.17 minutes while the mean ACO calculation time amounts to 86.39 minutes. Finally, it is important to highlight that the highly congested HWHL scenario is found to be the most time intensive case for both approaches.

4.3.5 MatPower/Matlab - PowerFactory comparison

Due to the inherited DPL language limitations, the developed non inter-temporal unit commitment methodology used in MatPower is not part of the PowerFactory model. The comparison between the two models is undertaken using the minimum limit unconstrained DC-OPF approach where the minimum output limits of the conventional generators are set to zero. Table 4.29 presents the results for the HWS case when PowerFactory and Matlab are employed.

One can observe that the results are similar but still some deviations are present. This is the result of the different solvers used in each case: the built-in PowerFactory solver and the IBM CPLEX for MatPower. Moreover, small deviations can also be attributed to the non-identical implementation as a result of the differences between the object-oriented PowerFactory DPL and the more C-like Matlab programming language. In any case, the PowerFactory implementation yielded lower total costs and upgraded fewer branches. It also introduced major calculation time speed-up.

In order to illustrate the solver differences, Table 4.30 presents the generators dispatch for the 1st hour selected by the k-means algorithm (314th hour of the year). The unconstrained case corresponds to the OPF performed during the statistical overload ranking.

Under the same demand and wind conditions, there is a deviation in the OPF results. For the unconstrained case, PowerFactory dispatches the coal generator at bus 38 to zero, while MatPower yields a zero output for the coal generator at bus 39. The results are further differentiated for the constrained case. In order to cover a 527 MW load at bus 20, MatPower dispatches the CCGT unit at bus 34 to 500 MW while PowerFactory to 93 MW. The additional power is covered by further increasing the output of the coal units at bus 38 and 39 and thus

Scenario	Base Case (BC)	
Method	LUCSIPO	ACO
Upgraded Branches	5	8
Curtailed Energy (%)	0.000	0.000
Curtailment Costs (M€)	0.000	0.000
Op. Policy Costs (M€)	0.000	0.000
Operational Costs (M€)	16.555	16.615
Investment costs (M€)	0.232	0.270
Upgraded Length(km)	231.4	268.5
Upgraded Branches	3 4 26 28 42	3 4x2 15x3 26 28
Total Costs (M€)	16.788	16.884
Calculation Time (sec)	851.8	4678.5

Table 4.27: ACO and LUCSIPO Results Comparison for the Base Case.

Scenario	High Wind (HW)	
Method	LUCSIPO	ACO
Upgraded Branches	9	6
Curtailed Energy (%)	0.75	0.81
Curtailment Costs (M€)	0.026	0.072
Op. Policy Costs (M€)	0.041	0
Operational Costs (M€)	14.069	14.134
Investment costs (M€)	0.428	0.304
Upgraded Length(km)	426.6	302.7
Upgraded Branches	3 4 10 26 27 28 31 35 42	3 4 26 27 28 42
Total Costs (M€)	14.564	14.510
Calculation Time (sec)	1468.8	5284.8

Table 4.28: ACO and LUCSIPO Results Comparison for the High Wind Case.

Software Tool	MatPower	PowerFactory
Curtailment Limit (%)	60	60
Upgraded Branches	4	3
Curtailed Energy (%)	0.46	0.36
Curtailment Costs (m euro)	0.041	0.032
Op. Policy Costs (m euro)	0	0
Operational Costs (m euro)	14.172	14.208
Investment costs (m euro)	0.178	0.146
Length (km)	177.5	145.0
Upgraded Branches	3 4 26 28	3 4 28
Total Costs (m euro)	14.392	14.385
Calculation Time	842.6	69.5

Table 4.29: *PowerFactory and MatPower Comparison for the HWS case.*

Generator dispatch for the 314 th hour of the year				
Generator Bus	Unconstrained		Constrained	
	PowerFactory	MatPower	PowerFactory	MatPower
30	0	0	0	0
31	732	732	732	732
32	0	0	0	0
33	0	0	0	0
34	0	0	92.67	499.78
35	0	0	0	0
36	0	0	0	0
37	965	965	812.67	812.67
38	0	1047.728	142.4	60.26
39	1047.73	0	1100	775.02
40	1072	1072	936.98	936.98
41	270	270	270	270

Table 4.30: *PowerFactory and Matpower dispatch comparison*

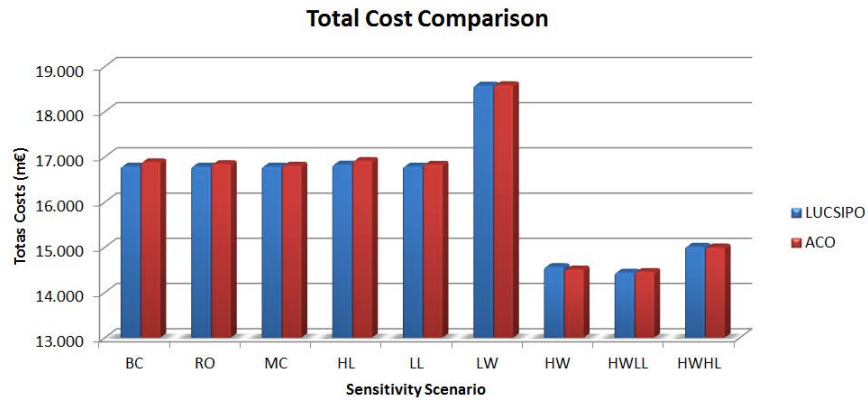


Figure 4.12: Total Cost Comparison for the LUCSIPO and the ACO approach.

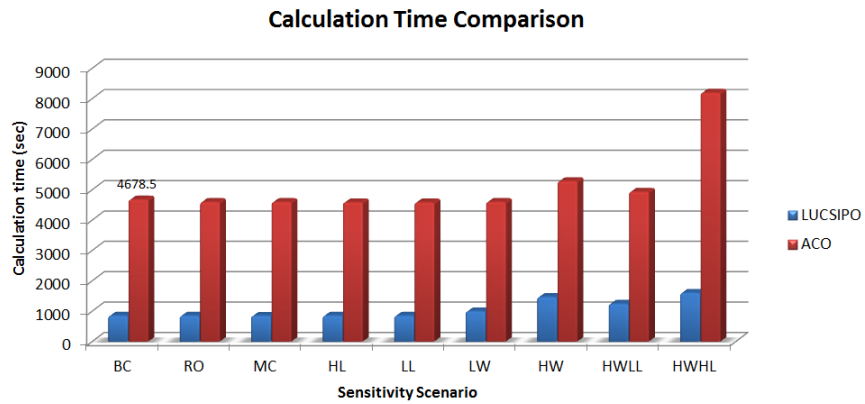


Figure 4.13: Calculation Time Comparison for the LUCSIPO and the ACO approach.

yields a lower cost solution. As a result, branch 27 is operated at 91% of its capacity in PowerFactory while only at 6% in MatPower. Therefore, it is reasonable to assume that the output is highly dependent on the employed solver used in the OPF.

4.4 Conclusions

This chapter presented the New England Test System which is the network model employed for assessing and comparing the two developed TEP methodologies. It comprises a small, flexible test system that contains the same modelling principles as the pan-European network model presented in chapter 5. Moreover, chapter 4 described the several sensitivity scenarios assumed, in order to validate the outcomes generated by the ACO and the LUCSIPO approach. The results include the upgrade candidate lists determined together with the cost and computation performance comparison of the achieved solutions. The figures displayed in this chapter, comprise information of high value for the analysis presented in the conclusion chapter.

Both TEP approaches were applied in a series of sensitivity analysis cases. The base case assumed a moderate wind capacity scenario, a 40% MRGCP limit, the feed-in-tariff scheme and the ICPPCRO ranking approach. The sensitivity scenarios included variations on the installed wind capacity, the MRGCP limit, the curtailment cost calculation approach and the ranking methodology followed.

The sensitivity analysis results prove the existence of an economic optimum between grid upgrades and RES curtailment. They further highlight the importance of network upgrades and high non-synchronous penetration limits for secure and cost-efficient large scale RES integration. The merit order effect is also pinpointed as a factor that has a direct impact on the trade-off between RES curtailment and grid extension.

The developed LUCSIPO approach has proved to be a simple and straight-forward TEP technique which is significantly faster than the ACO methodology. The final solution quality achieved, from a total system cost point of view, is comparable to the solutions obtained by the ACO technique. In some cases the LUCSIPO approach seems to produce even slightly more cost-effective results. Important to highlight is also the different upgrade list the two approaches produce. By making both options available to the planner, other factors such as environmental reasons or local opposition may favour the construction of one line over another.

Nevertheless, the ACO has not shown signs of absolute global convergence. Hence, it is reasonable to assume that finer tuning of its input parameters will augment its convergence to higher quality outputs. On the contrary, the LUCSIPO has most probably reached its performance limits.

Chapter 5

Flexible Computer Aided Transmission Network Modelling for Europe

This chapter describes the creation of a pan-European transmission system DC Load flow model, that was developed in cooperation with the Power Systems and Markets team in Ecofys Berlin. It deals with the design of a flexible, highly adjustable platform for network simulations, with the goal of applying the developed TEP methodologies. After presenting the main software tools employed, it outlines the setting up of a consistent dataset comprising of geo-referenced conventional and renewable generation, demand and network information. It also presents a step-by-step design guide for obtaining a fully functional and consistent network model. Finally, it introduces a short review on network reduction techniques and proceeds with suggestions about reducing the developed Pan European Network Model.

Figure 5.1 illustrates the main steps involved when constructing a DC - LF model from large datasets. A database management tool, such as PostgreSQL and a network simulation tool, such as DlgSILENT PowerFactory are necessary.

In this chapter the following terminology convention is followed:

- **Substation**

It refers to an actual geo-referenced substation provided by the external supplier.

- **Terminal**

It is a network simulation software object, used for representing the nodes of the grid model.

- **Region**

It refers to a geographical model region. Its surface (cover area) is used, among other, for determining the terminal objects that will represent the substations.

- **NUTS region**

It stands for Nomenclature of Units for Territorial Statistics. It is a multiple level region unit used for statistical reasons in Europe.

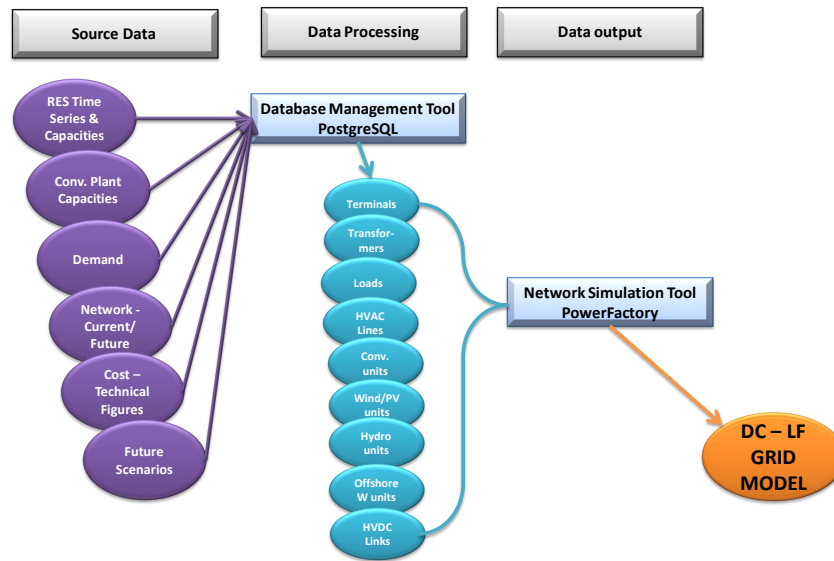


Figure 5.1: High Level Transmission System Network Modelling. .

5.1 Tools Overview

Developing a pan-European network model involves vast amounts of data. Dedicated software tools are needed in order to facilitate the handling of the dataset. A database management system, a Geographic Information System (GIS) tool and a network simulation tool need to be employed.

5.1.1 Database Management System

PostgreSQL, or simply *Postgres*, is used as the database management system. It is utilised for creating and storing a consistent dataset for the European power system including power plant datasets, RES installed capacity datasets, demand/generation time series and network parameters. Postgres functions as the interface between the network model and the dataset. It also serves as the backbone for the visualisation of modelling results, since it smoothly links with the GIS tool.

Postgres is an object-relational database system with an open source license. It has exhibited a 15 year proven track-record and comprises a highly flexible tool that is compatible with major programming languages and data formats [99]. Finally, an advantage of critical importance is the compatibility with PostGIS. PostGIS is an open source software that adds support for geographic objects to the PostgreSQL [100].

5.1.2 Geographic Information System

QuantumGIS is the GIS visualisation software, chosen due to its user-friendliness and smooth interface with the Postgres database. QuantumGIS, is an open source GIS that runs on several operational system and supports numerous data functionalities [101].

5.1.3 Network Simulation Tool

DIgSILENT PowerFactory is the network simulation tool employed for modelling the pan-European power system. Its data management system superiority is the reason that it was selected against MatPower. Nonetheless, a PL/pgSQL¹ interface with Matlab has been also designed.

5.2 Data Overview

One of the main goals of this thesis is to provide a consistent dataset for a European HV transmission system model, where the developed TEP methodologies can be applied; this consistent dataset comprises of

- Regionalised demand time series,
- Regionalised conventional power plant installed capacities,
- Regionalised wind and solar generation time series,
- Network infrastructure data.

Wind and solar time series data, together with the existing European grid infrastructure are provided by external data suppliers [23, 102–104] while reasonable assumptions must be taken for the:

- New network infrastructure,
- Conventional generation portfolios
- Installed wind - solar power
- Non wind - solar RES generation

based on publicly available data [105, 106] and studies [11, 15, 28, 107].

An overview of the available data together with their supplier and the year they correspond to is found in this section.

2012 Network Data

An external supplier, Platts, provided the PowerVision database [23]. It contains European wide information with regard to:

- Geo-referenced power lines,
- Geo-referenced substations
- Geo-referenced conventional (and not) Power Plants

Figure 5.2, presents the HVAC 220 kV - 380 kV and HVDC European transmission network, as provided by the Platts database. The ENTSO-e interconnected countries are shown in brown. Figure 5.3 provides a detail of Figure 5.2. It depicts the HV Network and conventional power plants in Germany. The darker areas correspond to the NUTS 2 regions of Germany. The Appendix Table B.1 presents the installed conventional capacities for major European countries according to the Platts database.

¹The procedural language used by Postgres.

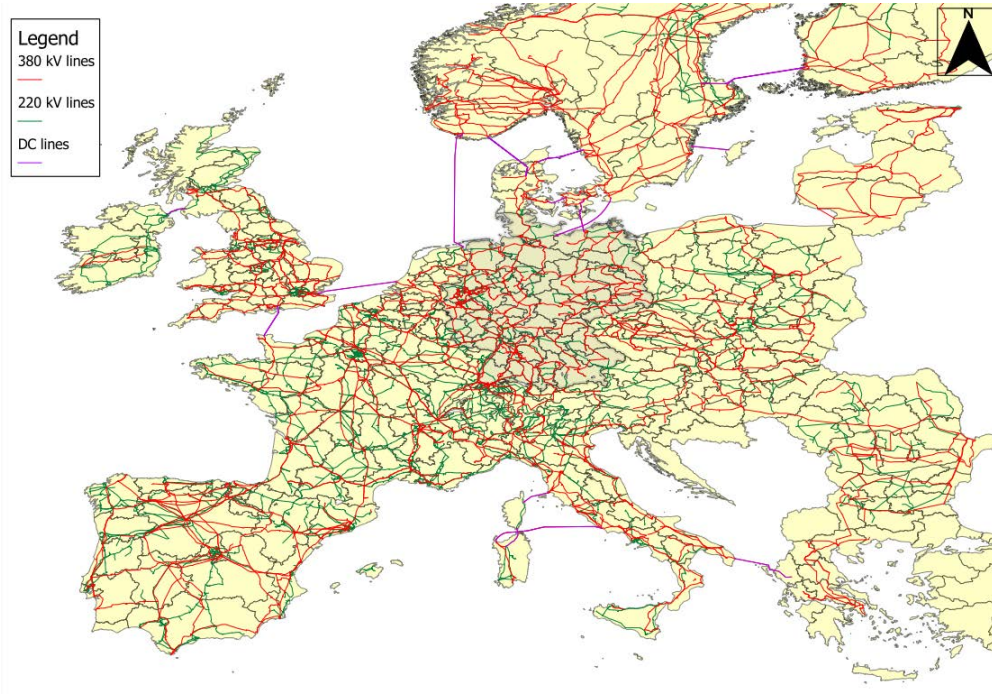


Figure 5.2: 2010 Transmission Network Corridors in Europe. Own representation based on [23].

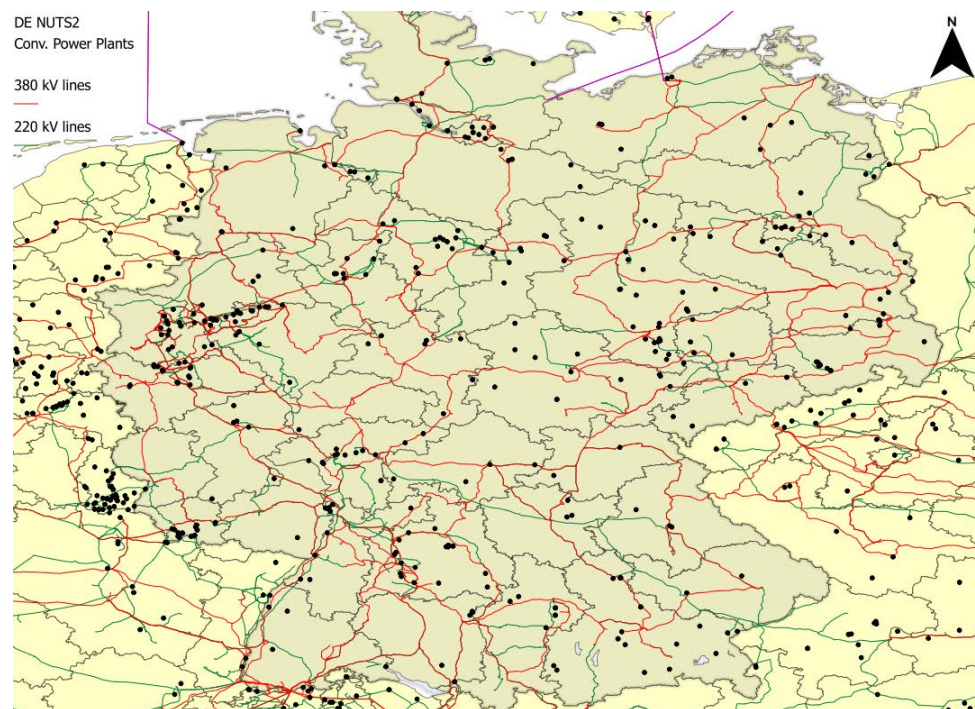


Figure 5.3: 2010 German Power Networks & Conventional Power Plants. Own representation based on [23].

Future Transmission Infrastructure

Two publicly available sources are utilised in order to integrate potential future changes in HV transmission infrastructure. For Germany, the data are extracted from the Netzentwicklungsplan (Network Development Plan) [31]. For the rest of Europe the ENTSO-e Ten Year Network Development Plan (TYNDP) [108] is used. For more realistic construction times, scenarios applying 5 and 10 year delays have been also assumed. Different paths and starting points can be used for integrating the transmission corridors assumed by each scenario.

Transmission Line Ratings

The Platts database does not provide detailed information on the capacity rating of each transmission corridor. The publicly available ENTSO-e statistical yearbook [109] is used for determining the capacity of the cross-border transmission lines. For national lines, typical values are used. Moreover, the publicly available ratings of the HVDC projects across Europe are also taken into account.

RES Generation Time Series

Data provided from an external supplier, EuroWind [102] are used as the hourly solar and wind in-feed time series. The data account for three model years:

- 2007: Extreme good wind year ($WYI^2 = 104\%$)
- 2008: Average wind year ($WYI = 99\%$)
- 2010: Extreme bad wind year ($WYI = 74\%$)

The EuroWind High Resolution Limited Area Model (HiRLAM) provides the wind data for selected regions in Europe. The model is using a horizontal resolution of 0.2°C which corresponds to a grid of about $20\text{km} \times 20\text{km}$. An actual temporal resolution of 3 hours is interpolated to an hourly resolution. The HiRLAM creates a model year on the basis of wind indices for a reference period between 2001 and 2010 [102]. Similarly, a Global Forecast System (GFS) model provides radiation data in a $100\text{ km} \times 100\text{ km}$ resolution, which after interpolation, produce the hourly radiation data for the requested years.

The data is provided in a country specific spatial resolution as shown in Table 5.1. The data contain both wind speeds/solar irradiation values but also normalised values which are scaled to the maximum instant per region. Moreover, EuroWind provides averaged offshore wind time series for ten European coastal areas, as selected by the industrial partner Ecofys. An overview of the selected regions is given in the Appendix Figure B.1.

Country	Resolution
DE	Two Digit Postal Code
IT,FR,ES,CH,CZ,PT,PO	NUTS 2
Rest	200 x 200 km grid

Table 5.1: *Spatial Resolution of the provided EuroWind data*

Due to lack of any other reliable source, monthly data for hydro production provided by ENTSO-e [111] are utilised in order to provide the hourly time series for hydro power plants. The monthly generation data has been divided by the number of hours of each month and distributed to the divergent forms of hydro generation.

²Wind Year Index as provided by [110].



Figure 5.4: Area (Longitude: 12° W to 30° E - Latitude: 35° S to 70° N) covered by HiRLAM. Source: [102]

Load - Demand Time Series

The publicly available ENTSO-e [105] database is used for the national demand profiles.

In order to avoid any confusion, the difference between the vertical load and the (actual) load is highlighted at this point. The vertical load, as provided by the entso-e transparency platform www.entsoe.net [18], is

The sum, positive or negative, of all power transferred from the transmission grid through directly connected transformers and power lines to distribution grids and final consumers [112].

On the contrary, the (actual) load as provided by www.entsoe.eu [105], is

The hourly average active power absorbed by all installations connected to the transmission network or to the distribution network. Load is the power consumed by the network including the network losses but excluding the consumption for pumped storage and excluding the consumption of generating auxiliaries [105]

The fundamental difference is that the vertical load does not account for the distributed generation since both solar farms but also the bulk of the wind power parks are connected to the distribution network. Thus, the national load profiles, provided by the second data portal are the ones used to represent the demand time series. This thesis deals only with (actual) load profiles.

The graphs in the appendix Figure B.2 illustrate the above described difference for a typical winter and spring week in Germany. The vertical load is highly distorted and does not provide actual consumption information.

Population

EU statistics [104] were used in order to obtain the European NUTS 3 regions populations. According to Bialek [15], the fraction of the region population over the national population suffices for an estimation of the regional load. Thus, dividing the region population obtained by Eurostat [104] with the national population yields a load fraction. Under the assumption that this load fraction is static for future years, the demand time series can be regionally distributed.

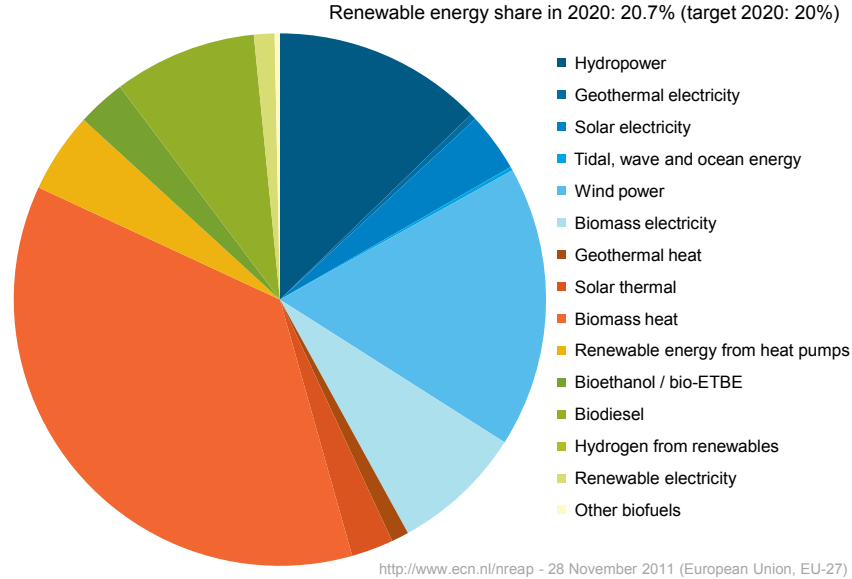


Figure 5.5: *Renewable shares in The EU - 2020.* Source: [115]

Installed RES Capacities

The publicly available 2010 Energymap [103] provide Germany’s PV, wind and biomass installed capacities. The spatial resolution of the data is the 5 digit German postal code area. For the rest of the EU Member States data are taken from Energia Electrica [113] and Eurostat [104]. Detailed colour code maps of the 2010 installed wind, solar and biomass capacities around Europe are shown in the Appendix Figures B.3, B.5 and B.4 respectively. Moreover, the Appendix Table B.2 presents the EU-27 national RES installed capacity for 2010 while Table B.1 contains the corresponding 2 digit postal code RES installed capacities in Germany.

Future RES Capacities

Defined in Article 4 of the European Renewable Energy Directive [114], each European Member State has provided a National Renewable Energy Action Plan (NREAP) to the European Commission. It contains RES capacity projections up to the year 2020, in order to meet the 20-20-20 [2] targets across the European Union (EU). Assigned by the European Environment Agency (EEA), the Energy research Centre of the Netherlands (ECN), has collected all energy-related data for all 27 European Union Member States (dated 28 November 2011) [39].

The pie graph of Figure 5.5 presents the share of Renewables in a 2020 European Union according to the NREAP. The graphs in Figures B.6 - B.9 of the Appendix depict the European Member States 2015 and 2020 targets. Those target values are used to scale up the existing regional RES capacities.

In order to separately account for offshore wind infrastructure, the publicly available 4coff-shore [106] platform provides both the current but also the future offshore wind parks capacities. The construction status information provided allows to project future capacity scenarios. Figure 5.6 portrays a visualization of the offshore wind farms in the Exclusive Economic Zones

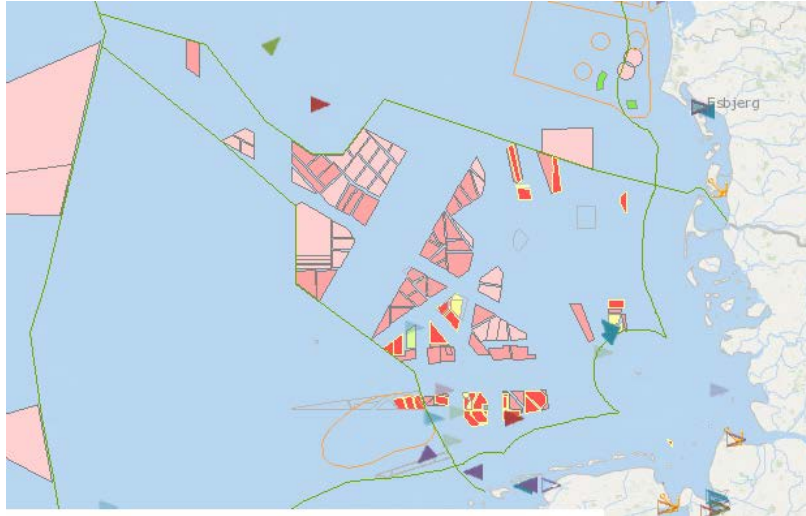


Figure 5.6: *Offshore Wind Farms at the North Sea. Source: [106]*

(EEZ) of Germany and Denmark at the North Sea. Actual data are presented in Tables B.5 and B.6.

Grid Expansion Costs

Cost of transmission infrastructure has been quite a widespread subject of literature during the past years. L'abbate and Miglavacca [97] have published a review paper that provides country specific prices per km of HVAC 380 and 220 kV lines together with cost indicatives of transformers and DC connections. Table B.7 presents average cost indicative figures for several transmission technologies.

5.3 The European DC-LF model

5.3.1 Interface between Postgres & PowerFactory

In order to construct the network DC-LF model, it is necessary to establish a proper interface between the database and PowerFactory. The described dataset needs to be transformed in a PowerFactory compatible format. Through the DGS interface, PowerFactory can read Postgres tables. PowerFactory is an object oriented modelling tool and handles all data as objects. Thus, each power plant unit becomes one row of the *ElmSym* table which contains all the synchronous machine objects. Each row will contain values that correspond to specific attributes of the PowerFactory object *ElmSym*.

PowerFactory handles three different object families:

- Element objects (e.g. out of service status, line length).
- Type objects (e.g. manufacturer data, R,X etc).
- Graphic objects (e.g. positions for graphical representation).

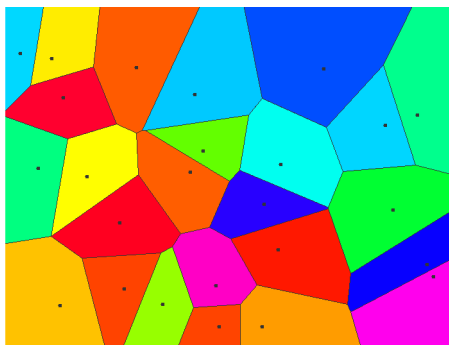


Figure 5.7: *Voronoi diagram. Source: [116]*

Each element object (e.g. *ElmSym*) created, also has a type object (e.g. *TypSym*) assigned to it. The demand and RES time series are stored in specific PowerFactory objects (*.ChaVec*), assigned to the load and generator objects respectively. The appendix Table B.4 presents the basic PowerFactory objects.

5.3.2 Network Model Regions

Spatial resolution flexibility was one of the major design principles during the development of the DC-LF modelling platform. Two basic options are covered; the Voronoi approach and the NUTS approach. The user can also specify a desired resolution that is a combination of both approaches. The underlying concept is the same for any choice: each model region is represented by a single node assuming there are no intra-region transmission line constraints (a.k.a. copper plates).

Voronoi

A voronoi diagram comprises the decomposition of Euclidean space into a predefined number of regions. Each Voronoi cell is the set of all points in the given space whose distance is shorter than the distance to the other cells. Figure 5.7 presents a decomposition of a euclidean plane into 25 cells performed on an on-line calculator from Cornell University.

The Voronoi approach is applied when high level of detail is required. The Euclidean space of the area under study is split into as many polygons as its number of geo-referenced HV substations. The Voronoi approach achieves the highest available spatial resolution. Every single power line is taken into account and the resulting network model is a nodal power flow model.

NUTS

On the contrary, the NUTS approach can be applied. The Nomenclature of Units for Territorial Statistics (NUTS) is an EU geocode standard for referencing the subdivisions of countries. For each EU member state, a hierarchy of three NUTS levels is established which does not necessarily correspond to administrative divisions within the country. NUTS 0 refers to country level while NUTS 1,2 and 3 include the divisions within each member state. NUTS 3 corresponds the highest spatial NUTS resolution available. A NUTS code begins with a two-letter code referencing the country, while the subdivisions are then referred with one number per hierarchy level [117]. For example, in Germany's case there are 429 NUTS 3 districts.

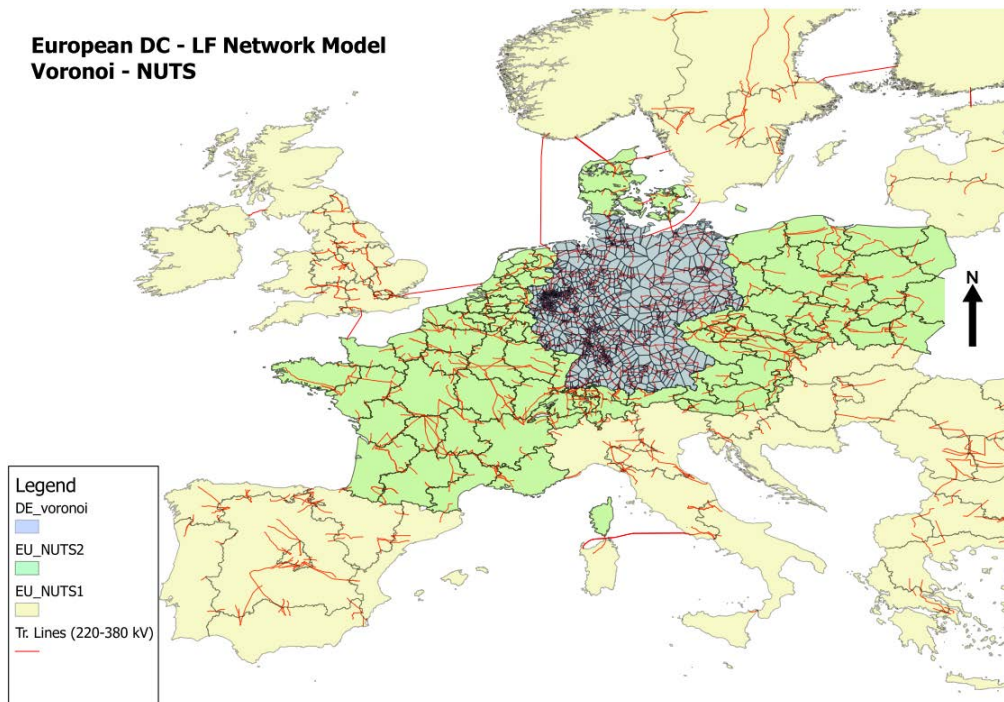


Figure 5.8: *DC-LF Network Model: Germany (Voronoi), surrounding countries (NUTS2) and rest of Europe (NUTS1).*

In case the NUTS approach is employed, the spatial resolution of the resulting grid model is significantly lower, varying with the level of NUTS hierarchy used. Since the model regions are assumed to be copper plates, the power lines connecting substations of neighbouring regions are only taken into account. The outcome is a zonal model, greatly reduced in comparison with the voronoi approach. This method is of great value for modelling system regions of lower focus. For example when the Spanish or Italian power systems are modelled for a study case that its main focus is Germany.

Figure 5.8 portrays the network model for the case where the Voronoi approach is employed for the region in focus (Germany). However, the NUTS concept has been used for modelling the Rest of the European System. Figure B.10 and B.11 of the Appendix depicts a NUTS-0 and a combined NUTS-1/NUTS-2 European model respectively.

5.3.3 High Level Region Components

The PowerFactory objects that correspond to each model region are assumed to follow the below defined nomenclature:

- region_name_Conv
- region_name_PV
- region_name_Wind
- region_name_Load

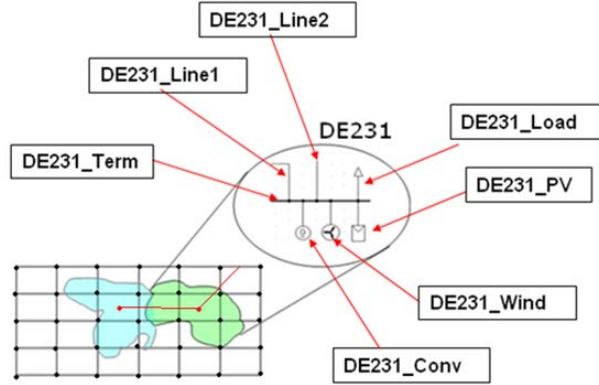


Figure 5.9: *High level components.*

- `region_name.Term`
- `region_name.Line`

Figure 5.9 gives an overview of the principles that the network model is based on. One can assume that the green area corresponds to the DE231 NUTS 3 region of Germany. DE231 is connected with the DE232 region (in blue). Each region is represented by a terminal object at which the disaggregated load, the conventional and renewable generation but also the inter-region transmission lines are accommodated. The overlay grid represents the spatial distribution of the renewable time series data supplied by the external partner. Overlapping this grid with each model region's cover area results in the extraction of the

- Wind and solar hourly in-feed
- Distributed load time series
- Installed wind, solar and biomass capacities

per model region.

The example presented in Figure 5.10 further illustrates the geo-processing undertaken for producing the distributed demand and RES figures. It represents the calculation of the hourly RES time series for the case that the EuroWind source data correspond to a 200 x 200 km spatial resolution (Table 5.1). Nonetheless the approach is the same for every case. An hourly output profile normalised for the capacities installed is given. Since this is different to the resolution required for input to the network model, geographical mapping is employed for rescaling the data to the desired output. Different shape sets are overlaid and the surface area fraction of the model region is calculated. As shown in Figure 5.10, the normalised profile will have to be multiplied by the corresponding installed capacity to obtain the actual output profile in MW. Then, 25% of the profile in cell B3, 60% of cell B4, 40% of cell B5, 40% of cell C4, 98% of cell C5 and 60% of cell C6 can be added to find the total solar and wind profile in the shaded model region.

5.3.4 Network Components Modelling

This section identifies key issues when modelling each separate component of the DC-LF model. It also presents the fundamental assumptions used for the development of this flexible platform.

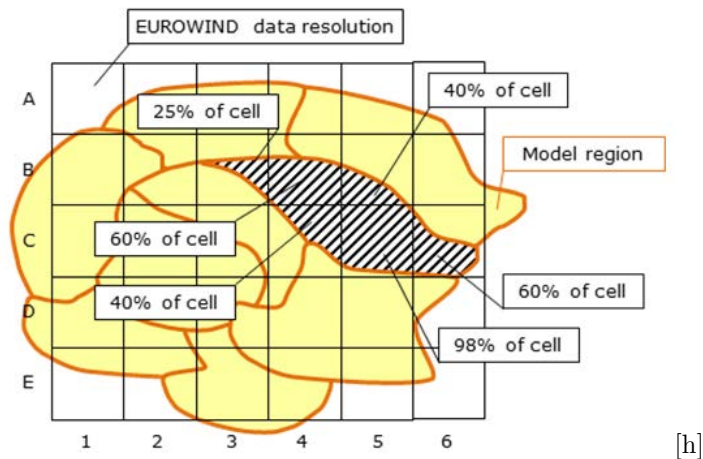


Figure 5.10: Geo processing. Source: [118]

Terminals

Each model region, either voronoi or NUTS, is represented by one PowerFactory terminal object (*ElmTerm*). In the case only, where two different voltage level transmission lines reach at the same geo-referenced region substation, two different terminal objects are built. This is due to the Platts database providing only maximum voltage information per substation. Figure 5.11 illustrates the decision process for constructing terminal objects out of the Platts substations for the voronoi approach.

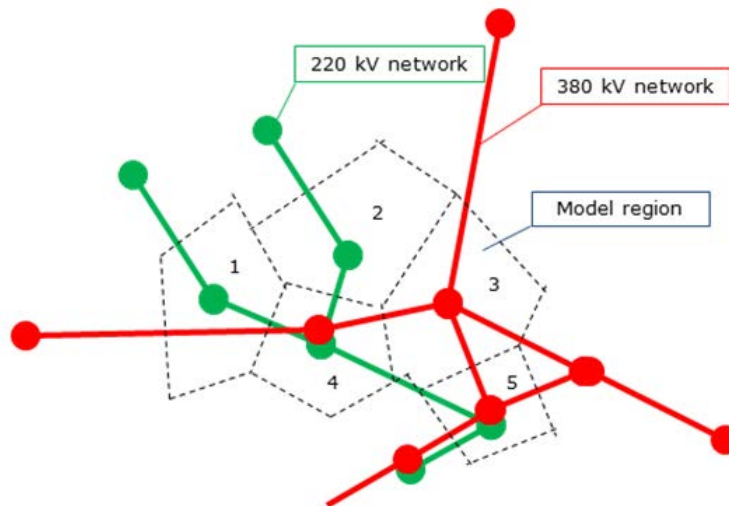


Figure 5.11: HV terminals modelling. Source: [118]

As shown in the example of Figure 5.11, the voronoi regions 1 and 2 have only 220 kV substations and region 3 has only a 380 kV substation. Regions 4 and 5 also have a single 380 Platts substation, but facilitate both HV Networks. Since the network model regions are based on Voronoi shapes around the HV substations, there will be one *ElmTerm* object for every model region that has a voltage level of either 380 kV or 220 kV. For regions 4 and 5,

two separate terminal objects are constructed. A similar approach is also used for the NUTS case. Due to the lower spatial resolution though, the case where both HV terminals exist is the norm.

Since all the middle/low voltage components are omitted, the loads used in this model are always high voltage (220 or 380 kV) loads, connected at the HV terminals. The power units are also directly connected to the HV terminals. In case there is only one terminal per model region, all the system components are connected to that terminal. On the contrary, if two PowerFactory nodes (*ElmTerm*) are employed, the convention used accommodates the conventional units at the 380 terminal, whereas the loads and RES units are assigned at the 220 kV bus-bars. The two terminal objects are connected via a transformer object as described in the following section.

Transformers

Transformers are used only in the case where power lines of different voltage levels reach the same region. In such a case, a transformer object (*ElmTr2*) is created in order to connect the two different voltage level terminals.

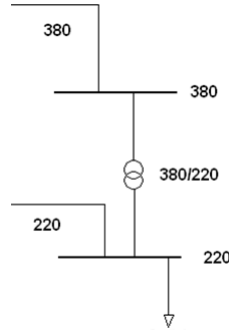


Figure 5.12: *Transformers modelling.*

The capacity rating is considered to be equal to the thermal rating of the strongest line the transformer is connected with. Nevertheless, transformers are not considered bottlenecks so their maximum capacity constraint is not activated during the model runs. For their impedance, a typical value of $U_k=12\%$ is assumed.

Loads

The load time series are provided by the ENTSO-e database in a country level. The national profile is then distributed in proportion with the NUTS 3 population according to the methodology suggested by Bialek [15]. The disaggregated load time series is then assigned to one characteristic vector (*ChaVec*) of a load (*ElmLod*) object.

Pre ENTSO-e unification (2010) data for specific countries were not included in the ENTSO-e dataset. Those data were obtained from the country state TSOs and specifically from Eirgrid [119], Ast [120], Svenska Kraftnet [121], Energinet [122], Fingrid [123], and National Grid [124]. In case of Norway and Lithuania, due to non availability of data, the ENTSO-e provided 2010 data were scaled in order to match the EURELECTRIC report [17] energy consumption value.

Further, different future consumption scenarios are assumed. The BMU LeadStudy [107] assumption of 13% load reduction by 2030 compared to 2008 values, is used as default. Other

studies' assumptions like Dena II [28] or Energynautics-Greenpeace [16] which assume stable or increasing demand profiles, have been also integrated. For enabling the modelling of every year between today and 2030, a linear approximation of the selected scenario rate is used in order to obtain the corresponding consumption figures.

Transmission Lines

An acceptable assumption for networks carrying bulk energy is to consider transmission lines only with voltage levels above and including 220 kV, i.e 220 and 380 kV. Although there is a significant amount of 110 kV lines in the European transmission network, their relatively small capacity renders them insignificant for a transmission network model [15]. Omitting the 110 kV lines is a limitation of the developed network model.

The actual transmission line dataset provided by the Platts database, is then used for creating the line objects that connect the neighbouring model regions. Standing out inconsistencies in the dataset were corrected manually by cross-checking the dataset with the ENTSO-e transmission system map. Since the Platts database lacks information on line impedance, typical transmission line impedance values per voltage level are assumed [125]. Expansion of this look up table is possible if further assumptions for different line capacities of the same voltage level are used, e.g. due to different bundling of the conductors. Moreover, other voltage level transmission lines found in UK and Norway (e.g. 345 or 300 kV) have been also modelled as 220 and 380 kV lines. Linear interpolation has been used in order to adjust the impedances found in Table 5.2.

Voltage(kV)	R (ohm/km)	X (ohm/km)
380	0.031	0.325
220	0.067	0.364

Table 5.2: Typical Transmission line Impedance values. Source: [125]

Further, for the line capacities, standardised values are used due to lack of information for intra-country transmission lines. Although information regarding the line distance is provided, no information is given about the line characteristics, such as conductor type, number of bundles or thermal capacity ratings. Since no other detailed data is publicly available, assumptions about these parameters are taken from the DENA-II Grid Study [28]. In this study different line ratings are assumed for existing and future lines due to improvements in transmission technology. Since values are given only for 380 kV lines, the 220 kV line rating value is extrapolated. This is done by assuming half the 380 kV line current due to half the number of bundles the 220 kV are usually built from. Equation (5.1) is used to calculate the transmission capacity ratings, which are in terms with values found in two German handbooks. All above mentioned figures can be found in Table 5.3. All apparent power ratings refer to active power ratings, since the developed network model is a DC-LF model.

$$S = \sqrt{3}VI \tag{5.1}$$

Conventional Power Plants

The Platts Database provides data for existing conventional power plant facilities in a unit detail. Information about plant lifetime and decommissioning date are also given. Fuel cost scenarios with efficiency assumptions depending on technology classes and installation year

Source	V(kV)	I (kA)	Bundles	S (MVA)
Dena II (existing lines)	380	2.72	4	1790
Dena II (new lines)	380	4	4	2633
Extrapolation (existing lines)	220	1.36	2	518
L'abbate and Miglavacca [46]	380	2.28	4	1500
Elektrische Energietechnik (1988)	220		2	625
	380		4	2500
Elektrische Kraftwerke und Netze (1978)	220		2	492
	380		4	1700

Table 5.3: *Line Ratings*

are also utilised. Each power unit is assigned to a PowerFactory synchronous generator object (*Elm.Sym*). As an example, Figure 5.13 shows the single line diagram of a typical gas turbine power plant. In this case, although the total rated capacity of the power plant is 300 MW, the total power actually comes from three units of 100 MW rated capacity each.

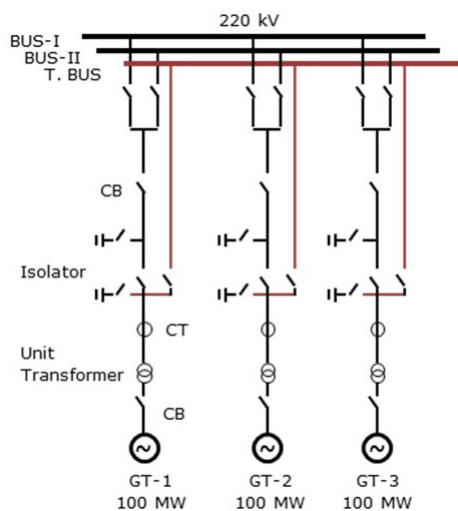


Figure 5.13: *Gas turbine power plant consisting of three units. Source: [118]*

Tables 3.1 and 4.2 of chapter 3 and 4 respectively present the assumptions used for the conventional generation technical figures and the future fuel price scenarios. Subclasses defined by construction year and extensions for co-generation that result in improved efficiencies are also integrated in the process.

Irrespective of the selected spatial resolution of the network model, the Voronoi regions are preliminarily utilised for determining the terminals that the conventional plants are connected with. In case the NUTS approach is selected, the plants are assigned to the NUTS region terminal that the Voronoi shapes are part of. Figure 5.14 depicts the decision making process that takes place based on the geo-information that comes with the Platts data. Further, Figure 5.15 presents an illustrating example. The conventional plants at regions 3 and 4 share the same coordinates with a HV substation so they are assigned to the corresponding terminal. On the contrary, fossil units at regions 1 and 2 are assigned to the HV terminal that is connected (through the MV line) with the substation on top of the unit. Finally, the non

substation connected unit in region 5 is accommodated at the terminals of the Voronoi region 5. In case a NUTS 3 resolution is selected, all the above plants are connected to a single 380 kV terminal.

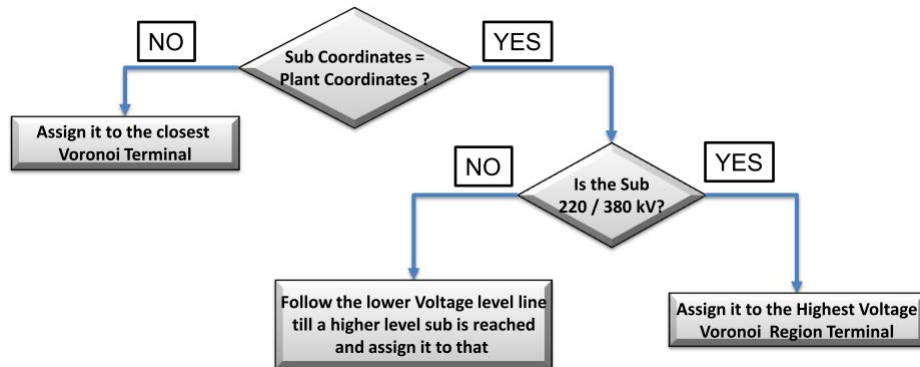


Figure 5.14: Assigning the plants at the voronoi regions decision making process. Sub refers to Substation.

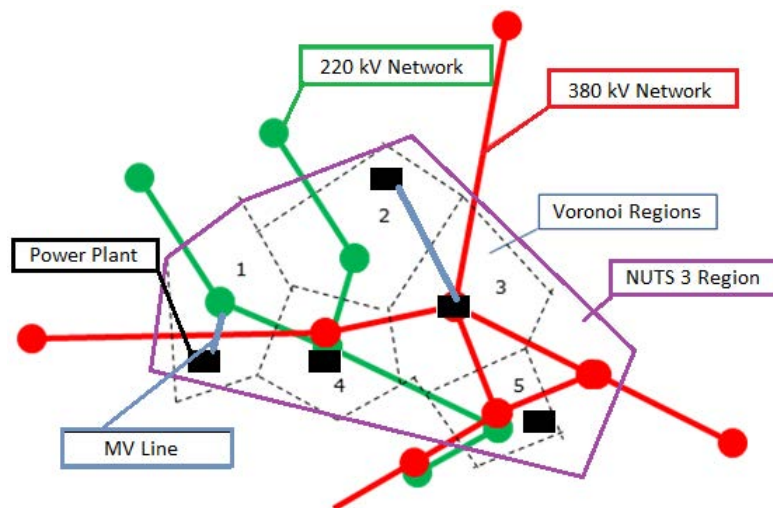


Figure 5.15: Assigning the plants.

In order to ease the computational effort and reduce calculation times, units of the same technology that belong to the same region, are aggregated into single synchronous machine (*Elm.Sym*) objects. The design is flexible in order to allow for aggregation up to a certain user defined absolute capacity limit. This step is of fundamental importance since not allowing for unit aggregation, ends up into the “explosion” of the problem constraint matrix. This may result in software inability to solve the power flow even in case the system is feasible.

As far as future conventional power plant portfolios are concerned, scaling up or down existing plant capacities is the most straight-forward option to be followed. The scaling takes place by evenly distributing the desired capacity per technology across the country. However, the Platts database provides also decommissioning information for the majority of the conventional units. For the rest, standard lifetimes per technology are assumed. Thus, in order to be consistent with the generic design of the model but also take into account upgraded technical figures due to improved learning curves, new units are also considered

for future scenarios. As a first step, identical (to the decommissioned) units are installed on the exact geographical spot. This is due to the fact that the location of the plants is highly dependent on the technology used. Mainly as a means to minimise fuel transportation costs. Specifically:

- Coal Plants are situated close to large rivers
- Lignite Units are located adjacent to lignite mines
- Natural Gas Plants are placed in the vicinity of natural gas pipelines
- Nuclear Plants are situated in areas abundant with water due cooling needs.

Solar & Wind units

Each model region cover area is used to produce the regionalised renewable profile after disaggregating the time series provided by EuroWind. The time series are then stored in a characteristic vector object (*ChaVec*) that is assigned to a synchronous generator object (*ElmSym*), used for simulating the PV/Wind production. Unlike the fossil plants which are modelled per individual unit, the wind and solar units are aggregated per model region.

The straight-forward approach to model the RES in-feed would have been to employ a static generator. Due to the focus of this study in the optimisation between RES curtailment and grid upgrades, all the units must participate in the system dispatch. The most efficient method to apply this concept is to use synchronous machine objects for modelling all available units.

The aggregated wind/solar farms are modelled as generators with maximum power rating equal to the available in-feed of each specific hour. The minimum production is preliminarily set to the same value as the maximum but it can be changed later to any user-defined fraction so that it is possible to reduce the wind power output in constrained areas. The marginal cost is set low, so that wind power plants always produces if not limited by grid constraints.

EuroWind provides capacity normalised time series. Thus a distributed generation capacity map (also provided by EuroWind) is required in order to determine the installed capacity regionally. This is implemented for Germany by using the Energymap data for Wind and PV capacities regionalised by postal code. For the rest of Europe the NREAP figures are utilised.

Hydro units

Three unit categories are established for effectively modelling the hydro technologies. Specifically:

- Dam - Reservoir (Dam) units,
- Run of River (RoR) units,
- Pump Storage (PS) units.

The Platts database is employed in order to determine the hydro units capacity. Nevertheless, its differentiation between the RoR and Dam technologies is not considered reliable. Therefore, a rule of thumb is applied through which, every unit below a certain parametrised value is considered to be a RoR unit while the rest are Dam units. Specifically for this study case, a 10 MW value is employed.

Nevertheless, hydro generation is dependent not only on the water flow of the neighbouring rivers, but also on factors specific for each technology. Modelling the time dependent generation poses different challenges for each of the three hydro classes. RoR generation dispatch can be simply modelled by normalising any available river flow time series but this does not hold true for Dam and PS units. Dam units are dependent on the water volume available in their reservoir while the PS units output is dispatched according to market rules.

The Tradewind project [126] presented the so called water - value approach for modelling the Dam units. According to this method, the marginal cost of the hydro Dam units is fluctuating relatively to the power already generated, i.e. to the amount of water left in the reservoir. For example, if high Dam power is dispatched, the unit's costs are set higher in order to account for the reduction of the reservoir water level. On the other hand, for the PS units, negative generation during times of low electricity price could be used for effectively simulating the pumping stage. Low electricity prices are present when the residual load is low.

Nevertheless, certain PowerFactory limitations led to the decision to utilise data derived from monthly production figures provided by entso-e [111]. The monthly hydro production data have been divided by the hours of each month and distributed to the different technologies. The flexible design allows to overcome the monthly flat production limitation if actual hourly hydro time series are employed.

In case of future portfolios, the desired capacity is distributed evenly to the existing units, by scaling accordingly their current capacity.

Biomass units

In contrast to all other RES, no time series are used for modelling the biomass units. Biomass plants are fully controllable since the fuel source is not fluctuating like the wind and solar in-feed. Biomass power also forms a relatively small share of the generation mix. Hence, a flat profile is applied. In order to also account for the units non availability, an adjustable fraction of the installed biomass capacities is used as the flat value; for this case study, it is set at 80%.

Biomass power plants substantially vary in size and fuel type, for which a reliable database is absent. Thus, a similar geo-processing approach to determine each region's installed capacity, as used for the wind and solar units, is also employed here. One biomass unit object is created for every model region via distributing the postal code Energymap capacities for Germany and the national figures for the rest of Europe.

For future capacity scenarios, a similar approach to the solar/wind units is followed and the installed capacities are scaled up or down accordingly.

Offshore Wind Units

EuroWind provides normalised time series for the offshore regions illustrated in Figure B.1 The installed (both current and future) capacities of offshore wind farms is taken from the publicly available 4coffshore platform [34]. Depending on the status of each farm (e.g consent authorised or application submitted), future offshore capacities are determined. Table [5.4] presents the aggregated capacities determined for Germany. One can observe that for 2030 the assumed capacities are quite higher than the BMU study [8] forecast, thus they have to be scaled down to meet the BMU figures. This holds true, as several of these project applications are abandoned or rejected in time. The actual capacities determined for Germany, are presented in the appendix tables B.5 and B.6.

The offshore wind farm modelling includes injections of power at certain onshore substations (e.g Diele, Borßum, Büttel). The grid connection points are also provided by the

Offshore capacities in Germany (GW)				
	2012	2015	2020	2030
North Sea	0.46	0.66	8.37	27.52
Baltic Sea	0.05	0.05	1.24	4.61
Sum	0.51	0.71	9.61	32.13
BMU	0.09	2.94	10	23.5

Table 5.4: *Installed Offshore capacities in Germany. Source: [106, 107]*

4coffshore platform; whenever information is not available, assumptions according to geographical allocation have been made. The coordinates of the farms connected at each onshore substation have been used in order to extract the percentage each EuroWind offshore area participates in the calculation of the offshore time series.

DC links

DC links can be modelled as different type of lines in PowerFactory. This applies specifically for the HVDC inter-connecting submarine cables in Europe. The main methodologies that can be applied for modelling the DC links, together with their limitations are presented below:

1. Apply normal AC line modelling but set impedances to zero
 - Problem with loop flows when a DC line is in parallel with AC lines
2. Use a pair of static generators at the nodes linked by a DC line
 - Static generators cannot be dispatched. Thus the flows need to be denoted before performing the OPF.
3. Use a pair of synchronous generators at the nodes linked by a DC line
 - The synchronous generators can be dispatched, but an iterative approach is required in order to converge at equal and opposite values. [127]

The latter option introduces further complexity without major gain. The second choice requires a market model run for every simulated hour in order to *a priori* determine the generator pair output. Hence, the first option is chosen. Since the HVDC capacity ratings are known, the HVDC are modelled as common 380 kV AC lines with very small (close to zero) impedances, for which the rated current is calculated using Equation 5.2.

$$I = \frac{S}{\sqrt{3}V} \quad (5.2)$$

Grid Expansion Costs

The values from Table B.7 comprise a first approximation of investment costs when extending the grid. L'abbate [97] also provides country specific figures. Furthermore, a path increase correction factor of 1.3 (TSO empirical value) [28] can be used in order to account for the meshed network that is not accurately represented by the network model branches. Finally, an in-crease of 20% for hilly and 50% for mountainous terrains is assumed when calculating the total costs [97].

Curtailement Costs

As also discussed in chapter 3, two different concepts have been developed with the purpose of monetising the cost of curtailment. They refer to a country specific approach for calculating the curtailment costs with regard to the compensation policy employed by the national TSO. In Europe, two trends are evident:

- The FIT concept followed mainly by Germany and Spain.
- The MC approach expressed either as premium on top of electricity market price (e.g. Denmark) or Renewable Obligation Certificates (ROC) on top of electricity price (e.g. Great Britain)

Specifically for Germany a policy of compensating the 95% of the originally agreed FIT price is currently applied [128].

5.3.5 Chronological Correlation

Demand and RES time series are chronologically correlated. In order to avoid inconsistencies due to time zone differences in European countries, all the time series have been transformed to the Central European Time (CET) zone. The daylight savings (DLS) time shift is not taken into account. Hence, the time zone used is the Universal Coordinate Time (UCT) plus one hour. The RES time series for all three base years were provided in UCT, and as a result they were shifted one hour. Nonetheless, for the demand time series, the bulk of which is provided by the ENTSO-e database, the time-stamp used is in CET, DLS considered. Therefore, for consistency reasons, the extra measurement in March has been deleted, while for the missing measurement in October, the demand figure prior to the missing value has been used. The demand profiles obtained from national TSOs have been also shifted to the CET zone.

One further point to highlight is that one of the base years, 2008, is a leap year. This can result in modelling inconsistencies since a leap year consists of 8784 hours instead of 8760. Due to this, all the time series corresponding to Friday, February 29th 2008 are removed. This option is selected against the choice to delete either January 1st or December 31st since February 29th is a “regular” Friday from a consumption perspective. On the contrary, the demand pattern in New Year’s eve is highly distorted when compared to any other regular week day. Hence, not accounting either for the first or the last day of the year can introduce loss of generality.

5.4 Network Reduction

Power systems have increased in complexity and size due to the rapid growth of widespread interconnections, the liberalisation of energy markets and the accelerated integration of distributed generation. This results in a highly meshed and complex European Power System that requires fast real time calculations which usually expand outside national borders or observation areas of TSOs.

For this specific study, certain network reduction techniques were investigated in order to bypass obstacles set by the large, complex European network model, with regard to:

- high computational times,
- potential inability of software solvers to deal with the complexity of the system,
- high simulation times that hinder debugging and further development.

5.4.1 Short Literature Review

While analysing a Power system, the behaviour of a certain sub-part of the system is of the main focus. Reduction or Equivalentencing is:

The process of reducing the complexity of the external system model while retaining its effect on the study system and maintaining acceptable accuracy with respect to a specific phenomenon [129].

From a network point of view, there are two major reduction technique families that depend mainly on the focus of the equivalent network model.

- Static reduction. It represents a snapshot of the system and it is employed for static analysis functions like power flows or network planning.
- Dynamic Reduction. It is applied when dynamic phenomena are under study and specifically for off-line transient stability analysis or on-line security analysis [129].

When a load flow type study is performed in large interconnected systems, an *internal* subsystem is usually of the main focus for the decision maker. Thus, it needs to be modelled in high detail. The remaining, less important, but still necessary *external* subsystem is represented by some equivalent, attached at the boundary buses [130]. The example of Figure 5.16 depicts a network model where the two sub-systems are interconnected through three tie lines.

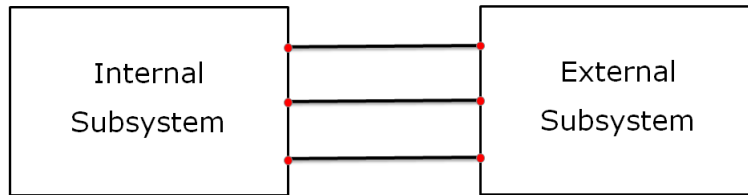


Figure 5.16: *Internal and External Subsystems of a Power System.*

There are several reduction techniques in literature suitable for static analysis studies that include:

- Ward-Type equivalents [131,132]
- Radial Equivalent Independent (REI) techniques [130,133,134]
- Sparsity of equivalents [135]
- Linearization approaches [130,136]
- Identification concepts [137,138]
- Sensitivity methods [139]
- Star-Delta Transformations [140]

The most widespread of the aforementioned reduction techniques is the Ward Reduction, developed by J.B.Ward in 1949. The Ward injection method performs Gaussian elimination³ and distributes the effects of the eliminated bus power around the boundary buses. Although,

³ Triangular reduction of the system's nodal admittance matrix

the extended ward equivalent outweighs the drawbacks of the classic ward method, i.e. the lack of VAR response, it is still dependent on the operational point of the system. Its major drawback is the requirement for complete network power flow prior to producing the reduced model [129-131].

Another technique that has been extensively used is the so called Radial Equivalent Independent method developed by Dimo in 1975. It first identifies groups of similar nodes and then replaces each group by a single virtual node while maintaining the power equilibrium. In other words, it concentrates the power at new fictitious nodes for which, neglecting losses, the power flow remains the same. Nevertheless, although it provides acceptable loss of accuracy in DC-LF studies, it exhibits similar drawbacks as the Ward - type reduction techniques [129] [130] [133].

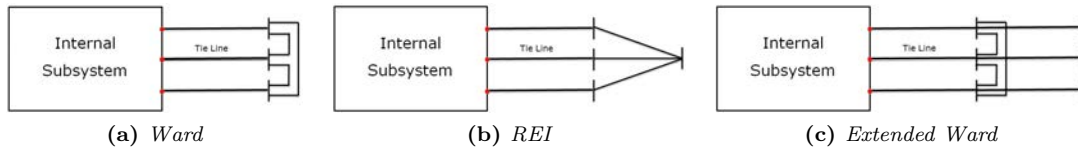


Figure 5.17: Major Reduced Network Equivalencing Techniques. based on [130] and [129]

From the rest of the network reduction techniques, none has exhibited significant approval or widespread use. On the other hand, market based reduction techniques are constantly gaining popularity since they lack the complexity of network related calculations. Those include:

- (a) Locational Marginal Price (LMP) based approaches. LMP reduction techniques perform aggregation of nodes with similar nodal prices, determined by an optimal power flow in the network. Methods, including hierarchical [141] and fuzzy [142] clustering are becoming more and more widespread. Figure 5.18 illustrates an example for the LMP calculation for a NUTS 2 Germany spatial resolution run of the developed DC-LF Model.

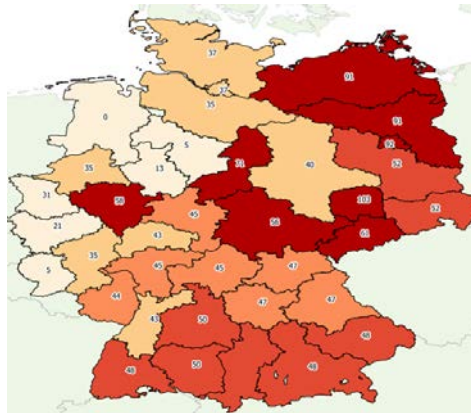


Figure 5.18: LMP Illustration. NUTS 2 Regions of similar color have similar nodal prices and thus can be further aggregated into wider regions.

- (b) Power Transfer Distribution Factors (PTDF) based approaches. The PTDF approach is a network reduction technique that has been applied in several European network studies (c.c. Table 2.2). It is based on the influence that a bilateral transfer of a marginal amount

of power has to the rest of the power network [129]. It measures the sensitivity of the system's power flows to a power transfer between two specific nodes and determines the power flows quasi analytically rather than iteratively.

5.4.2 Reducing the European DC-LF model

The size and complexity of the developed European DC-LF model dictates its reduction mainly due to solver constraints and unrealistic computation times. The spatial resolution flexibility of the developed DC-LF allows the reduction of the nodal model by employing the NUTS region approach. Equivalencing the network of Spain with a single NUTS 0 terminal where all generation and demand is aggregated in a single node does not produce significant loss of accuracy in case Germany is of the main focus. Nevertheless, reducing the complete German model into the 16 NUTS 1 regions that correspond to the 16 German Länder, and thus performing network reduction based on political division of countries does produce a great loss of generality that has to be tackled with another option.

Employing the robust PowerFactory built-in ward equivalent function seems attractive when equivalencing network regions other than the country in focus. It nevertheless, requires a time-intensive power flow before every simulation. Further, it is ambiguous whether it reduces the complexity of regions that need to be modelled in detail since for N boundary terminals, it produces N equivalent generators and $\frac{N(N-1)}{2}$ equivalent impedances. As seen in Figure 5.19, it constructs one equivalent generator for every boundary terminal and one equivalent impedance for every boundary terminal couple. This process renders the Ward method unsuitable for reducing the network complexity of multiple regions inside a wider region.

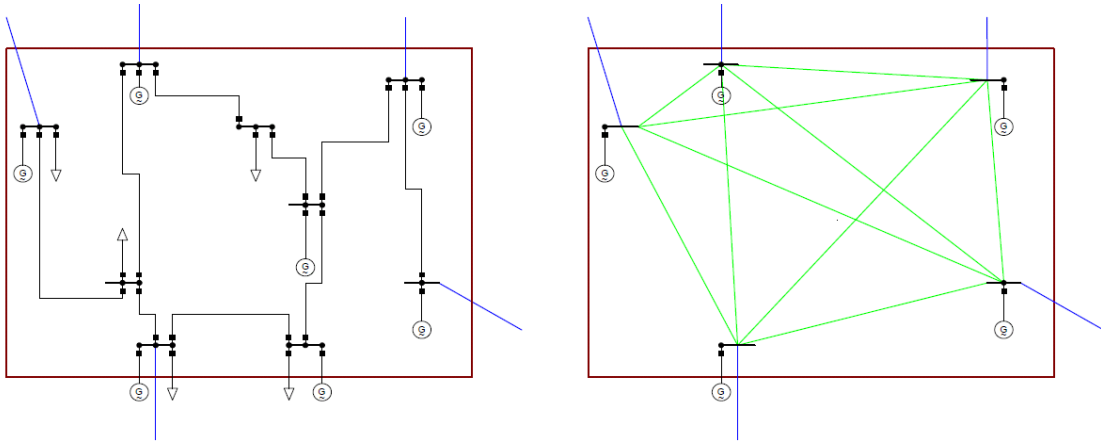


Figure 5.19: Original network and reduced network using the PowerFactory Ward reduction built-in function. In green the equivalent impedances between the 5 boundary buses.

Thus, employing the PTDF approach is not suitable for this study either, since the main tool employed is the OPF. PTDFs are mainly used as an alternative to the OPF and not as its supplementary. The LMP clustering of the Voronoi regions seems as the most suitable option but nevertheless, requires an OPF before every run. Further, performing a hierarchical or fuzzy clustering is not in the main focus of this thesis.

Instead, a combination of nodal and zonal modelling techniques is suggested. First, the NUTS region reduction is applied for regions of non high focus. The regions are considered

copper plates and the intra-region transmission lines are not taken into account. Next, a round-the-year statistical ranking, similar to the concepts presented in chapter 3 is employed, the outcomes of which are used for reducing the *internal* subsystem. The “reduction” takes place by considering the constraints of the overloaded lines only. Disregarding the loading constraints (but not the impedances) of the non - overloaded lines, reduces the size of the OPF constraint matrix and drastically decreases the computational time. A snapshot of the overloaded lines (in red) for the complete German model is presented in Figure 5.20.



Figure 5.20: *Voronoi Regions and Transmission Corridors for Germany. In Red the simulated above 80% loaded (N-1 overloaded) lines on 01:00:00 1/1/2010.*

5.5 Conclusions

The 5th chapter of this thesis described the development of a flexible platform for DC load flow network simulations of the Continental Europe (CE) network. It covered the modelling of renationalised conventional and renewable generation, distributed demand and geo-referenced network infrastructure. The spatial resolution flexibility is the novel feature that allows for modelling both nodal and zonal networks. The aim of the developed DC-LF model is to be used for the developed transmission expansion methodologies as an attempt to pinpoint pan-European network bottlenecks.

Chapter 6

Main Findings and Recommendation for Further Research

The increasing RES share in the European electricity mix poses new challenges to the power system. For reliable large scale RES integration and to facilitate the EU internal electricity market, the existing transmission system has to be upgraded.

This thesis described several concepts that contribute to the scientific discussion on transmission expansion planning in systems with high amounts of RES. The final section of this report draws conclusions arising from the results obtained from two TEP methodologies developed: the so-called Least Upgrade Curtailment Sensitive Iterative Pseudo Optimisation (LUCSIPO) and a modified Ant Colony Optimisation (ACO) methodology. The chapter first draws conclusions that can be deduced from the modelling results and then gives recommendations for further work.

6.1 Conclusions

The conclusions drawn in this section are based on the modelling outcomes, which are highly dependent on the network demand and wind time series used. Thus, the general statements presented have been carefully selected. Next, a discussion on the applied methodology follows, as well as the main conclusions yielded by a pan-European modelling exercise.

6.1.1 Potential savings in total costs and transmission line upgrades by network-optimised RES curtailment

The modelling results confirm that the annualised network upgrade and curtailment costs comprise a small fraction of the system's total system costs. In all sensitivity scenarios, the operational costs, including fuel and CO₂ equivalent costs, dominate the other costs by a factor of at least 20. The results also confirm the finding of previous studies that network upgrades can reduce the systems operational costs significantly once they release existing bottlenecks, and thus allow the electricity market to operate more efficiently. They allow higher utilization of RES which are commonly placed at the bottom of the merit order and thus reduce the electricity prices. Network upgrades are a cost-effective way to eliminate inefficiencies in the

power system but are often difficult to implement in practice due to public opposition by local stakeholders and, consequently, long licensing procedures.

Minor RES curtailment, however, e.g. of wind energy in the order of 1% of the available wind in-feed, allows for grid integration of RES with fewer network upgrades, at lower total costs. Some network upgrades are only required for those very few hours of the year, when the transmission of wind power to loads is at its peak. The related annualised investment costs of these transmission lines can be larger than the value of the respective extra RES energy integrated into the power system. Therefore, curtailment of the latter seems cost-effective from a societal viewpoint and desirable from a local stakeholder viewpoint.

For the chosen power system with high wind capacity, the results suggest that the curtailment and investment cost intersect for a curtailment limit¹ of about 30% of the installed capacity. The sum of curtailment and investment costs is minimised and thus regarded as the “optimum” in the flat region between 30-60%. The related wind energy curtailment amounts to 0.88% under the chosen conditions. The merit order effect, however, has a direct impact on the trade-off between RES curtailment and grid extension. The previously identified “optimum” is shifted to a curtailment limit of about 70-80% if the operational costs are also taken into account. The related wind energy curtailment amounts to about 0.75%. These findings confirm Jarass [13] suggestion that it would not be cost-effective to upgrade the network beyond integrating more than 80% of installed wind capacity.

On the other hand, any generalised conclusion that network-optimised RES curtailment would allow for less transmission lines to be built or upgraded in the future should be treated with much caution. The results from the sensitivity cases on the installed wind capacity show that an increase in the installed capacity (either as a long-term target compared to a mid-term target or from uncertainty about the actual development of RES in the future) still requires all of the network reinforcements that were identified for the base case. For the chosen power system, this holds even true for a curtailment limit that is lower (i.e. allows for more curtailment) in the case of increased installed wind capacity compared to the base case. Given the long licensing procedures for overhead lines, calling certain transmission lines dispensable would be obstructive from a long-term perspective.

6.1.2 Impact of a Minimum Required Conventional Generation Penetration (MRCGP) limit

From the results of the Minimum Required Conventional Generation Penetration (MRCGP) limit sensitivity cases, two conclusions can be drawn. First, that any requirement for a MRCGP limit may increase network congestion and, therefore, require more network upgrades than without such limit. This is, nevertheless, dependent on the resulting power flow patterns. Second, that the higher the MRCGP limit is, the more are the costs shifted from network congestion related curtailment expenditure to system balancing related operational policy costs. Therefore, extending the network to fully integrate the available RES in-feed will only be reasonable if any MRCGP limit is low enough to prevent operational policy related RES reduction.

6.1.3 Impact of the curtailment compensation scheme

he pseudo-optimum point proved to be almost insensitive to the value attributed to the curtailed energy as long as FIT and MC were in the same order of magnitude (which they were for the chosen power system). One can argue that curtailment costs are expected to be lower when the MC scheme is applied, since wind is curtailed during high wind situations which

¹Curtailment limit is the minimum power limit that the RES units can be dispatched to. It is defined as a fraction of either the installed capacity or the available in-feed.

usually result in low marginal costs. Nevertheless, the employed non inter-temporal unit commitment approach influences the actual marginal system costs. No definite conclusion can, therefore, be drawn on whether the FIT or MC approach results in lower total system costs and requires further research..

6.1.4 Methodology discussion

This thesis' major objective was to develop a consistent TEP methodology that would attempt to optimise the trade-off between network upgrades and RES curtailment. The outcome of this objective, is the LUCSIPO approach.

The LUCSIPO approach is a simple, straight-forward heuristic methodology that managed to prove the existence of an economic pseudo-optimum between grid extensions and curtailment. In order to validate its results, a proven state-of-the-art meta-heuristic approach, the ACO was employed. Results show that the LUCSIPO achieved solutions quite close to the ACO while introducing up to 5 times calculation speed-up. The solutions produced are similar on a total system cost perspective, but nevertheless result in differentiated list of network upgrades. Hence they enable other factors such as environmental reasons or local opposition to favour the construction of one line over another.

Moreover, for systems with high wind capacity, the LUCSIPO coupled with the investment cost ranking ICPPCRO achieved a higher quality solution than when the RO approach was applied. This is due to the ICPPCRO index selecting more cost-efficient (shorter) branches to be upgraded. It can be concluded that, accounting only for the line overload index but not considering the line length and related upgrade costs, would be insufficient to find the most cost-effective TEP result.

Finally, the employed k-means methodology efficiently represented the round-the-year system residual load. It resulted in a similar list of network upgrade candidates, while achieving computational time gains in the magnitude of 200 when compared to the round-the-year case. It can therefore be concluded that the k-means clustering technique can drastically reduce TEP studies simulation times.

6.1.5 Software Tools

The LUCSIPO methodology was developed both in MatPower and PowerFactory. Despite the limitations of the DPL language when compared to Matlab, PowerFactory introduced major calculation time speed-up in the minimum power limit unconstrained LUCSIPO implementation. It further yielded a solution with lower total system costs and fewer reinforced branches. The employed solver used in the OPF is considered to be the main cause of this behaviour. Therefore, it cannot be concluded which software is more suitable for transmission expansion studies. It is definite that the flexibility Matlab/MatPower provides cannot be outweighed by PowerFactory. Nevertheless, the superiority of the PowerFactory solver cannot be neglected in this case.

6.1.6 The European DC-LF model

Creating a consistent pan-European network model, based on publicly and commercially available data, is a challenging task that is prone to errors. The large amount of data requires dedicated database management tools but, data quality remains a major issue nevertheless. Moreover, the high model complexity makes complete European wide calculations unattractive. This is because solvers have to deal with too many problem constraints, an unrealistically long computational time is needed and interpretation of results is extremely difficult. Thus, reduced models are often required.

The developed flexible platform enables the modelling of both nodal (complete) and zonal (reduced) models. A combination of the zonal and nodal approach is proposed as a reliable model of prudent complexity.

6.2 Recommendations for further research

This thesis dealt with the static Transmission Expansion Problem, i.e. the optimisation for a single planning horizon in the future. Nevertheless, it is important not only to define where, but also when the grid reinforcements should be implemented. A first recommendation, thus, is the adjustment of the developed methodologies in order to perform dynamic transmission planning and therefore optimise through several intermediate stages between the base year and the final stage.

The PowerFactory implementation of the LUCSIPO approach exhibited higher quality results while significantly decreasing computation time. Nevertheless, its results should also be tested against the more complicated non-inter temporal unit commitment approach in order to allow for safer conclusions. Developing the ACO approach in PowerFactory can also be of further help for this cause. Further, the results appear to be dependent on the solver the two tools employ. MatPower allows the utilisation of a variety of solvers other than the IBM CPLEX (e.g. Gurobi or BPMPD) for solving the OPF. Therefore, evaluating the MatPower implementation coupled with a different solver, could lead to safer outcomes with regard to the influence the solver has on the final solution quality.

From a methodology perspective, the LUCSIPO approach has most probably reached its limits with regard to identifying the pseudo-optimal solution. Nonetheless, a finer step resolution for the curtailment limits between 70% and 100% may yield interesting results. Moreover, introducing an extra step where the algorithm attempts to locate a better solution in the vicinity of the feasible solution obtained from the previous step, could potentially lead to better solutions; at the expense of further increasing the computation time.

On the contrary, since the ACO approach has not shown signs of absolute convergence, it is reasonable to assume that finer tuning of its input parameters will produce higher quality outputs. Moreover, the curtailment sensitivity concept, applied in the LUCSIPO approach, has not been followed for the ACO method. Potential coupling could produce outcomes of significant value.

The validity of the LUCSIPO approach in realistic test systems needs also to be investigated. The delivered European DC-LF network model is a potential candidate. The industrial partner, Ecofys Berlin, will have to ensure the validity of the model prior to applying any of the developed TEP methodologies. The validation can take place by comparing the resulting power flows against publicly available physical cross-border flow snapshots published by ENTSO-e.

Employing parallel computing both for the ACO and the LUCSIPO approach would significantly reduce the simulation times required. Matlab provides the Parallel Computing Toolbox which introduces the parallel for loop concept. Since both approaches solve independent snapshots of the same problem, separate Matlab workers can be employed. The ACO methodology can utilise parallel computing for its local search part while LUCSIPO can separately solve the TEP for every curtailment limit of its outer loop. Parallel computing will enable the adoption of higher time resolution for the TEP simulations, so round-the-year simulations could be performed instead of the representative 100 hour solution that is currently implemented.

Bibliography

- [1] Sir Nicholas Stern “Stern review: The economics of climate change”, London, 30 October 2006. [Online]. Available: <http://webarchive.nationalarchives.gov.uk/+http://www.hm-treasury.gov.uk/sternreview_index.htm>.
- [2] European Parliament, Council of the European Union, “*The EU climate and energy package*”, Brussels, 2010 [Online]. Available: <http://ec.europa.eu/clima/policies/package/index_en.htm>.
- [3] H. Zhang et al., “A mixed-integer linear programming approach for multi-stage security-constrained transmission expansion planning” *Power systems*,” *IEEE Trans. Power Syst.*, vol. 27, no. 2, pp. 1125-1133, 2012.
- [4] M. Osthues et al., “Scenario-based analysis of investment needs for the German transmission grid” in *PowerTech, 2011 IEEE, Trondheim* , pp. 1-5, 2011.
- [5] I. Fuchs et al, “Improved method for integrating renewable energy sources into the power system of northern Europe” in *Transmission expansion planning for wind power integration 2011, 10th International Conference on : Environment and Electrical Engineering (EEEIC)*, pp. 1-4, 2011.
- [6] Mo Chen (Dec 2009) - Matlab central home, “K-means cluster”, [Online], Available: <<http://www.mathworks.com/matlabcentral/fileexchange/24616-kmeans-clustering>>, [Nov 2012].
- [7] Mapsof.net, ”A collection of world, country and city maps: Interactive and printable maps anywhere in the world”, [Online], Available: <<http://mapsof.net/>>,[Dec 2012].
- [8] J. Nitsch et al, Leitstudie 2010: Langfristszenarien und Strategien für den Ausbau der Erneuerbaren Energien in Deutschland bei Berücksichtigung den Entwicklung in Europa und Global”, 2010.
- [9] J. Bertsch et al., “Flexibility options in European electricity markets in high RES-e scenarios: Study on behalf of the International Energy Agency (IEA),” October 2012.
- [10] A. R. Ciupuliga et al., “Round-the-year security analysis with large-scale wind power integration Sustainable Energy”, *IEEE Trans. on Sust. Energy*, vol. 3, no. 1, pp. 85-93, 2012.
- [11] M. Fürsch and L. Glotzbach, Roadmap 2050 - a closer look: Cost efficient RES-E penetration and the role of grid extensions. Köln: EWI, 10/2011.

- [12] L. Fried et al., “Global wind energy outlook 2012”, GWEC, Greenpeace International, 2012.
- [13] L. Jarass and G. M. Obermair, “Efficient grid extension for strongly fluctuating energy sources”, *Zeitschrift für Energiewirtschaft*, vol. 34, no. 3, pp. 223-233, 2010.
- [14] W. Winter et al., “European Wind Integration Study (EWIS): Towards a successful integration of large scale wind power into European electricity grids”, 31/03/2010.
- [15] Q. Zhou and J. Bialek, “pproximate model of european interconnected system as a benchmark system to study effects of cross-border trades”, *IEEE Trans. Power Syst.*, vol. 20, no. 2, pp. 782-788, 2005.
- [16] E. Tröster et al., “European grid study 2030/2050”, 18 January 2011.
- [17] EURELECTRIC, “Power statistics & trends 2011”, 05 December 2011.
- [18] Entsoe.net, “The transparency platform on electricity in Europe (former ETSOVISTA), [Online], Available: <<https://www.entsoe.net/home.aspx>>, [2012, May. 15].
- [19] Satel-Light, “The European database of daylight and solar radiation”, [Online], Available: <<http://www.satel-light.com/core.htm>>, [03/2012].
- [20] NOAA, “Climate prediction center reanalysis project”, [Online], Available: <<http://www.cpc.ncep.noaa.gov/products/wesley/reanalysis.html>>, [03/2012].
- [21] C. Hewicker et al, “Power perspectives 2030: On the road to a de-carbonised power sector”, 2011.
- [22]P. Capros et al., ”EU energy trends to 2030”, 04/08/2010. [23] PowerVision, “EMEA price assessments and indices Platts”, [Online], Available: <<http://www.platts.com/Products/powervision>>, [03/2012].
- [24] Michaela Fürsch et al, “The role of grid extensions in a cost-efficient transformation of the European electricity system until 2050”, February 2012.
- [25] K. Schaber et al., “Parametric study of variable renewable energy integration in Europe: Advantages and costs of transmission grid extensions”, *Energy Policy*, vol. 42, pp. 498-508, 2012.
- [26] K. Schaber et al., “Transmission grid extensions for the integration of variable renewable energies in Europe: Who benefits where?”, *Energy Policy*, vol. 43, pp. 123-135, 2012.
- [27] A. Ciupiliga et al., “A market-based investigation of large-scale renewable energy integration in North-western Europe” in *Power and Energy Society General Meeting, 2012 IEEE*, pp. 1-82012
- [28] German Energy Agency, “Integration of renewable energy sources in the German power supply system from 2015-2020 with an outlook to 2025”, 2010.
- [29] Fraunhofer Institute for Wind, “Wind measuring network and 200 meter measuring mast - energy and energy system technology”, [Online], Available: <http://www.iwes.fraunhofer.de/en/labore/Windmessnetz_und_200-Meter-Messmast.html>, [03/2012].

- [30] SoDa Service, “Knowledge in solar radiation”, [Online], Available: <<http://www.sodais.com/eng/index.html>>, [03/2012].
- [31] B. Schucht et al., “Der Netzentwicklungsplan 2012: The network development plan 2012”, 15/08/2012.
- [32] H. Seifi and M. S. Sepasian, *Electric power system planning: Issues, algorithms and solutions*, Heidelberg, Springer, 2011.
- [33] S. Boyd and L. Vandenberghe, *Convex Optimization*, Cambridge University Press, seventh Ed., 2004.
- [34] Optimization Problem Types, “Convex optimization - front-line systems”, [Online], Available: <<http://www.solver.com/probconvex.htm>>, [July 2012].
- [35] S.P. Bradley et al., *Applied mathematical programming*, Addison-Wesley, 1977.
- [36] A. M. Leite da Silva et al., “Performance comparison of metaheuristics to solve the multi-stage transmission expansion planning problem”, *Generation, Transmission & Distribution, IET*, vol. 5, no. 3, pp. 360-367, 2011.
- [37] G. Latorre et al., “Classification of publications and models on transmission expansion planning”, *IEEE Trans. Power Syst.*, vol. 18, no. 2, pp. 938-946, 2003.
- [38] S. Binato and G. C. Oliveira, , “A heuristic procedure to cope with multi-year transmission expansion planning”, 1995.
- [39] E. Platts et al., “A method for horizon-year transmission planning”, *IEEE Trans. Power App. Syst.*, vol. PAS - 89, pp. 1356-1361, 1972.
- [40] Karsten Burges, Ecofys, Private communication, July 2012.
- [41] K. J. Kim et al., “Optimal long term transmission expansion planning based on maximum principle”, *IEEE Trans. on Power Syst.*, vol. 3, no. 4, pp. 1494-1501, 1988.
- [42] R. Villasana et al., “Transmission network planning using linear programming”, *IEEE Trans. Power App. Syst.*, vol. 104, no. 2, pp. 349-356, 1985.
- [43] H. K. Youssef and R. Hackam, “New transmission planning model”, *IEEE Trans. on Power Syst.*, vol. 4, no. 1, pp. 9-18, 1989.
- [44] Y. P. Dusonchet and A. El-Abiad, “Transmission planning using discrete dynamic optimizing”, *IEEE Trans. Power App. Syst.*, vol. 92, no. 4, pp. 1358-1371, 1973.
- [45] B. Alizadeh and S. Jadid, “Reliability constrained coordination of generation and transmission expansion planning in power systems using mixed integer programming”, *Generation, Transmission & Distribution, IET*, vol. 5, no. 9, pp. 948-960, 2011.
- [46] A. P. Meliopoulos et al., “Optimal long range transmission planning with AC load flow”, *IEEE Trans. Power App. Syst.*, vol. 101, no. 10, pp. 4156-4163, 1982.
- [47] C. Barbulescu and S. Kilyeni, “Congestion management. Transmission expansion planning considering large wind power plants”, in *2011 6th IEEE International Symposium on Applied Computational Intelligence and Informatics (SACI)*, pp. 559-564, 2011.

- [48] G. A. Orfanos et al., "Transmission expansion planning in deregulated electricity markets for increased wind power penetration", in *2010 7th International Conference on the European Energy Market (EEM)*, pp. 1-7, 2010.
- [49] S. Dehghan et al., "Transmission network expansion planning using a dea-based benders decomposition", in *2010 18th Iranian Conference on Electrical Engineering (ICEE)*, pp. 955-960, 2010.
- [50] R. Romero and A. Monticelli, "A hierarchical decomposition approach for transmission network expansion planning", *IEEE Trans. on Power Syst.*, vol. 9, no. 1, pp. 373380, 1994.
- [51] E. N. Asada et al., "A branch-and-bound algorithm for the multi-stage transmission expansion planning", in *IEEE Power Engineering Society General Meeting, 2005*, pp. 171-176 Vol. 1, 2005.
- [52] M. J. Rider et al., "Branch and bound algorithm for transmission network expansion planning using dc models", in *2007 IEEE Lausanne : Power Tech*, pp. 1350-1355, 2007.
- [53] R. Fischl and W. R. Puntel, Ed., *Computer aided design of electric power transmission network*, 1972.
- [54] J. Bennon and A. P. Meliopoulos, "Use of sensitivity analysis in automated transmission planning", *IEEE Trans. Power App. Syst.*, vol. PAS-101, pp. 53-59, Jan. 1982.
- [55] M. V. F. Pereira and L. M. V. G. Pinto, "Application of sensitivity analysis of load supplying capability to interactive transmission expansion planning", *Power Eng. Rev., IEEE*, vol. 5, no. 2, p. 39, 1985.
- [56] A. Monticelli, et al., "Interactive transmission network planning using a least-effort criterion", *IEEE Trans. Power App. Syst.*, vol. 101, no. 10, pp. 3919-3925, 1982.
- [57] R. C. G. Teive et al., "A cooperative expert system for transmission expansion planning of electrical power systems", *IEEE Trans. on Power Syst.* vol. 13, no. 2, pp. 636-642, 1998.
- [58] V. A. Levi and M. S. Calovic, "A new decomposition based method for optimal expansion planning of large transmission networks", *IEEE Trans. on Power Syst.*, vol. 6, no. 3, pp. 937-943, 1991.
- [59] G. Latorre-Bayona and I. J. Perez-Arriaga, "Chopin, a heuristic model for long term transmission expansion planning", *IEEE Trans. on Power Syst.*, vol. 9, no. 4, pp. 1886-1894, 1994.
- [60] V. Asadzadeh et al., "Economics-based transmission expansion planning in restructured power systems using decimal codification genetic algorithm", in *2011 IEEE Jordan Conference on Applied Electrical Engineering and Computing Technologies (AEECT)*, pp. 1-8, 2011.
- [61] L. S. Rezende et al., "Artificial immune systems and differential evolution based approaches applied to multi-stage transmission expansion planning", in *ISAP 09: 15th International Conference on Intelligent System Applications to Power Systems*, pp. 16, 2009.
- [62] G. A. Orfanos et al., "Transmission expansion planning by enhanced differential evolution", in *2011 16th International Conference on Intelligent System Application to Power Systems (ISAP)*, pp. 1-6, 2011.

- [63] A. M. L. Da Silva, et al., "Evolution strategies to transmission expansion planning considering unreliability costs," in *PMAAPS 2006 International Conference on Probabilistic Methods Applied to Power Systems*, pp. 1-7, 2006.
- [64] I. Fuchs and T. Gjengedal, "Ant colony optimization and analysis of time step resolution in transmission expansion computations for wind power integration", in *2011 16th International Conference on Intelligent System Application to Power Systems (ISAP)*, pp. 1-6, 2011.
- [65] A. Verma et al., "Transmission network expansion planning with adaptive particle swarm optimization", *2009 NaBIC World Congress on Nature & Biologically Inspired Computing*, pp. 1099-1104, 2009.
- [66] P. Ren and N. Li, "Optimal expansion planning of high-voltage transmission network using the composite particle swarm optimization", in *2010 International Conference on Artificial Intelligence and Computational Intelligence (AICI)*, vol. 1, pp. 170-173, 2010.
- [67] M. Eghbal et al., "Transmission expansion planning by meta-heuristic techniques: A comparison of shuffled frog leaping algorithm, PSO and GA," in *2011 IEEE Power and Energy Society General Meeting*, pp. 1-8, 2011.
- [68] Jingran Wang, et al., "Discrete monkey algorithm and its application in transmission network expansion planning", in *2010 IEEE : Power and Energy Society General Meeting*, pp. 1-5, 2010.
- [69] R. Romero et al., "Transmission system expansion planning by simulated annealing", in *1995 IEEE Power Industry Computer Application Conference*, pp. 278-283, 1995.
- [70] S. Binato et al., "A greedy randomized adaptive search procedure for transmission expansion planning", *IEEE Trans. on Power Syst.*, vol. 16, no. 2, pp. 247-253, 2001.
- [71] H. Mori and H. Kakuta, "Multi-objective transmission network expansion planning in consideration of wind farms", in *2011 2nd IEEE PES International Conference and Exhibition on Innovative Smart Grid Technologies (ISGT Europe)*, pp. 1-7, 2011.
- [72] N. P. Padhy, "Congestion management under deregulated fuzzy environment", in *2004 IEEE International Conference on Electric Utility Deregulation, Restructuring and Power Technologies (DRPT 2004)*, vol. 1, pp. 133-139 Vol.1, 2004.
- [73] H. Yu et al., "Robust transmission network expansion planning method with taguchi's orthogonal array testing in Power Systems," *IEEE Trans. on Power Syst.*, vol. 26, no. 3, pp. 1573-1580, 2011.
- [74] D. Fudenberg and J. Tirole, *Game Theory*. MIT Press, Boston, 1983.
- [75] M. V. F. Pereira et al., "A decomposition approach to automated generation/transmission expansion planning", *IEEE Power Eng. Rev.*, vol. 5, no. 11, pp. 30-31, 1985.
- [76] L. d. Mello Honorio et al., "A cluster and gradient-based artificial immune system applied in optimization scenarios", *IEEE Trans. Evol. Comput.*, , vol. 16, no. 3, pp. 301-318, 2012.
- [77] M. Dorigo et al., "Ant colony optimization", *IEEE Comput. Intell. Mag.*, vol. 1, no. 4, pp. 28-39, 2006.

[78] Wikipedia-Ant colony optimization, “Ant colony optimization algorithms”, [Online], Available: <http://en.wikipedia.org/wiki/Ant_colony_optimization>, [08/2012].

[79] Sistemas Adaptativos Complejos, “Observando comportamiento de ejambre durante su diseno evolutivo”, [Online], Available: <<http://cas-chile.blogspot.nl/2009/05/observing-swarm-behaviour-du.html>>, [08/2012].

[80] A. M. L. da Silva et al., “Tabu search applied to transmission expansion planning considering losses and interruption costs”, in *PMAPS 08, Proceedings of the 10th International Conference on Probabilistic Methods Applied to Power Systems*, pp. 1-7, 2008.

[81] H. S. Wio et al., “An introduction to stochastic processes and nonequilibrium statistical physics”. Singapore, New Jersey, London, World Scientific, rev. ed. , 2012.

[82] DiGSILENT, “Powerfactory flyer”, [Online], Available: <http://www.digsilent.de/tl_files/digsilent/files/PowerFactory/PowerFactory_Flyer.pdf>, [2012, May 15].

[83] Dr. Francisco M. Gonzalez-Longatt, “DiGSILENT powerfactory: Digsilent tutorials”, [Online], Available: <http://www.fglongatt.org.ve/Tutorial_DigSilent_EN.html>, [2012, May. 15].

[84] DiGSILENT, “Powerfactory V14 documentation, v1.13”, [Online], Available: <<http://www.klgsystel.com/pdf/dig-silent/pf-v14-software.pdf>>, [2012, May. 15].

[85] DiGSILENT, “DGS interface documentation version 19.10.2009”.

[86] MathWorks United Kingdom, “MathWorks united kingdom - Matlab and Simulink for technical computing”.

[87] R. D. Zimmerman et al., “Matpower: Steady-state operations, planning, and analysis tools for power systems research and education”, *IEEE Trans. on Power Syst.* , vol. 26, no. 1, pp. 12-19, 2011.

[88] J. J. Grainger and W. D. Stevenson, *Power system analysis*. New York: McGraw-Hill, 1994.

[89] Göran Andersson, “Power system analysis: Power flow analysis, fault analysis, power system dynamics and stability”, ETH, September 2012.

[90] A. Pinar et al, “Computing criticality of lines in power systems”, *ISCAS 2007, IEEE International Symposium on Circuits and Systems*, pp. 65-68, 2007.

[91] Power Optimisation, “Software for unit commitment and dispatch within electricity industry”, [Online], Available: <<http://dawhois.com/site/powerop.co.uk.html>>, [01/2013].

[92] D. Saxena and et al., “Application of computational intelligence in emerging power systems”, *International Journal of Engineering, Science and Technology*, vol. 2, no. 3, pp. 1-7, 2010.

[93] M. Honarkhah and J. Caers, “Stochastic simulation of patterns using distance-based pattern modeling”, *Mathematical Geosciences*, vol. 42, no. 5, pp. 487-517, 2010.

[94] 50Hertz Transmission GmbH, Amprion GmbH, TransnetBW GmbH, TenneT TSO GmbH, “EEGJahresabrechnungen”, 8/1/2012.

- [95] Eurostat, "Eurostat news release: Euro indicators", 1/31/2013, [Online], Available: <http://epp.eurostat.ec.europa.eu/cache/ITY_PUBLIC/2-28022013-AP/EN/2-28022013-AP-EN.PDF> [02/2013].
- [96] Bundesnetzagentur, "Beschluss BK4-11-304", 11/2/2011.
- [97] L'abbate and Miglavacca, "Review of costs of transmission infrastructures, including cross-border connections", 2011.
- [98] Ecofys, "All Island TSO Facilitation of Renewables studies: Eirgrid", Work Package 3 Final Report, 2010.
- [99] PostgreSQL, "The world's most advanced open source database", [Online], Available: <<http://www.PostgreSQL.org/about/>>, [2012, May 15].
- [100] Wikipedia, "Postgis", [Online], Available: <<http://en.wikipedia.org/wiki/PostGIS>>, [2012, May 15].
- [101] Quantum GIS, "Quantum GIS - open source geographic information system", [Online], Available: <<http://www.qgis.org/>>, [07/2012].
- [102] EuroWind GmbH, "Accredited energy and weather information", [Online], Available: <<http://www.windprognose.de/english/index.php>>, [03/2012].
- [103] Deutsche Gesellschaft für Sonnenenergie (DGS) e.V, Energymap.info. Konsolidierte und Plausibilisierte Datenbank der Stammdaten Von EEG-Anlagen in Deutschland", [Online], Available: <<http://energymap.info/>>, [2012, May 15].
- [104] European Commission, "European commission: Your key to european statistics, browse/search database", [Online], Available: <http://epp.eurostat.ec.europa.eu/portal/page/portal/statistics/search_database>, [2012, May 15].
- [105] ENTSOE, "European network of transmission system operators for electricity. data portal", [Online], Available: <<https://www.entsoe.eu/resources/data-portal/consumption/>>, [04/2012].
- [106] 4coffshore, "Global offshore wind farms database", [Online], Available: <<http://www.4coffshore.com/offshorewind/>>, [2012, May 15].
- [107] J. Nitsch et al, "Leitstudie 2012: Langfristszenarien und Strategien für den Ausbau der Erneuerbaren Energien in Deutschland bei Berücksichtigung den Entwicklung in Europa und Global", 2012.
- [108] ENTSO-e, "Ten year network development plan 2010-2020", 05/07/2012.
- [109] ENTSO-e, "Entso-e statistical yearbook 2011", 20/11/2011.
- [110] Bundesverband WindEnergie e.V., "Windjahr in prozent zum langjährigen mittel", [Online], Available: <>, [2012, May 15].
- [111] ENTSO-e, "Detailed monthly production data", [Online], Available: <<https://www.entsoe.eu/data/data-portal/production/>>, [2012, May 15].
- [112] 50Hertz, "50Hertz Transmission GmbH Vertical load", [Online], Available: <<http://>>

www.50hertz.com/cps/rde/xchg/trm_de/hs.xsl/149.htm?rdeLocaleAttr=en&rdeCOQ=SID-23A3BF0E-023605F1], [2012, May 15].

[113] Energía Eléctrica, “Registro de instalaciones - energía eléctrica - energía - energía y turismo Spain”, [Online], Available: <<http://www.minetur.gob.es/energia/electricidad/regimenespecial/registro/paginas/registroinstalacionesre.aspx>>, [2012, May 15].

[114] European Parliament Council of the European Union (2009), “Promotion of the use of energy from renewable sources and amending and subsequently repealing directives”, 25/06/2009.

[115] ECN, National renewable energy action plans”, [Online], Available: <<http://www.ecn.nl/units/ps/themes/renewable-energy/projects/nreap/>>, [05 / 2012].

[116] Paul Chew 2007, “Online Voronoi diagram/Delaunay triangulation applet”, [Online], Available: <<http://www.cs.cornell.edu/home/chew/Delaunay.html>>, [10/2012].

[117] Wikipedia, “Nomenclature of territorial units for statistics”, [Online], Available: <http://en.wikipedia.org/wiki/Nomenclature_of_Territorial_Units_for_Statistics>, [03/2012].

[118] R. Kuwahata, “Ecofys integrated power system modelling tool”, Internal document, 07/08/2012.

[119] Eirgrid, “System demand”, [Online], Available: <<http://www.eirgrid.com/operations/systemperformancedata/systemdemand/>>, [09/2012].

[120] AST, “Demand, net exchange and production”, [Online], Available: <http://www.ast.lv/eng/power_system/current_situation_in_power_system/planned_and_actual_demand_net_exchange_and_production/>, [09/2012].

[121] Svenska Kräftnet, “Elstatistik för hela sverige”, [Online], Available: <<http://www.svk.se/Energimarknaden/El/Statistik/Elstatistik-for-hela-Sverige/>>, [09/2012].

[122] Energinet, “Download of market data”, [Online], Available: <<http://www.energinet.dk/EN/El/Engrosmarked/Udtraek-af-markedsdata/Sider/default.aspx>>, [09/2012].

[123] Fingrid, Fingrid - load and generation”, [Online], Available: <<http://www.fingrid.fi/en/electricity-market/load-and-generation/Pages/default.aspx>>, [09/2012].

[124] National Grid, “National grid: Metered half-hourly electricity demands”, [Online], Available: <<http://www.nationalgrid.com/uk/Electricity/Data/Demand+Data/>>, [09/2012].

[125] Erik Delarue et al., “Development of a comprehensive electricity generation simulation model using a mixed integer programming approach”, *Engineering and Technology*, vol. 28, 2007.

[126] Frans Van Hulle et al, “Tradewind - integrating wind: Developing Europe’s power market for the large-scale integration of wind power”, May 2009.

[127] R.Kuwahata, Ecofys, “DC modeling in PowerFactory”, Private Communication, April 2012.

[128] BMU, Act on granting priority to renewable energy sources: Renewable energy sources act eeg, 2012.

- [129] G. A. Antonis Papaemmanouil, "On the reduction of large power system models for power market simulations", ETH, [Online], Available: <http://www.eeh.ee.ethz.ch/uploads/tx_ethpublications/PSCC2011_Antonios.pdf>, [09/2012].
- [130] S. Deckmann et al., "Studies on power system load flow equivalencing, *IEEE Trans. Power App. Syst.*, vol. 99, no. 6, pp. 2301-2310, 1980.
- [131] J. B. Ward, "Equivalent circuits for power-flow studies", *Transactions of the American Institute of Electrical Engineers*, vol. 68, no. 1, pp. 373-382, 1949.
- [132] K. L. Lo et al., "Extended ward equivalent of external system for on-line security analysis", in *APSCOM-93 2nd International Conference on Advances in Power System Control, Operation and Management*, pp. 5459 vol.1, 1993.
- [133] P. Dima, *Nodal Analysis of Power Systems*. Kent and England: Abacus Press, 1975.
- [134] F. Milano and K. Srivastava, "Dynamic REI equivalents for short circuit and transient stability analyses", *Electric Power Systems Research*, vol. 79, no. 6, pp. 878-887, 2009.
- [135] S. Deckmann et al., "Numerical testing of power system load flow equivalents", *IEEE Trans. Power App. Syst.*, vol. 99, no. 6, pp. 2292-2300, 1980.
- [136] A. Monticelli et al., "Real-time external equivalents for static security analysis", *IEEE Trans. Power App. Syst.*, vol. 98, no. 2, pp. 498-508, 1979.
- [137] G. Contaxis and A. S. Debs, "Identification of external system equivalents for steady-state security assessment", *IEEE Trans. Power App. Syst.*, vol. 97, no. 2, pp. 409-414, 1978.
- [138] A. S. Debs, "Estimation of external network equivalents from internal system data", *IEEE Trans. Power App. Syst.*, vol. 94, no. 2, pp. 273-279, 1975.
- [139] H. K. Singh and S. C. Srivastava, "A sensitivity based network reduction technique for power transfer assessment in deregulated electricity environment", in *IEEE/PES Transmission and Distribution Conference and Exhibition 2002 Asia Pacific*, vol. 3, pp. 1976-1981 vol.3, 2002.
- [140] S.D. Wang and C.H. Sun, "Transformations of star-delta and delta-star reliability networks", *IEEE Trans. Rel.*, vol. 45, no. 1, pp. 120-126, 1996.
- [141] B. Burstedde, "From nodal to zonal pricing a bottom-up approach to the second-best" in *2012 9th International Conference on the European Energy Market (EEM 2012)*, Florence, pp. 885-893, 2012.
- [142] Y.Y. Hong et al., "Determination of congestion zones in deregulated electricity markets using fuzzy clustering" in *14th PSCC, Sevilla 2002*, pp. 2-1, 2002.

Appendix A

TEP Simulation Results

Table A.1: *LUCSIPO MC Scenario Results*

Curtailed Limit(%)	20	30	40	50	60	70	80	90	100
Upgraded Branches	2	2	2	2	2	2	5	5	5
Curtailed Energy(%)	3.27	3.27	3.27	3.27	3.27	3.27	0.00	0.00	0.00
Curtailed Costs (M€)	0.339	0.339	0.339	0.339	0.339	0.339	0.000	0.000	0.000
Op. Policy Costs (M€)	0	0	0	0	0	0	0	0	0
Operational Costs (M€)	16.878	16.878	16.879	16.879	16.879	16.879	16.555	16.555	16.555
Investment costs p.a. (M€)	0.096	0.096	0.096	0.096	0.096	0.096	0.232	0.232	0.232
Upgraded Length(km)	95.7	95.7	95.7	95.7	95.7	95.7	231.4	231.4	231.4
Total Costs (M€)	17.313	17.313	17.314	17.314	17.314	17.314	16.788	16.788	16.788

Table A.2: *LUCSIPO HW Scenario Results*

Curtailed Limit(%)	20	30	40	50	60	70	80	90	100
Upgraded Branches	2	2	2	2	4	4	9	9	15
Curtailed Energy(%)	10.16	10.16	10.16	10.16	0.88	0.88	0.75	0.75	0.74
Curtailed Costs (M€)	0.910	0.910	0.910	0.910	0.078	0.078	0.067	0.026	0.000
Op. Policy Costs (M€)	0.000	0.000	0.000	0.000	0.000	0.000	0.000	0.041	0.066
Operational Costs (M€)	15.135	15.136	15.136	15.136	14.394	14.394	14.075	14.069	14.048
Investment costs p.a. (M€)	0.096	0.096	0.096	0.096	0.178	0.178	0.428	0.428	0.665
Upgraded Length(km)	95.7	95.7	95.7	95.7	177.5	177.5	426.6	426.6	661.9
Total Costs (M€)	16.141	16.143	16.143	16.143	14.651	14.651	14.570	14.564	14.778

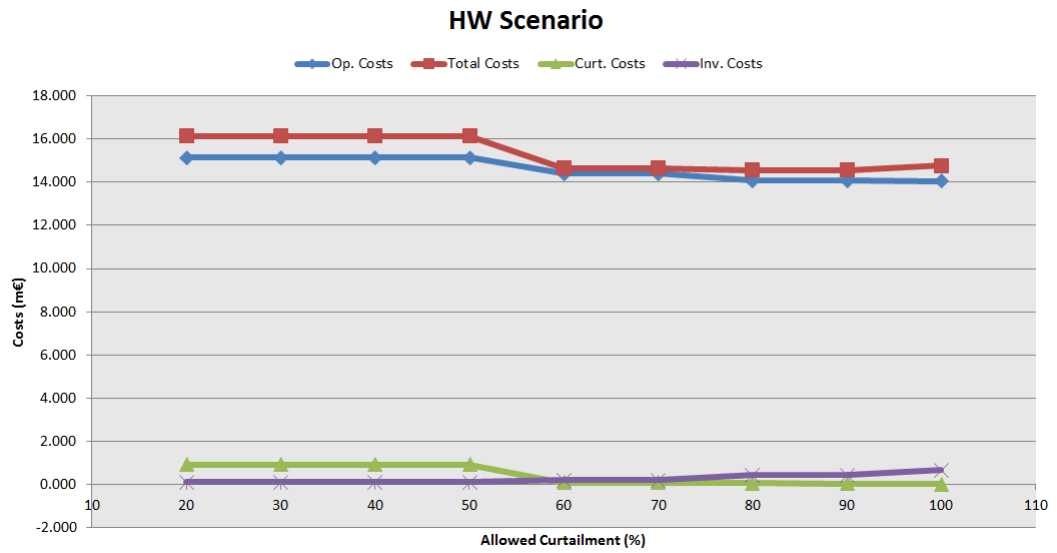


Figure A.1: HW Scenario Cost Factors. Source: Own Representation

Table A.3: LUCSIPO HW Scenario upgraded branches

Curtailment Limit (%)	Upgraded Branches
20	3 4
30	3 4
40	3 4
50	3 4
60	3 4 26 28
70	3 4 26 28
80	3 4 10 26 27 28 31 35 42
90	3 4 10 26 27 28 31 35 42
100	3 4x2 7 10 25 26x2 27 28x2 30 31 35 42

Table A.4: *LUCSIPO HWS Scenario Results*

Curtailement Limit (%)	20	30	40	50	60	70	80	90	100
Upgraded Branches	2	4	4	4	4	9	9	15	15
Curtailed Energy (%)	10.16	0.88	0.88	0.88	0.88	0.75	0.75	0.74	0.74
Curtailement Costs (M€)	0.910	0.078	0.078	0.078	0.063	0.041	0.007	0.000	0.000
Op. Policy Costs (M€)	0.000	0.000	0.000	0.000	0.015	0.026	0.060	0.066	0.066
Operational Costs (M€)	15.136	14.395	14.395	14.395	14.388	14.069	14.069	14.048	14.048
Investment costs p.a. (M€)	0.096	0.178	0.178	0.178	0.178	0.428	0.428	0.665	0.665
Upgraded Length(km)	95.7	177.5	177.5	177.5	177.5	426.6	426.6	661.9	661.9
Total Costs (M€)	16.143	14.652	14.652	14.652	14.645	14.564	14.564	14.778	14.778

Table A.5: *LUCSIPO HWS Upgraded Branches*

Curtailement Limit (%)	Upgraded Branches
20	3 4
30	3 4 26 28
40	3 4 26 28
50	3 4 26 28
60	3 4 26 28
70	3 4 10 26 27 28 31 35 42
80	3 4 10 26 27 28 31 35 42
90	3 4x2 7 10 25 26x2 27 28x2 30 31 35 42
100	3 4x2 7 10 25 26x2 27 28x2 30 31 35 42

Table A.6: *LUCSIPO LW Scenario Results*

Curtailed Limit(%)	20	30	40	50	60	70	80	90	100
Upgraded Branches	2	2	2	2	2	2	2	7	7
Curtailed Energy(%)	0.08	0.08	0.08	0.08	0.08	0.08	0.08	0.00	0.00
Curtailed Costs (M€)	0.004	0.004	0.004	0.004	0.004	0.004	0.004	0.000	0.000
Op. Policy Costs (M€)	0	0	0	0	0	0	0	0	0
Operational Costs (M€)	18.497	18.497	18.497	18.497	18.497	18.497	18.497	18.234	18.234
Investment costs p.a. (M€)	0.096	0.096	0.096	0.096	0.096	0.096	0.096	0.347	0.347
Upgraded Length(km)	95.7	95.7	95.7	95.7	95.7	95.7	95.7	345.7	345.7
Total Costs (M€)	18.596	18.596	18.596	18.596	18.596	18.596	18.596	18.581	18.581

Table A.7: *LUCSIPO LW Scenario Upgraded Branches*

Curtailed Limit (%)	Upgraded Branches
0.2	3 4 6 17 26 42
0.3	3 4 6 17 26 42
0.4	3 4 6 17 26 42
0.5	3 4 6 17 26 42
0.6	3 4 6 17 26 42
0.7	3 4 6 17 26 42
0.8	3 4 6 17 26 42
0.9	3 4 6 17 26 42
1	3 4 6 17 26 42

Table A.8: LUCSIPO LL Scenario Results

Curtailement Limit(%)	20	30	40	50	60	70	80	90	100
Upgraded Branches	2	2	2	2	2	2	5	5	5
Curtailed Energy(%)	3.27	3.27	3.27	3.27	3.27	3.27	0.00	0.00	0.00
Curtailement Costs (M€)	0.223	0.223	0.223	0.223	0.223	0.223	0.000	0.000	0.000
Op. Policy Costs (M€)	0	0	0	0	0	0	0	0	0
Operational Costs (M€)	16.878	16.878	16.879	16.879	16.879	16.879	16.555	16.555	16.555
Investment costs p.a. (M€)	0.096	0.096	0.096	0.096	0.096	0.096	0.232	0.232	0.232
Upgraded Length(km)	95.7	95.7	95.7	95.7	95.7	95.7	231.4	231.4	231.4
Total Costs (M€)	17.197	17.197	17.198	17.198	17.198	17.198	16.788	16.788	16.788

Table A.9: LUCSIPO HL Scenario Results

Curtailement Limit(%)	20	30	40	50	60	70	80	90	100
Upgraded Branches	2	2	2	2	2	2	5	5	5
Curtailed Energy(%)	3.40	3.40	3.40	3.40	3.40	3.40	0.34	0.34	0.34
Curtailement Costs (M€)	0.231	0.231	0.231	0.231	0.231	0.231	0.023	0.023	0.000
Op. Policy Costs (M€)	0.000	0.000	0.000	0.000	0.000	0.000	0.000	0.000	0.023
Operational Costs (M€)	16.885	16.885	16.885	16.885	16.885	16.885	16.576	16.576	16.576
Investment costs p.a. (M€)	0.096	0.096	0.096	0.096	0.096	0.096	0.232	0.232	0.232
Upgraded Length(km)	95.7	95.7	95.7	95.7	95.7	95.7	231.4	231.4	231.4
Total Costs (M€)	17.212	17.212	17.213	17.213	17.213	17.213	16.831	16.831	16.831

Table A.10: LUCSIPO HWHL Scenario Results

Curtailement Limit(%)	20	30	40	50	60	70	80	90	100
Upgraded Branches	2	2	2	2	9	9	11	11	9
Curtailed Energy(%)	9.39	9.39	9.39	9.39	3.16	3.16	3.44	3.44	3.54
Curtailement Costs (M€)	0.824	0.824	0.824	0.824	0.274	0.241	0.152	0.027	0.000
Op. Policy Costs (M€)	0.000	0.000	0.000	0.000	0.000	0.033	0.146	0.271	0.307
Operational Costs (M€)	15.176	15.178	15.178	15.178	14.280	14.283	14.277	14.276	14.259
Investment costs p.a. (M€)	0.096	0.096	0.096	0.096	0.459	0.459	0.502	0.502	0.459
Upgraded Length(km)	95.7	95.7	95.7	95.7	457.5	457.5	499.6	499.6	457.5
Total Costs (M€)	16.097	16.098	16.098	16.098	15.014	15.017	15.077	15.075	15.026

Table A.11: LUCSIPO HWHL Scenario Upgraded Branches

Curtailement Limit (%)	Upgraded Branches
20	3 4
30	3 4
40	3 4
50	3 4
60	3 4x2 26 27 28 31 35 42
70	3 4x2 26 27 28 31 35 42
80	3 4x2 10 26x2 27 28 31 35 42
90	3 4x2 10 26x2 27 28 31 35 42
100	3 4x2 26 27 28 31 35 42

Table A.12: *LUCSIPO HWLL Scenario Results*

Curtailed Limit (%)	20	30	40	50	60	70	80	90	100
Upgraded Branches	2	2	2	2	4	4	4	8	15
Curtailed Energy (%)	10.09	10.09	10.09	10.09	0.54	0.54	0.54	0.19	0.00
Curtailed Costs (M€)	0.906	0.906	0.906	0.906	0.048	0.048	0.048	0.017	0.000
Op. Policy Costs (M€)	0.000	0.000	0.000	0.000	0.000	0.000	0.000	0.000	0.000
Operational Costs (M€)	15.109	15.111	15.111	15.111	14.346	14.346	14.346	14.046	13.996
Investment costs p.a. (M€)	0.096	0.096	0.096	0.096	0.178	0.178	0.178	0.377	0.665
Upgraded Length(km)	95.7	95.7	95.7	95.7	177.5	177.5	177.5	375.5	661.9
Total Costs (M€)	16.111	16.113	16.113	16.113	14.572	14.572	14.572	14.440	14.660

Table A.13: *LUCSIPO HWLL Scenario Upgraded Branches*

Curtailed Limit (%)	Upgraded Branches
20	3 4
30	3 4
40	3 4
50	3 4
60	3 4 26 28
70	3 4 26 28
80	3 4 26 28
90	3 4 10 26 27 28 31 42
100	3 4x2 7 10 25 26x2 27 28x2 30 31 35 42

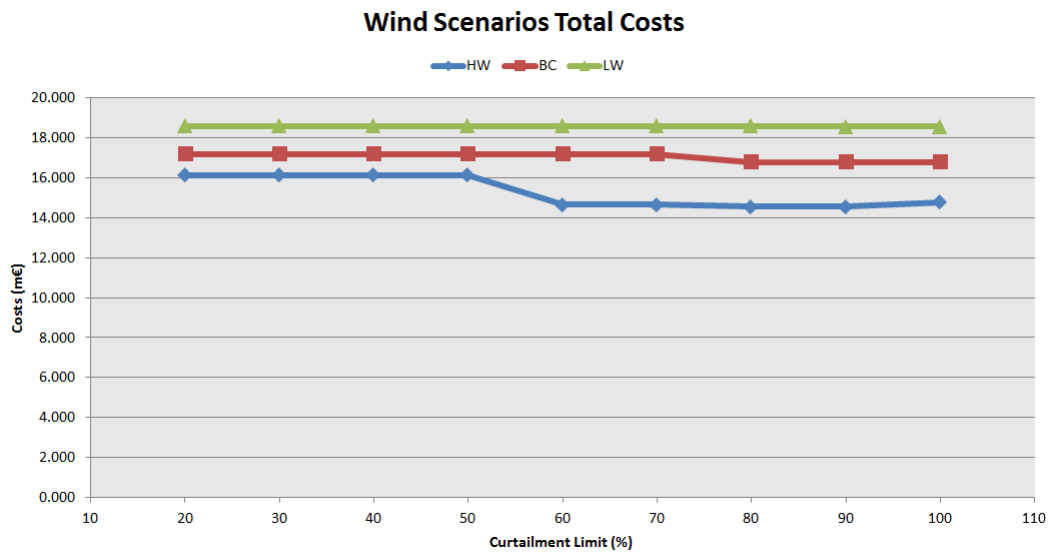


Figure A.5: Total Cost Comparison for the three wind cases, HW, BC and LW.

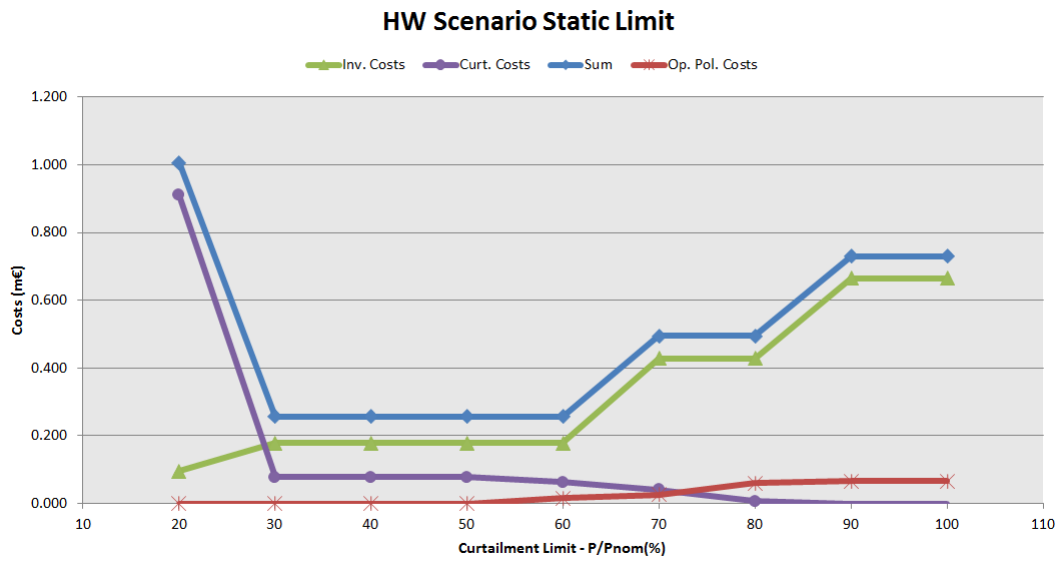


Figure A.2: Curtailment and investment costs for the static limit case.

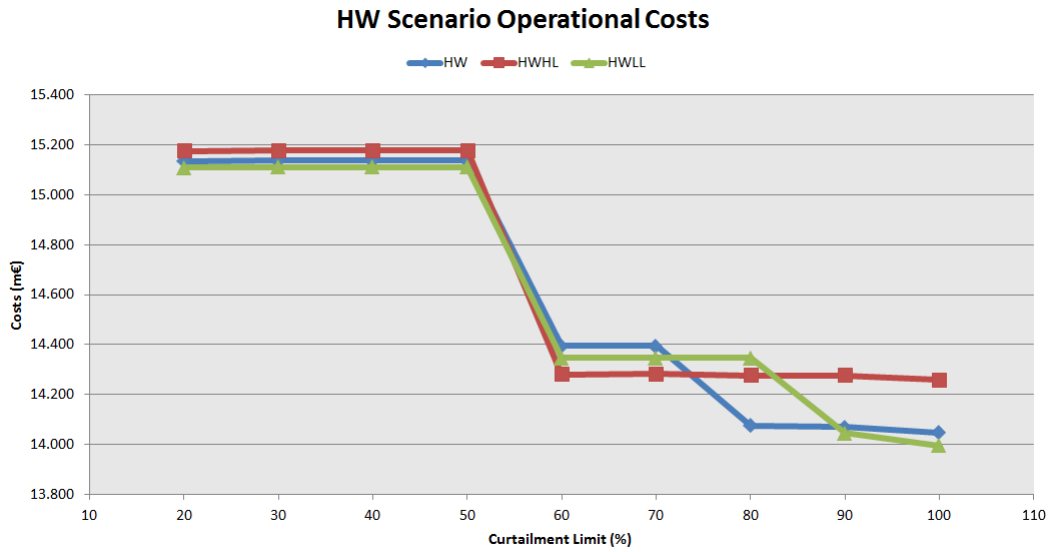


Figure A.3: *LUCSIPO*. Comparing the conventional power integration limits for the HW case from an operating costs point of view.

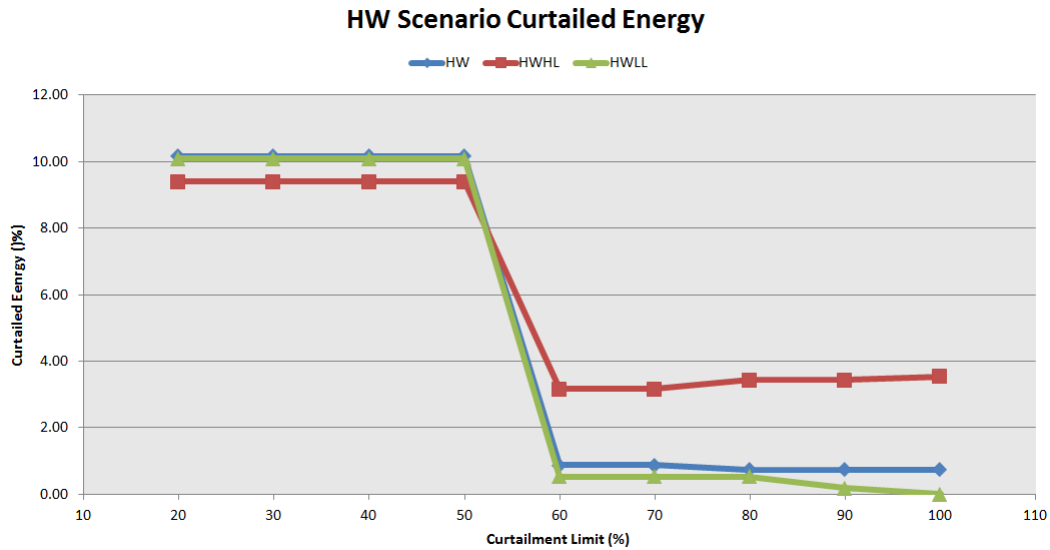


Figure A.4: *LUCSIPO*. Comparing the conventional power integration limits for the HW case from a curtailed energy point of view.

Table A.14: LUCSIPO HWRO Scenario Results

Curtailement Limit(%)	20	30	40	50	60	70	80	90	100
Upgraded Branches	2	2	2	2	4	4	12	12	15
Curtailed Energy(%)	10.16	10.16	10.16	10.16	0.88	0.88	0.75	0.75	0.74
Curtailement Costs (M€)	0.910	0.910	0.910	0.910	0.078	0.078	0.067	0.026	0.000
Op. Policy Costs (M€)	0.000	0.000	0.000	0.000	0.000	0.000	0.000	0.041	0.066
Operational Costs (M€)	115.135	15.136	15.136	15.136	14.394	14.394	14.066	14.060	14.048
Investment costs p.a. (M€)	0.096	0.096	0.096	0.096	0.178	0.178	0.550	0.550	0.665
Upgraded Length(km)	95.7	95.7	95.7	95.7	177.5	177.5	548.2	548.2	661.9
Total Costs (M€)	16.141	16.143	16.143	16.143	14.651	14.651	14.683	14.677	14.778

Table A.15: LUCSIPO HWRO Scenario Upgraded Branches

Curtailement Limit (%)	Upgraded Branches
20	3 4
30	3 4
40	3 4
50	3 4
60	3 4 26 28
70	3 4 26 28
80	3 4x2 7 10 26x2 27 28 31 35 42
90	3 4x2 7 10 26x2 27 28 31 35 42
100	3 4x2 7 10 25 26x2 27 28x2 30 31 35 42

Table A.16: *ICPPCRO/RO ranking comparison for a 90% curtailment limit. The first ranking corresponds to the original network while the second takes place after one branch has been already reinforced.*

Ranking Positions. $P_{curt}=90\%$							
1 st Ranking				2 nd Ranking			
HW		HWRO		HW		HWRO	
ICPPCRO (M €)	ID	RO (%)	ID	ICPPCRO (M €)	ID	RO (%)	ID
0.47	4	68.66	4	0.85	3	52.27	3
0.87	26	45.82	3	0.90	26	28.96	26
0.96	3	33.37	42	1.60	42	26.90	42
1.29	42	30.07	26	1.67	28	23.59	28
1.67	28	23.59	28	10.15	27	5.62	27
7.18	31	7.05	31	12.46	31	4.06	31
10.15	27	5.62	27	28.36	4	1.14	4
37.04	10	0.89	35	38.14	10	0.89	35
45.84	35	0.21	10	45.84	35	0.20	10
138.82	25	0.20	25	472.43	25	0.06	25
2701.34	45	0.02	45	827.98	7	0.05	7
22502.02	38	0.00	38	2701.34	45	0.02	45
n\a	n\a	n\a	n\a	4137.74	24	0.02	24
n\a	n\a	n\a	n\a	6600.29	6	0.01	6
n\a	n\a	n\a	n\a	22502.02	38	0.00	38

Table A.17: *ICPPCRO/RO ranking comparison for a 90% curtailment limit. The 8th ranking corresponds to the last ranking the two approaches selected the same branch for reinforcement. For the 9th ranking the two approaches pinpoint a different branch.*

Ranking Positions. $P_{curt}=90\%$							
8 th Ranking				9 th Ranking			
HW		HWRO		HW		HWRO	
ICPPCRO (M €)	ID	RO (%)	ID	ICPPCRO (M €)	ID	RO (%)	ID
34.11	35	1.19898	35	35.97	10	0.48717	4
35.97	10	0.48717	4	58.42	26	0.44567	26
58.42	26	0.44567	26	66.39	4	0.21144	10
66.39	4	0.21144	10	137.70	25	0.20001	25
233.21	28	0.16913	28	477.24	7	0.08156	7
280.48	25	0.09819	25	549.95	28	0.07172	28
477.24	7	0.08156	7	2701.34	45	0.01637	45
1337.80	6	0.04652	6	n\a	n\a	n\a	n\a
2701.34	45	0.01637	45	n\a	n\a	n\a	n\a

Table A.18: LUCSIPO IFLH Scenario Results

Curtailement Limit (%)	20	30	40	50	60	70	80	90	100
Upgraded Branches	0	0	4	6	6	6	6	10	10
Curtailed Energy (%)	16.61	16.61	6.10	3.73	3.73	3.73	3.73	3.26	3.25
Curtailement Costs (M€)	1.858	1.858	0.662	0.405	0.341	0.140	0.087	0.003	0.000
Op. Policy Costs (M€)	0.000	0.000	0.000	0.000	0.064	0.265	0.317	0.351	0.352
Operational Costs (M€)	15.799	15.799	14.098	13.721	13.719	13.735	13.735	13.434	13.435
Investment costs (M€)	0.000	0.000	0.138	0.242	0.242	0.242	0.242	0.439	0.439
Upgraded Length(km)	0.0	0.0	137.7	240.9	240.9	240.9	240.9	437.6	437.6
Total Costs (M€)	17.657	17.657	14.898	14.368	14.365	14.381	14.381	14.227	14.227

Table A.19: *LUCSIPO IFLH Scenario Upgraded Branches*

Allowed Curtailment (%)	Upgraded Branches
0.2	
0.3	
0.4	3 4 10 26
0.5	3 4 10 26 28 42
0.6	3 4 10 26 28 42
0.7	3 4 10 26 28 42
0.8	3 4 10 26 28 42
0.9	3 4 7 8 10 26 27 28 30 42
1	3 4 7 8 10 26 27 28 30 42

Table A.20: *ACO and LUCSIPO Results Comparison for the Low Wind Case.*

Scenario	LW	
	LUCSIPO	ACO
Method		
Upgraded Branches	7	9
Curtailed Energy (%)	0.00	0.00
Curtailment Costs (M€)	0.000	0.000
Op. Policy Costs (M€)	0.041	0.000
Operational Costs (M€)	18.234	18.181
Investment costs (M€)	0.347	0.406
Upgraded Length(km)	345.7	404.0
Upgraded Branches	3 4 26 28 31 35 42	3 4 19 25 26 27 28 35 42
Total Costs (M€)	18.581	18.587
Calculation Time	998.1	4602.1

Table A.21: *ACO and LUCSIPO Results Comparison for the High Wind High Limit Case.*

Scenario	HWHL	
	LUCSIO	ACO
Method		
Upgraded Branches	9	8
Curtailed Energy (%)	3.16	3.14
Curtailment Costs (M€)	0.274	0.272
Op. Policy Costs (M€)	0.000	0.000
Operational Costs (M€)	14.280	14.303
Investment costs (M€)	0.459	0.423
Upgraded Length(km)	457.5	421.2
Upgraded Branches	3 4x2 26 27 28 31 35 42	3x2 4 26 27 28 35 42
Total Costs (M€)	15.014	14.999
Calculation Time	1606.4	8197.3

Table A.22: *ACO and LUCSIPO Results Comparison for the High Wind Low Limit Case.*

Scenario	HWLL	
	LUCSIO	ACO
Method		
Upgraded Branches	8	9
Curtailed Energy (%)	0.19	0.10
Curtailment Costs (M€)	0.017	0.009
Op. Policy Costs (M€)	0.000	0.000
Operational Costs (M€)	14.046	14.019
Investment costs (M€)	0.377	0.428
Upgraded Length(km)	375.5	426.6
Upgraded Branches	3 4 10 26 27 28 31 42	3 4 10 26 27 28 31 35 42
Total Costs (M€)	14.440	14.456
Calculation Time	1244.2	4938.02

Table A.23: *ACO and LUCSIPO Results Comparison for the Low Limit Case.*

Scenario	LL	
	LUCSIO	ACO
Method		
Upgraded Branches	5	9
Curtailed Energy (%)	0.00	0.00
Curtailment Costs (M€)	0.000	0.000
Op. Policy Costs (M€)	0.000	0.000
Operational Costs (M€)	16.555	16.355
Investment costs (M€)	0.232	0.474
Upgraded Length(km)	231.4	472.4
Upgraded Branches	3 4 26 28 42	3 4 26 27 28 31 35 42 45
Total Costs (M€)	16.788	16.830
Calculation Time	850.8	4582.7

Table A.24: *ACO and LUCSIPO Results Comparison for the High Limit Case.*

Scenario	HL	
	LUCSIO	ACO
Method		
Upgraded Branches	5	9
Curtailed Energy (%)	0.34	0.34
Curtailment Costs (M€)	0.023	0.023
Op. Policy Costs (M€)	0.000	0.000
Operational Costs (M€)	16.576	16.534
Investment costs (M€)	0.232	0.356
Upgraded Length(km)	231.4	354.2
Upgraded Branches	3 4 26 28 42	3 4 18 25 26 28 29 35 42
Total Costs (M€)	16.831	16.912
Calculation Time	853.12	4586.9

Table A.25: *ACO and LUCSIPO Results Comparison for the Marginal Cost Case.*

Scenario	MC	
	LUCSIO	ACO
Method		
Upgraded Branches	5	9
Curtailed Energy (%)	0.00	0.00
Curtailment Costs (M€)	0.000	0.000
Op. Policy Costs (M€)	0.000	0.000
Operational Costs (M€)	16.555	16.356
Investment costs (M€)	0.232	0.453
km	231.4	451.5
Upgraded Branches	3 4 26 28 42	3 4 25 26 27 28 31 35 42
Total Costs (M€)	16.788	16.809
Calculation Time	848.67	4597.4

Table A.26: *ACO and LUCSIPO Results Comparison for the RO Case.*

Scenario	RO Ranking (RO)	
	LUCSIO	ACO
Method		
Upgraded Branches	5	9
Curtailed Energy (%)	0.00	0.00
Curtailment Costs (M€)	0.000	0.000
Op. Policy Costs (M€)	0.000	0.000
Operational Costs (M€)	16.555	16.410
Investment costs (M€)	0.232	0.433
Upgraded Length (km)	231.4	431.0
Upgraded Branches	3 4 26 28 42	3 4 26 27 28 30 31 36 42
Total Costs (M€)	16.788	16.843
Calculation Time	851.8	4597.3

Table A.27: *NE Test System Branch Information*

Branch Number	From Bus	To Bus	Length (km)	Transformer
1	1	2	150.38	
2	1	39	91.22	
3	2	3	55.25	
4	2	25	40.43	
5	2	30	0.00	1
6	3	4	77.80	
7	3	18	48.65	
8	4	5	46.76	
9	4	14	47.12	
10	5	6	9.51	
11	5	8	40.94	
12	6	7	33.61	
13	6	11	30.00	
14	6	31	0.00	1
15	7	8	16.83	
16	8	9	132.61	
17	9	39	91.22	
18	10	11	15.74	
19	10	13	15.74	
20	10	32	0.00	1
21	12	11	0.00	1
22	12	13	0.00	1
23	13	14	36.97	
24	14	15	79.38	
25	15	16	34.43	
26	16	17	32.55	
27	16	19	71.33	
28	16	21	49.30	
29	16	24	21.54	
30	17	18	30.00	
31	17	27	63.25	
32	19	20	0.00	1
33	19	33	0.00	1
34	20	34	0.00	1
35	21	22	51.12	
36	22	23	35.07	
37	22	35	0.00	1
38	23	24	127.85	
39	23	36	0.00	1
40	25	26	118.33	
41	25	37	0.00	1
42	26	27	53.84	
43	26	28	173.52	
44	26	29	228.81	
45	28	29	55.29	
46	29	38	0.00	1
47	25	41	0.00	1
48	21	40	0.00	1

Appendix B

European Network Model Data

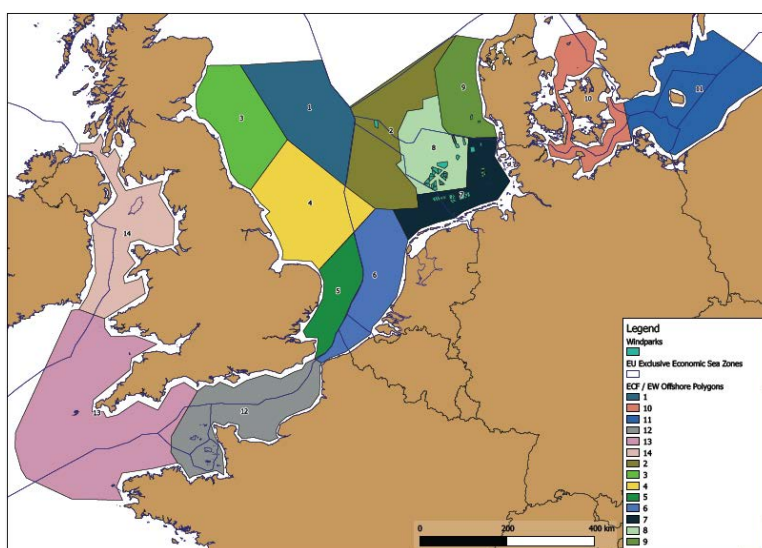


Figure B.1: Offshore Regions. Source: Representation by LEnGISS.

Table B.2: Installed RES capacities in EUROPE on 2010. Source: [113] [104]

EUROPE									
INSTALLED RES-E CAPACITIES 2010 (MW)									
MS	Biomass	Biogas	Inciner.	PV	Wind	Hydro (L)	Hydro (M)	Hydro (S)	CHP
EU 27	14006	4199	5688	25375.6	64429	89682	9604	2992	0
EU 15	12903	4027	5637	25314.6	63336	76305	8676	2475	0
BE	442	88	185	563	911	52	50	8	2090
BG	0	0	0	6	375	1890	300	51	1370
CZ	468	71	3	466	215	753	300	155	4820
DK	558	81	303	5	3752	0	4	5	5370
DE	0	5626	1301	18001	27580	2104	960	640	2225

Continued on next page

Table B.2 – Continued from previous page

MS	Biomass	Biogas	Inciner.	PV	Wind	Hydro (L)	Hydro (M)	Hydro (S)	CHP
ES	10	2	0	0	77	0	0	5	0
IE	0	29	0	0	1028	196	50	27	0
GR	0	40	0	205	1208	2319	114	44	400
ES	0	697	189	4129	19243	11232	2200	314	5916
FR	265	120	827	789	5660	18823	2500	543	5110
IT	2131	349	1113	2032	5797	11190	3000	516	6730
CY	0	0	0	0	0	0	0	0	0
LV	3	7	0	0	28	1511	50	48	0
LT	16	8	0	0	54	90	50	34	0
LU	0	6	9	26	42	0	50	3	110
HU	356	19	42	1	295	37	0	4	190
MT	0	0	0	0	0	0	0	0	0
NL	405	167	506	64	2237	37	0	0	8970
AT	2024	121	431	49	1011	7040	1000	385	3650
PL	40	52	0	1	1107	672	300	86	8780
PT	293	13	77	102	3898	3634	400	32	1090
RO	15	0	0	1	462	6009	400	69	4690
SL	48	9	0	8	0	873	100	76	340
SK	147	4	6	0	3	1542	65	25	2150
FI	1757	0	0	8	143	2786	420	41	0
SE	2761	24	423	8	814	15436	1450	160	0
UK	513	996	273	23	3406	1456	108	65	0
IS	0	0	0	0	0	0	49	0	0
NO	79	0	25	8	360	27150	1048	48	0
CH	0	32	332	45	18	13475	0	0	0
HR	0	0	0	0	28	1749	32	1	0
TR	69	33	0	0	364	13582	231	16	0

Table B.3: 2010 Installed RES Capacities (MW) in Germany per 2 Digit Postal Code

DE - Installed RES per 2 digit postal code (MW). Source: [103]					
2 Digit PLZ	Biomass	Hydro	PV	Wind	Geothermal
10	0.55	0.00	8.58	0.00	0.00
12	29.53	0.06	28.61	0.00	0.00
13	2.39	0.00	16.76	36.65	0.00
14	52.23	0.22	339.33	850.78	0.00
15	115.12	0.42	276.69	593.78	0.00
16	104.73	1.47	381.34	1441.21	0.00
17	136.41	7.05	342.60	1216.80	0.00
18	45.41	1.56	144.86	569.79	0.00
19	94.05	2.63	350.00	650.40	0.22
20	0.24	0.00	1.53	0.00	0.00
21	60.83	0.59	130.09	610.97	0.00

Continued on next page

Table B.3 – *Continued from previous page*

2 Digit PLZ	Biomass	Hydro	PV	Wind	Geothermal
22	29.03	0.17	26.47	26.51	0.00
23	63.23	5.31	115.78	685.37	0.00
24	185.02	2.24	344.32	575.38	0.00
25	133.64	0.00	515.64	2339.95	0.00
26	196.48	2.08	568.60	2027.44	0.00
27	172.79	0.00	302.47	1408.90	0.00
28	17.30	1.19	63.23	244.81	0.00
29	165.36	6.95	246.98	894.63	0.00
30	12.45	5.16	86.58	152.07	0.00
31	130.43	14.51	386.67	727.30	0.00
32	58.57	13.13	347.10	241.55	0.00
33	71.82	1.70	332.38	347.25	0.00
34	49.12	22.12	379.72	380.79	0.00
35	13.09	9.31	219.12	156.56	0.00
36	32.35	9.89	229.59	189.35	0.00
37	56.02	17.58	185.87	190.43	0.00
38	58.48	16.98	145.46	605.65	0.00
39	184.69	2.88	258.68	1685.90	0.00
40	5.88	0.04	43.43	5.68	0.00
41	51.14	0.32	139.88	158.23	0.00
42	2.60	4.03	34.82	24.37	0.00
44	26.20	1.32	88.57	19.84	0.00
45	68.44	20.56	120.05	70.29	0.00
46	71.87	3.24	340.97	221.46	0.00
47	49.17	7.76	297.00	191.99	0.00
48	117.76	1.09	687.94	751.72	0.00
49	258.70	0.48	875.00	1010.79	0.00
50	2.42	0.05	59.71	64.21	0.00
51	5.29	10.45	68.43	12.80	0.00
52	23.49	3.61	148.18	326.16	0.00
53	12.72	1.84	180.00	106.87	0.00
54	37.07	18.86	286.57	646.24	0.00
55	26.84	8.76	206.08	309.62	0.00
56	49.71	9.30	195.53	291.63	0.00
57	13.10	11.40	88.34	124.77	0.00
58	21.82	36.45	66.94	56.52	0.00
59	85.80	24.86	325.02	449.07	0.00
60	14.64	4.20	14.94	0.00	0.00
61	10.88	2.84	134.39	172.33	0.00
63	47.93	21.60	358.08	261.83	0.00
64	15.36	5.86	146.51	319.78	0.00
65	43.26	5.88	210.52	72.09	0.00
66	31.08	13.91	366.63	442.92	0.00
67	31.77	2.81	357.61	268.89	0.00
68	67.18	7.45	134.08	12.11	0.00
69	16.17	47.85	105.30	83.98	0.00
70	3.92	12.90	44.06	0.50	0.00
71	18.85	12.24	165.19	0.01	0.00

Continued on next page

Table B.3 – *Continued from previous page*

2 Digit PLZ	Biomass	Hydro	PV	Wind	Geothermal
72	60.85	37.64	395.04	50.56	0.00
73	65.99	19.96	295.51	88.75	0.00
74	117.17	54.35	595.95	75.67	0.00
75	45.31	13.60	167.99	15.13	0.00
76	34.02	21.39	288.51	65.39	3.55
77	45.08	19.56	199.57	69.43	0.00
78	41.71	16.28	317.56	52.16	0.00
79	52.59	100.57	325.15	68.82	0.00
80	2.41	5.69	25.28	1.50	0.00
81	1.62	24.90	32.57	4.52	0.00
82	19.15	29.63	230.23	5.04	3.60
83	70.37	92.57	390.65	8.69	0.00
84	108.12	33.98	974.21	10.68	0.17
85	100.22	20.09	519.62	18.31	0.00
86	164.46	74.95	994.63	18.99	0.00
87	49.03	98.22	485.66	46.48	0.00
88	94.46	21.00	621.27	13.33	0.00
89	109.61	29.36	591.13	68.51	0.00
90	11.44	4.91	117.80	13.19	0.00
91	113.45	19.79	741.10	118.46	0.00
92	88.97	22.35	499.67	28.59	0.00
93	44.63	30.74	490.35	28.16	0.00
94	67.38	71.23	1178.52	19.07	0.00
95	48.02	23.53	261.44	109.53	0.00
96	49.22	31.19	356.76	41.46	0.00
97	45.55	80.70	788.58	321.52	0.00
98	26.57	3.77	77.17	1.77	0.00
99	88.24	6.23	228.37	606.23	0.00

Table B.1: Installed conventional capacities in DE and surrounding countries on 2012. Source: [23].

Conventional Technology Capacities (MW)						
MS/Fuel	Coal	Natural Gas	Other Gas	Oil	Lignite	Uranium
Austria	617	962	1	149	0	0
Belgium	0	1755	3	377	0	2984
Czech Republic	0	368	0	100	10669	6848
Denmark	82	2234	35	871	0	0
France	2008	2108	0	0	0	6960
Germany	32829	27672	493	3051	24586	12027
Luxemburg	0	428	0	1	0	0
Netherlands	3495	9558	0	0	0	0
Norway	0	1106	58	0	0	0
Poland	0	467	0	0	5112	0
Sweden	0	1255	21	1242	0	6631
Switzerland	20	151	26	25	0	6420

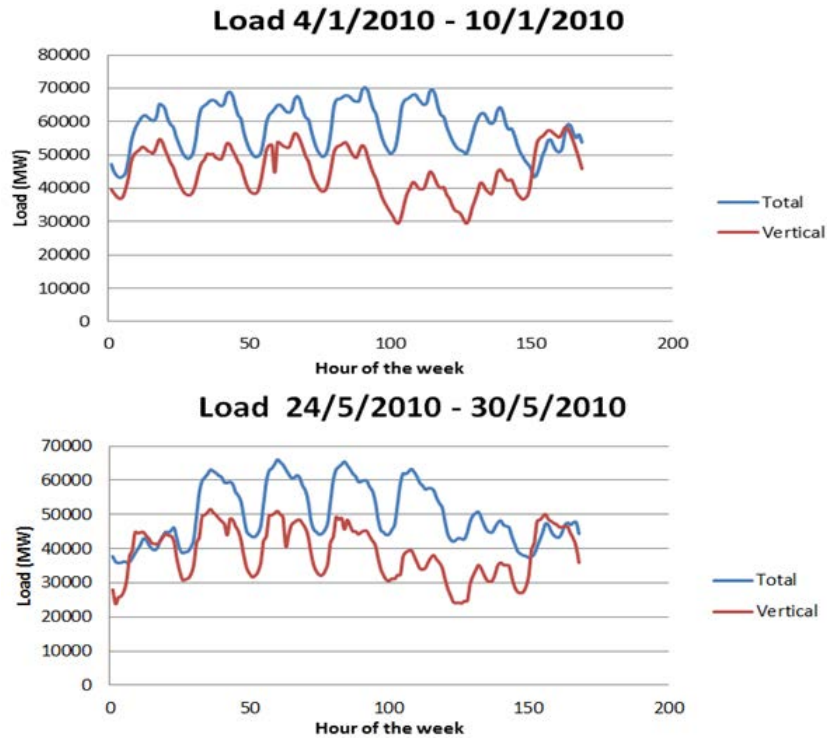


Figure B.2: Typical German winter and spring week. Total [105] and Vertical [18] Load comparison

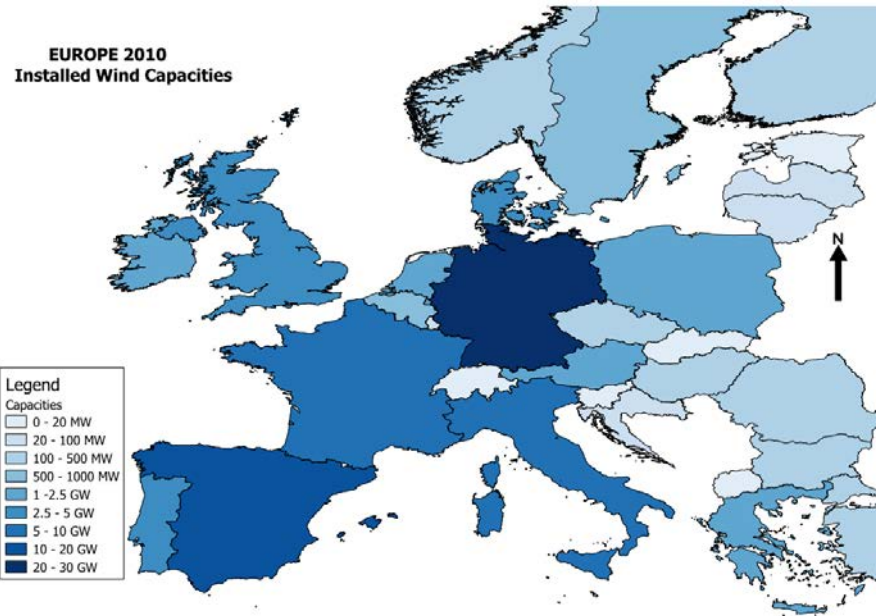


Figure B.3: EU Wind Capacities in 2010. Own Representation based on [104] [113]

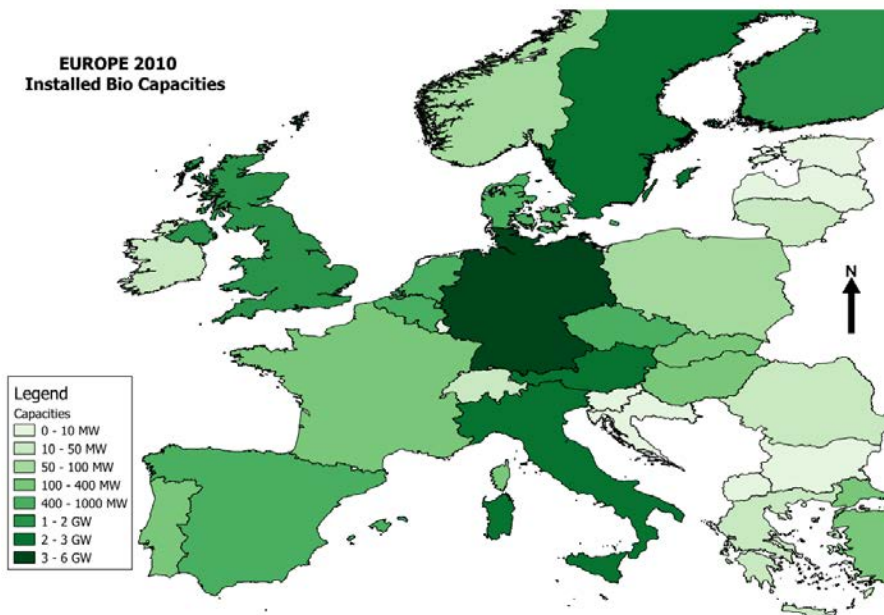


Figure B.4: EU Biomass and Biogas Capacities in 2010. Own Representation based on [104] [113].

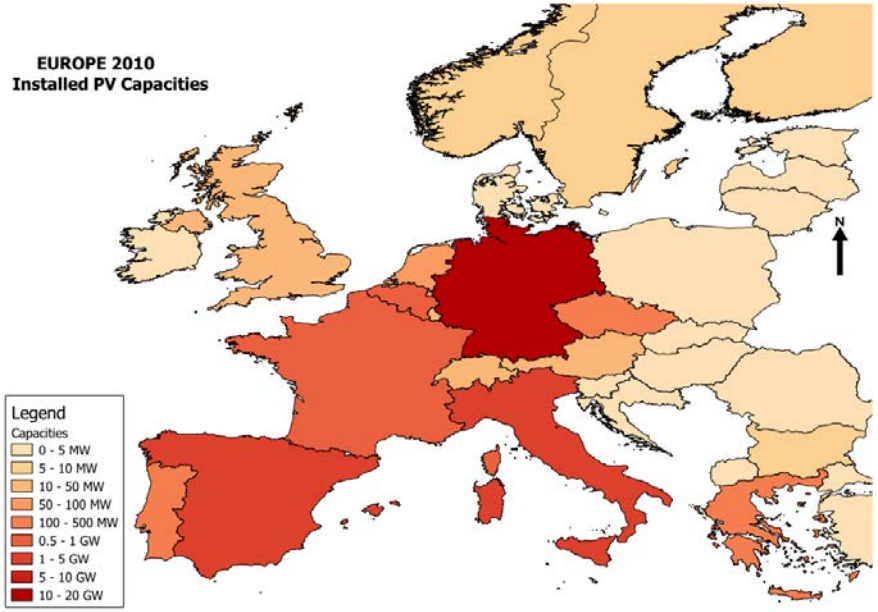


Figure B.5: EU Solar Capacities in 2010, Own Representation based on [104] [113].

Figure B.6: EU Solar Capacities (GW). Source: [115]

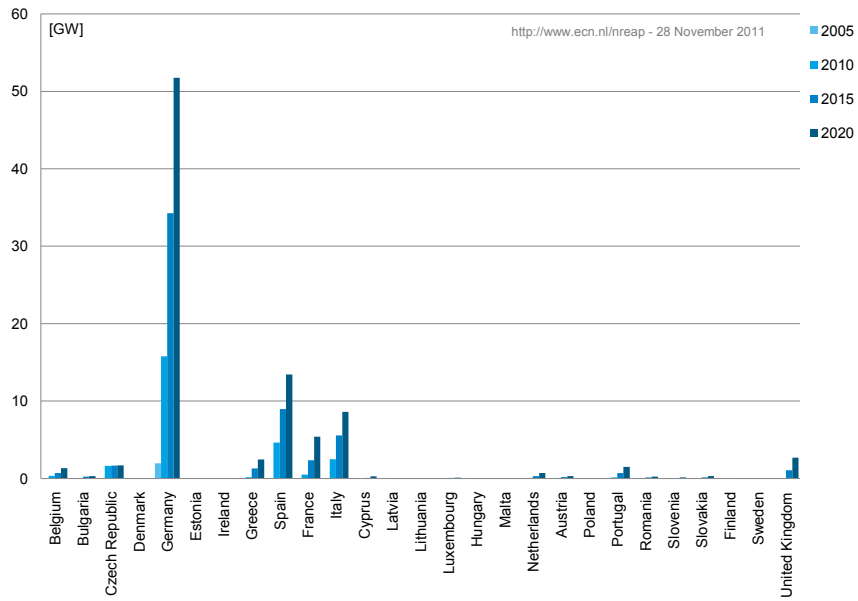


Figure B.7: EU Wind Capacities (GW). Source: [115]

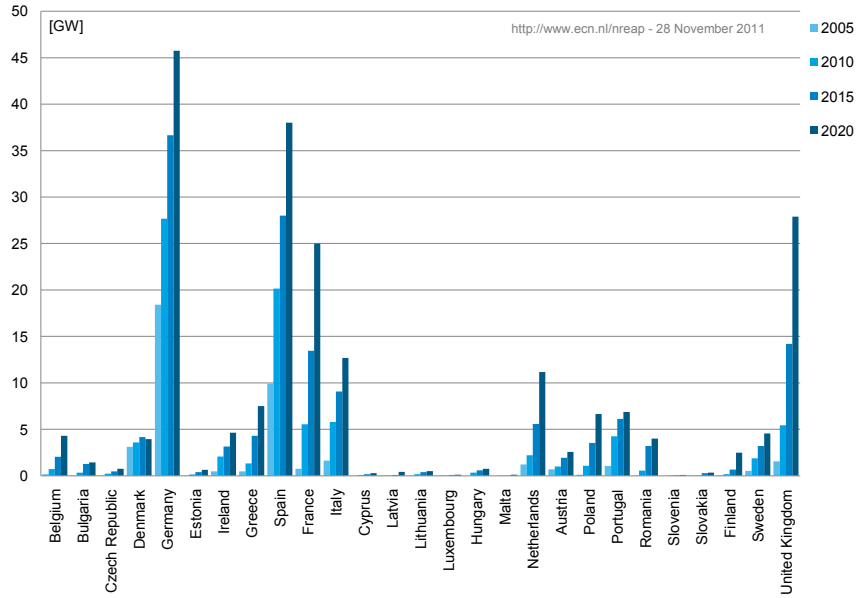


Figure B.8: EU Hydro Capacities (GW). Source: [115]

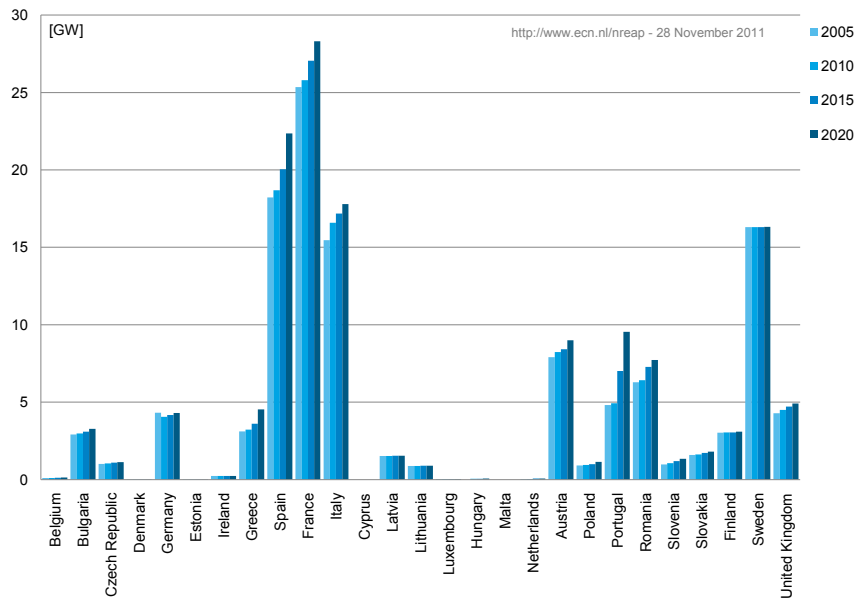


Figure B.9: *EU Biomass Capacities (GW). Source: [115]*

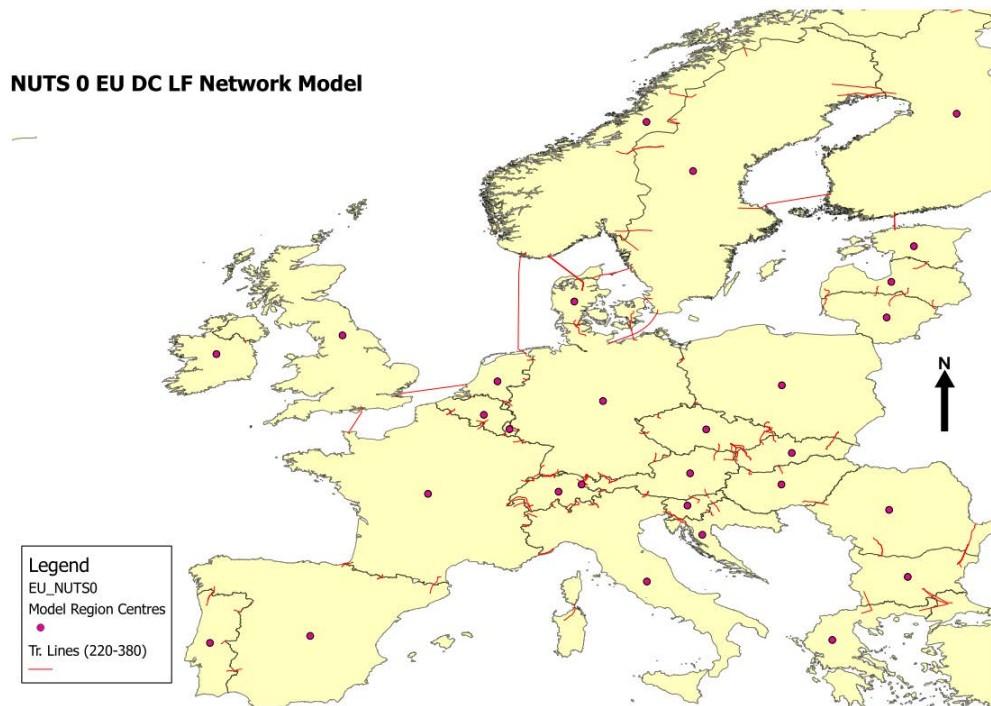
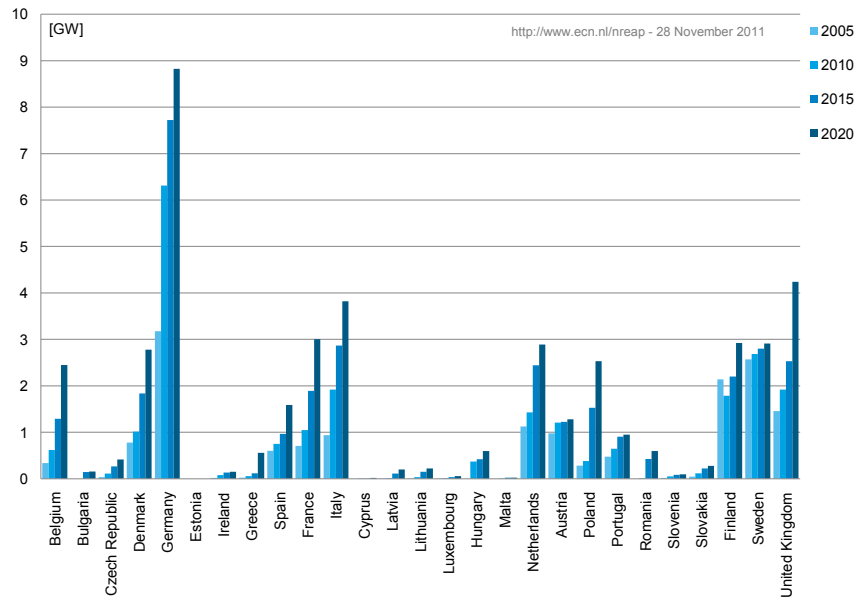


Figure B.10: *DC-LF Network Model: EU NUTS0.*

Table B.4: *Basic PowerFactory objects*

PF object	Name	Comments
General	General information	DGS Interface version
ElmNet	Main Grid	Parent Folder (nothing in fold_id field)
ElmTerm	Terminal Elements	
ElmLod	Load Elements	
TypLod	Load Types	
ElmSym	Sync. Machines Elements	
TypSym	Sync. Machines Types	
ElmAsm	Asyn Machines Elements	
TypAsmo	Asyn Machines Types	
ElmTr2	Transformer Element 2wind	
TypTr2	Transformer Types 2wind	
ElmLine	Line Elements	
TypLne	Line Types	
StaCubic	Cubicle element	Used for connection between branch elements
StaSwitch	Switch element	Used together with cubicles
IntFold	Folder for libraries	Equipment type library
ElmGenstat	Static Generator	Commonly used for RES generation
Vsc	Rectifier/Inverter object	May be used for the HVDC links
chavec	Characteristic vector	Used for time series and scaling
Scale	Scale object	The characteristic vectors time scale

Table B.5: *DE North Sea Offshore Capacities. Source: [106]*

North Sea -Sum of Capacity [MW]		
Consent application submitted	Brunsubttel	1205
	Buttel	815
	Diele	11969
	Diele -lkraftwerk Eemshaven	400
	Diele/Borssum	215
	H2-Speicher	400
	?	4150
Consent application submitted Total		19154.2
Consent authorised	Buttel	2343
	Diele	3895
	Diele/Borssum	400
	Dorpen west	852
	Emden Borssum	108
	Inhausen	110.7
Consent authorised Total		7708.9
Operational	Diele	400
	Hagermarsch	60
Operational Total		460
Under Construction	Dorpen west	200
Under Construction Total		200
Grand Total		27523.1

Table B.6: *DE Baltic Sea Offshore Capacities. Source: [106]*

Baltic Sea -Sum of Capacity [MW]		
Consent application submitted	Bentwisch	500
	Gohl	150
	Lubmin	737
	Stralsund	350
	?	1630
Consent application submitted Total		3367
Consent authorised	Bentwisch	288
	Gohl	25
	Lubmin	880
Consent authorised Total		1193
Fully commissioned	Bentwisch	48
Fully commissioned Total		48
Grand Total		4608

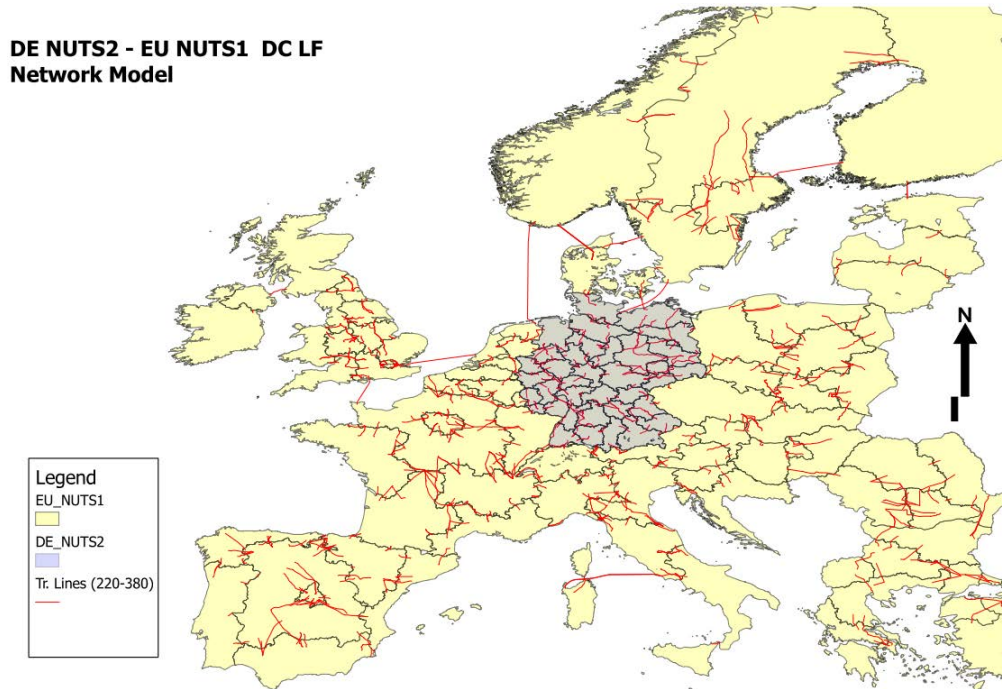


Figure B.11: DC-LF Network Model: Germany (NUTS2) and rest of Europe (NUTS1).

System	Voltage level	Power rating	Cost	Cost Unit
HVAC OHL, single circuit	380 kV	1500 MVA	400-700	kEUR/km
HVAC OHL, double circuit	380 kV	2 x 1500 MVA	500-1000	kEUR/km
HVAC underground XLPE cable, single circuit	380 kV	1000 MVA	1000 - 3000	kEUR/km
HVAC underground XLPE cable, double circuit	380 kV	2 x 1000 MVA	2000-5000	kEUR/km
HVDC OHL, bipolar	$\pm 150 - \pm 500$ kV	350 - 3000 MW	300 - 700	kEUR/km
HVDC underground cable pair	± 350 kV	1100 MW	1000 - 2000	kEUR/km
HVDC undersea cable pair	± 350 kV	1100 MW	1000 - 2500	kEUR/km
HVDC Voltage Source Converter (VSC) terminal, bipolar	$\pm 150 - \pm 350$ kV	350 - 1000 MW	60 - 125	kEUR/MW
HVDC Current Source Converter (CSC) terminal, bipolar	$\pm 350 - \pm 500$ kV	1000 - 3000 MW	75 - 110	kEUR/MW

Table B.7: Average Indicative costs for different grid technologies. Source: [97]